University of Nottingham

UK | CHINA | MALAYSIA

Bowel MRI imaging to investigate drug delivery from coated capsules

Thesis submitted to the University of Nottingham for the degree of Doctor of Philosophy

Sarah Sulaiman

School of Medicine

University of Nottingham, UK

March 2023

Table of Contents

List of abbreviations

^{99m}Tc	99m-Technetium
^{111}In	111-Indium
AC	ascending colon
Ach	acetylcholine
ATP	adenosine triphosphate
AUC	area under the curve
ANOVA	analysis of variance
COV	coefficient of variation
CTT	colon transit time
DC	descending colon
EC	ethylcellulose
ENS	enteric nervous system
FODMAP	fermentable oligosaccharides, disaccharides, monosaccharides and polyols
GC	geometric centre
GE	gastric emptying
GI	gastrointestinal

GABA	γ-aminobutyric acid
HAPS	high-amplitude propagating sequences
HPLC	high-performance liquid chromatography
HPMC	hydroxy-propyl-methyl-cellulose or hypromellose
IBD	Inflammatory Bowel Disease
IBS	Inflammatory Bowel Syndrome
ICJ	ileo-caecal junction
IQR	interquartile range
IJJ	interstitial cells of Cajal
LHBT	lactulose hydrogen breath test
LUBT	lactose ureide breath test
MCC	microcrystalline cellulose
MMC	migrating motor complex
MRI	Magnetic Resonance Imaging
NO	nitric oxide
OCTT	oro-caecal transit time
PG	prostaglandin
PR	prolonged release

PCDC	pressure-controlled colon delivery capsules
ROM	radio-opaque marker
RPRs	rhythmic propulsive ripples
RTC	radiotelemetry capsule
RPMC	rhythmic propulsive motor complexes
SC	sigmoid colon
SEM	standard error of the mean
SIT	small intestinal transit
STD	standard deviation
STDJac	standard deviation of the Jacobian
Sm_2O_3	samarium oxide
TC	transverse colon
UC	ulcerative colitis
WGT	whole gut transit
WAPS	median average weighted position score

Related Publications and Abstracts

Publications

Senekowitsch S, Schick P, Abrahamsson B, Augustijns P, Gießmann T, Lennernäs H, Matthys C, Marciani L, Pepin X, Perkins A, Feldmüller M, **Sulaiman S**, Weitschies W, Wilson CG, Corsetti M, Koziolek M. Application of *In Vivo* Imaging Techniques and Diagnostic Tools in Oral Drug Delivery Research. Pharmaceutics. 2022 Apr 6;14(4):801. doi: 10.3390/pharmaceutics14040801. PMID: 35456635; PMCID: PMC9025904.

Sulaiman S, Gershkovich P, Hoad CL, Calladine M, Spiller RC, Stolnik S, Marciani L. Application of *In Vivo* MRI Imaging to Track a Coated Capsule and Its Disintegration in the Gastrointestinal Tract in Human Volunteers. Pharmaceutics. 2022 Jan 24;14(2):270. doi: 10.3390/pharmaceutics14020270. PMID: 35214003; PMCID: PMC8879863.

Schütt, M.; O'Farrell, C.; Stamatopoulos, K.; Hoad, C.L.; Marciani, L.; **Sulaiman, S**.; Simmons, M.J.H.; Batchelor, H.K.; Alexiadis, A. Simulating the Hydrodynamic Conditions of the Human Ascending Colon: A Digital Twin of the Dynamic Colon Model. Pharmaceutics 2022, 14, 184. https://doi.org/10.3390/pharmaceutics14010184

O'Farrell C, Hoad CL, Stamatopoulos K, Marciani L, **Sulaiman S**, Simmons MJH, Batchelor HK. Luminal Fluid Motion Inside an *In Vitro* Dissolution Model of the Human Ascending Colon Assessed Using Magnetic Resonance Imaging. Pharmaceutics. 2021 Sep 23;13(10):1545. doi: 10.3390/pharmaceutics13101545. PMID: 34683837; PMCID: PMC8538555.

Stamatopoulos K, Karandikar S, Goldstein M, O'Farrell C, Marciani L, **Sulaiman S**, Hoad CL, Simmons MJH, Batchelor HK. Dynamic Colon Model (DCM): A Cine-MRI Informed Biorelevant In Vitro Model of the Human Proximal Large Intestine Characterized by Positron Imaging Techniques. Pharmaceutics. 2020 Jul 13;12(7):659. doi: 10.3390/pharmaceutics12070659. PMID: 32668624; PMCID: PMC7407282.

Sulaiman S, Marciani L. MRI of the Colon in the Pharmaceutical Field: The Future before us. Pharmaceutics. 2019 Mar 27;11(4):146. doi: 10.3390/pharmaceutics11040146. PMID: 30934716; PMCID: PMC6523257.

Conference abstracts

Gastrointestinal and Liver Research Showcase Event, UK, June 2022. **S Sulaiman**, P Gershkovich, C L Hoad, M Calladine, R C Spiller, S Stolnik, L Marciani. Application of *in vivo* MRI imaging to track a coated capsule and its disintegration in the gastrointestinal tract in human volunteers

UNGAP Annual Meeting, Slovenia, February 2020. **S Sulaiman**, S Stolnik-Trenkic, P Gershkovich, M Corsetti, L Marciani. Colon targeted delivery: novel MRI insights.

UNGAP Annual Meeting, Germany, February 2019. **S Sulaiman**, C O'Farrell, K Stamatopoulos, A Alexiadis, H Batchelor, M Simmons, M Corsetti, L Marciani. MRI of the colon in the pharmaceutical field: the future before us.

Oral Presentations

UNGAP Annual Meeting, Slovenia, February 2020. Colon targeted delivery: novel MRI insights.

Acknowledgements

Undertaking this PhD has been a truly life-changing experience for me and it would not have been possible to do without the support and guidance that I received from many people.

First and foremost, I would like to express my sincere gratitude and appreciation to my supervisor Prof Luca Marciani for his guidance, encouragement and inspiring mentorship. I am grateful for his commitment to my success and support in my academic and personal struggles. I could not have asked for a better mentor; working under his supervision has been very enjoyable and I have learnt and grown a lot.

I would also like to thank Prof Snow Stolnik, Dr Pavel Gershkovich and Prof Robin Spiller for co-supervising this work and the Precision Imaging Beacon of Excellence for this PhD scholarship.

I am also thankful to the Tech Team of the Nottingham Biomedical Research Centre and, especially, the Biodiscovery Institute lab members. Everyone has been instrumental to the completion of this work and it has been a pleasure to work alongside.

To my family and my partner, thank you for always believing in me and encouraging me to follow my dreams. Without you, this would not have been possible.

Abstract

Background

Magnetic resonance imaging (MRI) has the potential to provide new physiological insights into oral dosage forms in the undisturbed human GI tract. This potential has been recently shown in the literature, however these initial studies principally focused on the upper GI tract. Applications to the lower GI tract and particularly to MRI imaging of coated capsules remain to be explored to date.

Aims

Building on the available literature, this work therefore aimed to:

1. Design and manufacture coated capsules with the potential to reach the lower human intestine and at the same time to be MRI-visible
2. Develop and demonstrate a new MRI method to track the transit of the coated capsule and its disintegration in the lower human intestine
3. Load the coated capsule with an active pharmaceutical ingredient (API) and correlate the MRI findings with the API's absorption kinetic
4. Explore additional MRI measurements of GI function of interest for oral dosage forms, such as small bowel motility measurements, by comparing MRI with concomitant perfused manometry

Key results

Size 0 (21 mm × 7 mm) capsules, consisting of a hydroxypropyl methylcellulose (HPMC) shell, dip-coated with different amounts of synthetic

polymer Eudragit® S 100 were designed and manufactured manually in house. The capsules were filled with 0.65 mL of olive oil as MRI-visible marker fluid. Standard, basket apparatus disintegration tests showed that the capsules were able to withstand the upper gastrointestinal tract acid conditions and that disintegration time in intestinal condition increased with weight gain due to coating. The capsules could also be visualised *in vitro* using MRI.

The *in vivo* imaging feasibility study in 10 healthy adult participants showed that it was possible to track capsules with varying amounts of coating in the human gastrointestinal tract. The capsules' loss of integrity was imaged exploiting the ability of MRI to image fat and water separately, and in combination. By the 360 min end of the study, out of the 10 participants, the capsules were imaged in the small bowel in 9 participants, in the terminal ileum in 8 participants and in the colon in 4 participants. Loss of capsule's integrity was observed for 8 participants out of 10, occurring predominantly in distal intestinal regions.

After this, 75 mg of caffeine was added in suspension to the olive oil inside the capsules. The selection of this dose was based on literature searches and aimed to provide a safe active pharmaceutical ingredient marker, and also a marker that could be adequately absorbed from the unfavourable environment of the large intestine and then be detected in saliva. For this purpose, a pre-existing high-performance liquid chromatography (HPLC) assay was used. The conditions, peak shapes and run time for the injections were optimised for this study and the assay's lower limits of detection

characterised. Nine healthy participants were then administered capsules manufactured with varying amounts of Eudragit® S 100 coating from 0 mg to 36 mg weight gain. The timing of the first loss of capsule integrity detected in the body using MRI correlated well with the onset of increase in caffeine concentration in the saliva from the baseline level ($R^2 = 0.76$, $p = 0.0022$).

Lastly, the work explored the ability of MRI to monitor small bowel motility using retrospective data whereby 18 healthy volunteers underwent concomitant MRI and perfused manometry monitoring of duodenal motility. Total of 393 data sets could be compared showing limitations of the MRI protocol and a modest ($R^2 = 0.1214$) but significant ($p < 0.0001$) correlation between the values of motility indexes derived from MRI and corresponding perfused manometry values. The association between MRI peaks of motility and MMC III events was statistically significant ($p < 0.0001$).

Conclusion

Building on initial reports in the literature this work has successfully developed and tested *in vivo* a coated capsule using a new concept for the MRI-visible filling. MRI was able to determine location and disintegration times of these coated capsules in the distal intestine, and this correlated well with absorption kinetics of a model active pharmaceutical ingredient, caffeine in this case.

This work adds to the field new methods to study performance of coated capsules *in vivo* in an undisturbed bowel. The new data and techniques will in turn help to make *in vitro* pharmacopoieial tests and kinetic and bench

dynamic modelling more *in vivo* relevant. MRI has also the potential to assess other parameters of gastrointestinal function which are relevant for dosage form transit and disintegration such as small bowel motility. However such methods have limitations and more work to incorporate them with the MRI tracking of coated capsules remains to be done.

1 Introduction

This chapter will first introduce the gastrointestinal (GI) tract and the challenges of delivering drugs to the lower GI tract. It will then set the scene of imaging studies of drug delivery to the lower GI tract leading to the aims and hypothesis of this work.

1.1 The gastrointestinal tract

The GI tract comprises the main organs for digestion. It has a tubular structure and a multifunctional role such as food reception and accommodation, propulsive movement of its contents, mechanical and chemical breakdown of food, absorption of water, electrolytes, vitamins and nutrients, and it is also responsible for waste elimination [1-3]. In addition, it constitutes a barrier and regulates the microbiota [3, 4].

The GI tract is divided into a proximal or upper part (mouth, oesophagus, stomach, duodenum, jejunum) and a more distal or lower part (ileum, caecum, colon, rectum and anus). Organs complementary to food processing in the GI tract are the salivary glands, pancreas, liver and gallbladder (Figure 1.1).

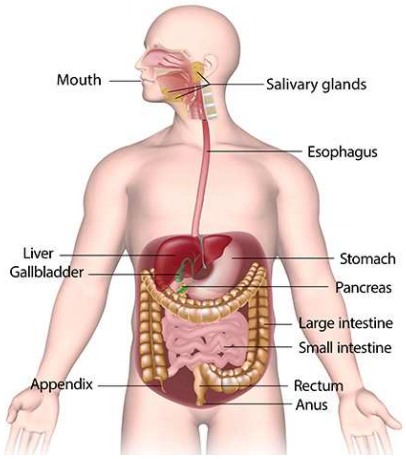

Figure 1.1. The human GI tract. Taken from [5]**.**

The walls of the GI tract comprise many layers which are the mucosa (absorption and secretion function), the submucosa (which includes nerves, lymphatics and the connective system), the smooth muscle (longitudinal and circular muscle) and the outer serosal layer as depicted below (Figure 1.2) [3].

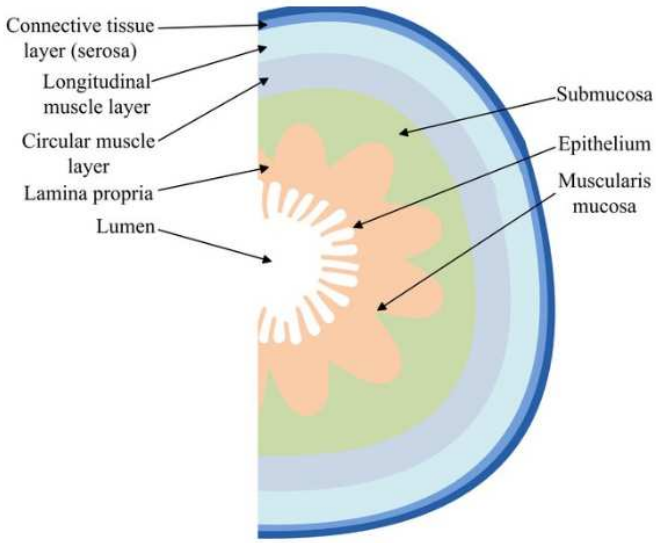

Figure 1.2. Transverse cut of the layers of human GI tract. Taken from [6]**.**

Intake of food happens via the mouth and oesophagus which have limited volume capacity and mucosa surface. The stomach acts as a reservoir having a larger and adaptive volume capacity but limited mucosa surface. On the other hand, the small intestine is the organ responsible for much of the intraluminal and mucosal-associated digestion and absorption. It therefore has the largest mucosal surface area (around 30 m^2) compared to other whole organs and compared to its overall volume. Lastly, the large intestine is a reservoir organ because of its large volume capacity and a smaller surface area (around 2 m^2). The surface of the mucosa of the digestive tract equals approximately half the size of a badminton court (32 m^2) [1]. When the digesta passes the ileo-caecal valve and arrives in the colon, it is considered as faeces and is gradually propelled to the rectum and anal canal [3]. The daily GI fluid flux is of the order of 9 L and this juice contains digestive enzymes, mucus, ions, water and bile [3].

The pH is very acidic in the fasted stomach due to hydrogen ion secretion. The stomach pH becomes higher in the fed state but returns in its acidic state 1 hour later (pH = 1.5-3.5). The luminal pH then becomes progressively alkaline in the distal GI. It is alkaline in the small intestine mainly because of the buffering bicarbonate anions in the alkaline fluid from the pancreas and bile secretions (pH = 5-7). Fermentation in the lower intestine also increases pH values (pH = 5.5-7) [7]. The presence of absence of nutrients in the GI tract is a major driver of the pH values throughout the GI tract.

1.2 Gastrointestinal characteristics related to drug absorption processes

The luminal pH values are in turn a key determinant of the fate of ionisable drugs. Solubility and dissolution of ionisable drugs are highly favourable in their ionized state. Lipophilic drugs are subject of passive membrane absorption when they are unionized [7].

Different uptake mechanisms, with different substrate characteristics, exist throughout the GI tract. Passive diffusion requires the molecule to be lipophilic while active transport requires the molecule to be substrate for a protein-carrier (the latter is regulated by its interaction with the lipids and the membrane fluidity). Membrane fluidity also regulates the absorption of large molecules. The lipid (phospholipids, glycolipids, cholesterol and free fatty acids) structure of the brush border and the basolateral membranes of the enterocyte determine whether and how (passive, active, facilitated and endocytosis/pinocytosis) nutrients and drugs are absorbed [7].

Understanding GI parameters such as fluid content and distribution, motility, transit and flow is crucial for the effective design and performance of oral drug formulations. Our knowledge of the upper GI characteristics has grown profoundly. More specifically, the small bowel has been studied extensively as it is the main GI site of interest for oral drug absorption [8, 9]. However, the importance of drug performance in the lower intestine (terminal ileum, caecum and colon) has lagged behind and its relevance has only recently been

recognised under specific circumstances, drawing increasing scientific interest [9].

1.3 Physiology and function of the small and large bowel

1.3.1 Anatomy and function of the small bowel

Anatomically the small bowel begins at the pylorus and consists of 3 parts: the duodenum, jejunum and ileum and has a length of 6 – 7 m. Its main function is to be the main site for systemic absorption (primarily in the duodenum and proximal jejunum) and it's also responsible for the absorption of lipids, fat-soluble vitamins, electrolytes, food components and water. Secretion of acid, bile and digestive enzymes occurs in the small bowel too [10].

In-between meals and under GI fasting conditions, there is a regular behaviour of contractility in the upper GI tract named as the ''migrating motor complex'' or MMC [10, 11]. It has typical electrical characteristics and it travels through the entire small intestine. The MMC is established as the intestinal housekeeper of the GI tract and its dysregulation may lead to eating disorders [11]. The MMC has a role in the promotion of the gastric products and in the regulation of the topical bacterial presence [10].

The MMC is a recurrent motility event that requires a total of 1.5 – 2 h to travel from the stomach to the most distal part of the small intestine. The onset of food consumption overrides the start of the MMC activity and the

propulsion of food components to the small bowel is a hinder of the MMC in the whole small intestine [10, 12]. The MMC's onset occurs 2 – 3 h after food digestion and absorption have been completed.

The MMC is commonly divided in Phases I-IV. Phase I is associated with the absence of contractions, Phase II has random activity of contractions, Phase III has an abrupt start of contractions and an end of a burst of movement with the highest amplitude and time and Phase IV follows with a sudden reduction of contractions [10, 12, 13].

It has been reported that Phase III spontaneously starts from the stomach (70%) but it can also be initiated from the proximal duodenum (18%), the distal duodenum (10%), and the proximal jejunum (1%). Phase I will start once Phase III is over until is interrupted by meal consumption [14]. Phase III: contractions last for approximately 7 min and have an average duodenal amplitude of 30 mmHg. Its propagating velocity reduces from 11.4 cm/min in the proximal duodenum to 7.4 cm/min in the distal duodenum. Because of the rapid activity of Phase III and its absence in Phase I, absorption of nutrients and drugs is more likely to happen during Phase I [10].

Food, enteric nervous system and gut hormones such as motilin regulate the presence or absence of the MMC. Increased presence of motilin initiates Phase III contractions. Food consumption created a different contraction activity which permits a bigger contact time with the mucus and therefore transit is being prolonged and absorption is favoured [10].

1.3.2 Anatomy and function of the large intestine

As depicted in Figure 1.3, the large intestine consists of 5 parts (caecum, ascending colon, transverse colon, descending and sigmoid colon) which comprise many sacculations and haustra [1]. Villi are absent in the colon lumen and microvilli are less abundant [7].

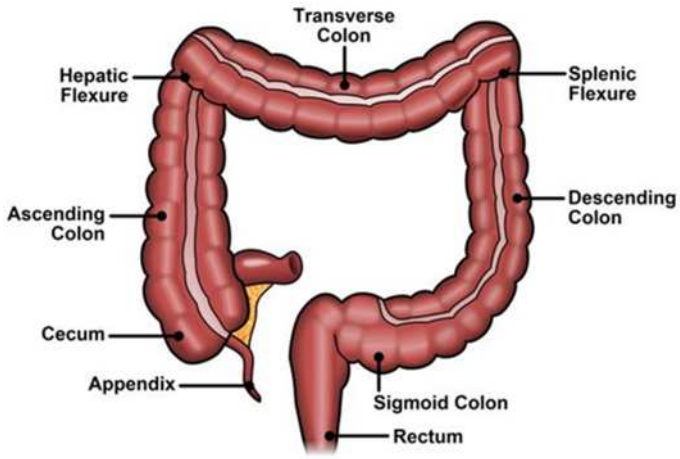

Figure 1.3. Anatomy of the large intestine. Taken from [15]**.**

The large intestine absorbs mainly water, sodium (Na+) and other minerals and it is a natural host of the majority of the human microbiota. Another role of the large intestine is the production and absorption of fatty acids [7]. The large intestine is also responsible for transforming the chyme into faeces (solidification) and faeces accommodation [3]. Well organised switching of smooth muscle between contraction and relaxation results in propagating and non-propagating (mixing) movements of the intestinal contents. The presence of food does not affect the continuity of all intestinal contractions [2]. Molecules that treat immunological diseases (e.g. IBD and rheumatoid arthritis) could potentially affect the balance of intestinal physiology and

functionality. For instance, they could cause diarrhoea or colitis as adverse effects [2].

Precise determination of the intestinal dimensions (mucosal and villous surface, microvilli, length and diameter) is challenging because the gut has a dynamic character and its anatomy can vary due to inter- and intra-subject variability and study conditions. Factors that can determine gut characteristics are also diet and microbiota [1]. Colonic length and diameter have been estimated to be between 90-190 cm and 4.1-4.8 cm respectively, using different methods of investigation (laparotomy, computed tomographic colonography and double contrast barium enema) and patient conditions (abdominal disease or asymptomatic, prepared bowel, post-mortem measurements) [1-7].

1.3.3 Colonic motility

Intestinal motility has been traditionally studied using manometric catheters and more recently fibre-optic catheters [16-21]. The application of high-resolution fibre-optic manometry in the investigation of colon motility in 10 healthy volunteers in the fasted and the fed state has been able to identify 4 types of propagation patterns in the colon. More specifically, propagating activity consists of cyclic motor patterns (at 2-6/min), short single motor patterns, long single motor patterns and slow, erratic retrograde movement. The effect of food administration created another type of movement called high-amplitude propagating sequences (HAPS) with the simultaneous increase of retrograde cyclic activity [22].

Recently, colonic motility was investigated and correlated with anal motility. 17 healthy volunteers and 10 patients with delayed colonic transit were recruited and underwent colonoscopy during which high-resolution manometry was applied. This work reported pressure increase in amplitude and time in all colonic sensors when the anal sphincter was relaxed. This motor pattern was named ‘’pan-colonic pressurizations”, occurred mainly after meal consumption, created urges for gas evacuation and their incidence was less likely in patients [23].

Regulators of colon motility are the Enteric Nervous System (ENS) which consists of motor neurons, interneurons and intrinsic sensory neurons, the autonomic nervous system, the Interstitial Cells of Cajal (ICC), hormones and proteins/peptides. The colon self-regulates its motility but is also affected by external factors too (e.g. neurons, proteins, hormones) [2]. Processes of mixing and propagation are results of: 1) rhythmic propulsive ripples (RPRs)/phasic contractions which derive from the ICC, are slow and mixing, 2) tonic contractions and 3) ultra-propulsive (peristaltic) contractions or else rhythmic propulsive motor complexes (RPMCs)/colonic migrating motor complexes/ giant migrating complexes. The RPRs is mainly for mixing and less for propagation [2].

Intestinal motility is affected by xenobiotics, drugs and human diseases and affect mostly the RPMCs which when slow they lead to higher water uptake and dry faeces, constipation and abdominal discomfort whereas when quick they lead to diarrhoea. Inter-individual and intra-individual variability can also

affect the residence times in each segment of the colon, which in turn could influence drug bioavailability. The main intestinal neurotransmitter is acetylcholine (Ach) which causes contractions, substance P and neurokinin A. Inhibition is primarily caused by nitric oxide (NO), vasoactive intestinal peptide, gamma amino butyric acid (GABA), adenosine triphosphate (ATP) and prostaglandins (PGs) [2].

1.3.4 Colonic chyme and fluid

The study of chyme characteristics and of water volumes in the colonic region is difficult. This organ is poorly accessible in the physiological unprepared state but water distribution is a key determinant for oral drug absorption. Since standard MRI images are based on water hydrogen proton imaging, MRI could provide unique insights in the colonic undisturbed physiological chyme and fluid state. MRI sequences typically used for cholangiopancreatography studies collect high signal from freely mobile fluids, which have long transverse relaxation time T2. These MRI sequences are ideal to identify pockets of fluid in the body though signal from less fluid ('thick') components such as mucous which is lost (Figure 1.4).

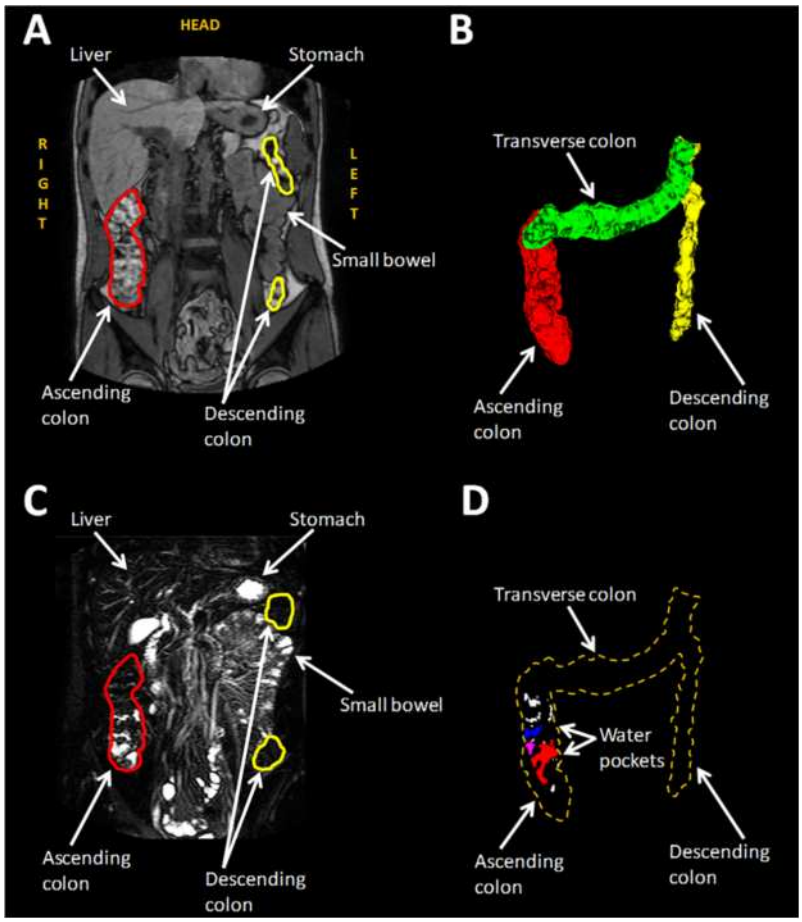

Figure 1.4. (A) MRI bowel image. (B) 3-D reconstruction of the bowel. Red, green and yellow stand for ascending, transverse and descending colon respectively. (C) Highly T2 weighted image with the same angle of (A). Unbound liquid appears white whereas bound and less mobile liquid seem darker. (D) Unbound liquid of the colon. Taken from (37).

There are a few pivotal scientific articles in the literature and these are mentioned below (Table 1.1).

Table 1.1. Investigation of fluid volumes in the large intestine.

Reference	Aims	Methods	Outcomes
Schiller et al., [24]	Estimation of intestinal water distribution	12 healthy subjects consumed non-disintegrating capsules on fasted and fed conditions	Food ingestion had minimum effect on colonic water volumes but increased the number of colonic pockets ($p < 0.005$). Fasting inter-subject variability of colonic volumes was high (1-44 ml) and water pockets were mainly located in the caecum, AC and DC with total capacity of (median) 2 ml. Variability remained high after the meal consumption too (2-97 ml) which increased the number of water pockets ($p < 0.005$) but did not affect their volume capacity [(mean) 1 ml]
Placidi et al., [25]	Estimation of freely mobile water content	18 healthy subjects ingested mannitol (secretory diarrhoea model) and capsules of placebo or loperamide or loperamide and simethicone	Placebo arm increased water distribution in the AC 45 min following the mannitol ingestion. At 0-135 min, the two active interventions reduced the AC water distribution ($p < 0.004$). At 135-270 min, placebo behaved the same way as loperamide whereas, loperamide combined with simethicone decreased the ascending colon water. MRI images of the placebo administration showed that the presence of water in the ascending colon was similar to loperamide with or without simethicone administration.
Marciani et al., [26]	Effect of PEG electrolyte ingestion on colonic expansion	12 healthy volunteers ingested 2 L or 1 L twice of PEG electrolyte	The 2 L solution exerted a greater increase on the total volume of the large intestine than the split dose, $p = 0.0332$. The formulation affected mostly the AC and the TC rather than the DC.

Reference	Aims	Methods	Outcomes
Pritchard et al., [27]	Estimation of the gut segmental liquid presence in IBS-D patients and healthy volunteers	25 IBS-D patients and 75 healthy subjects were scanned in the fasted and fed (rice pudding) state	Fasted segmental volume in both groups was similar. In the healthy group, feeding caused higher ileo-colonic activity and 10 % expansion of the AC content whereas the last parts of the meal induced a smaller expansion in the same region. In the IBS-D patients, feeding resulted in a smaller increase of the AC volume and later a greater TC one.
Pritchard et al., [28]	Gut water quantification	IV administration of CRH and cold water hand immersion on the intestinal environment of 18 healthy volunteers divided in two groups (saline and CRH injection)	CRH injection expanded the intestinal water presence, $p = 0.002$. Comparison of ice water immersion to warm water immersion revealed no differences, $p = 0.730$. The consumption of the meal did not increase significantly the ascending colon water volume on CRH injection. On saline injection, warm and ice immersion increased water volume significantly. TC water volumes were only significantly affected (decreased) only on water immersion ($p = 0.0107$). Water distribution in the descending colon was unaffected in any case.
Sandberg et al., [29]	Assessment of regional colonic water	4 healthy subjects	Median (IQR) of total colon volume was 819 ml (687-898.5). Regarding each segment, the volume of the AC was determined as 200 ml (169.5-260), TC as 200.5 ml (113.5-242.5), DC as 148 ml (121.5-178.5) and SC-rectum as 277 ml (192-345).
Coletta et al., [30]	Effect of gluten on colonic	12 healthy subjects	Fasted total colonic volume on a GFB diet was (mean ± SEM) 748 ± 258 ml, on NGCB 659 ± 291 ml and on AGCB 576 ± 252 ml. Segmental respective volumes were estimated as following: AC

Reference	Aims	Methods	Outcomes
	volume and gas		250 ± 119 ml, 256 ± 149 ml, 224 ± 128 ml, TC 289 ± 95 ml, 212 ± 73 ml, 178 ± 86 ml and DC 209 ± 73 ml, 187 ± 92 ml, 172 ± 77 ml. Statistical differences were only detected in the case of the volume of the transverse colon which was higher after the GFB diet compared to NGCB and AGCB diets ($p = 0.02$).
Lam et al., [31]	Effect of a laxative PEG electrolyte formulation on gut volumes	24 patients with functional constipation and 24 with IBS-C	The volumes of the ascending colon 120 min after the PEG electrolyte ingestion which were 597 (170) mL and 389 (169) mL respectively ($p < 0.01$) and the total large intestinal volumes 1505 (387) mL and 1039 (418) mL respectively ($p < 0.01$) at the same time.
Wilkinson-Smith et al., [32]	Effect of consuming glucose, fructose and inulin on intestinal water volumes	29 healthy volunteers and 29 IBS patients	Intestinal volume was primarily affected by fructose and inulin rather than glucose in both groups.
Murray et al., [33]	Timeline of total and segmental unbound water in terms	12 healthy volunteers on the administration of 240 mL of water (the first team to	The number of bound colonic water pockets water in the fasted state were 11 ± 5 and each of them contained approximately 2 ± 1 mL in total. 30 min after the water ingestion the colonic liquid reached the peak of 7 ± 4 mL divided in 17 ± 7 pockets. By time, the number of the liquid pockets and their volumes decreased but, one hour later, only the

Reference	Aims	Methods	Outcomes
	of volume and number of liquid pockets in the large intestine	conduct this kind of study)	amount of the colonic pockets peaked again (17 ± 7) while their volumes remained in lower levels (3-4 mL). The main site of the freely liquid was the ascending colon.
Major et al., [34]	Regional and total bowel water in healthy and constipated volunteers	9 healthy subjects and 20 constipated patients on maltodextrin (placebo), 10.5 g and 21 g of psyllium	In both groups, in the fasting state colonic volumes were risen on the psyllium arm ($p < 0.05$). Segmentally, significant differences occurred while on the placebo arm in the colonic volumes of the fasted state between patients and healthy subjects ($p < 0.05$) mainly because of higher volumes in the AC and the TC.
Sloan et al., [35]	Effect of FODMAP diet with the co-administration of either oligofructose or maltodextrin on intestinal water with MRI	37 healthy volunteers	Both oligofructose and maltodextrin exerted a positive effect on the intestinal volume. When it comes to segmental colonic volumes only oligofructose was capable to rise the volumes' values in the ascending, transverse and distal colon. There was no significant difference between the two substances.

Reference	Aims	Methods	Outcomes
Wilkinson-Smith et al., [36]	The role of foods in modulating gut water content	15 subjects and either a bread meal, a rhubarb meal or a lettuce meal	The bread meal created an AUC [mean (SEM)] of 78 (43) mL whereas the rhubarb and the lettuce meal created a much higher rise of 291 (89) mL ($p < 0.01$ Wilcoxon) and 409 (231) mL respectively

Abbreviations: AC: ascending colon; AUC: area under the curve; AGCB: added gluten content bread; CRH: corticotrophin releasing hormone; DC: descending colon; FODMAP: fermentable oligosaccharides, disaccharides, monosaccharides and polyols; GFB: gluten-free bread; IV: intravenous; IBS: Irritable Bowel Syndrome; IQR: interquartile range; IBS-C: Irritable Bowel Syndrome with constipation; IBS-D: Irritable Bowel Syndrome with diarrhoea; MRI: Magnetic Resonance Imaging; NGCB: normal gluten content bread; PEG: Polyethylene glycol; SEM: Standard Error of the Mean; TC: transverse colon.

1.3.5 Colon transit and luminal flow

The fate of meals in the GI tract is determined by the various GI processes (e.g. motility, transit and flow) and physiology. Oral drug formulations are subject to the same GI processes as meals and in combination with the food presence or absence their efficacy assessment is not always straightforward and reproducible [37].

The transit time of the oral dosage form exert a significant role on its efficacy [38]. Modified release oral formulations and colon-targeted drugs have to release their active substance in the colon. It is reasonable to expect that changes in the transit and flow patterns may affect drug release [39-41]. MRI has been increasingly used to study the transit times. Key articles found reviewing the literature, are summarised in Table 1.2. Pritchard et al. evaluated the application of the novel MRI technique of tagging to study the ascending colonic flow in 11 healthy and 11 constipated volunteers on macrocol administration. Briefly, the method of tagging is the application of tag lines on the MRI images. Tag lines are dark stripes and the observation of how and if they shift (blurring of the tags) correlates positively with flow motion through the average coefficient of variation (%COV). The %COV indicates movement and mixing events. Analysis of the baseline revealed weak flow procedures regardless volunteer group [healthy 20% (14-23) [median (interquartile range, IQR), constipated 12% (11-20), p = 0.1). Sixty min after macrogol administration, dislocation of the tags could be observed mainly in the healthy group [30% (26-35), p = 0.002, Wilcoxon test] rather than the constipated one [17% (13-230, p = 0.57].

Table 1.2. Location and transit of contents relating to the large intestine with various MRI techniques.

Reference	Aims	Methods	Outcomes
Schiller et al., [24]	Assessment of the intestinal transit by MRI	12 healthy volunteers were scanned in fasted and fed state and after consumption of gel-filled capsules	Location of the capsules was affected by food consumption (in the large intestine: fasted vs fed state was 3 vs 17 capsules respectively, $p < 0.01$)
Buhmann et al., [42]	Assessment of new MRI technique of estimating intestinal transit with per os capsules containing gadolinium-saline solution	7 females and 8 males (all healthy) consumed 5 capsules	Mean transit time for female and male volunteers was 41 ± 9 h and 31 ± 10 h respectively
Hahn et al.,[43]	Application of ^{19}F and ^{1}H MRI on intestinal transit	2 healthy subjects consumed perfluoro-[15]-crown-5-ether capsules: 1 each on scanning day 1 and 2 each on scanning day 2	Single capsule tracking: total transit lasted 27 h and 32 h for subjects A and B respectively (mean capsule velocity was 1.0 mm/s and 1.0 mm/s respectively). Capsule found outside the stomach 170 min and 220 min respectively
Chaddock et al.,[44]	Validate MRI technique towards OCTT and WGT measurements	21 healthy subjects OCTT estimated by the arrival of the head of the meal into the beginning of the large bowel with MRI and by LUBT	MRI measurement of OCTT was [median(IQR)] 225 (180-270) min and of WGT was 28 (4-50) h

Reference	Aims	Methods	Outcomes
Marciani et al.,[26]	Investigation of the effect of oral PEG electrolyte in two dosing regimens on colonic motility	12 healthy subjects consumed the split dose (1L before the first scanning day and 1L on the scanning day) and the other 12 healthy volunteers the single dose (2L on the first scanning day) Each volunteer ingested MRI marker pills the day before the MRI transit scan (days 8,14,28)	No differences due to dosing regimens based on mean position score of split vs single dose at Day 8, p = 0.2527; Day 14, p = 0.6076; Day 28, p = 0.3327. No differences between the days regardless dosing: Day 8 vs 14: p = 0.7750 Day 8 vs 28: p = 0.2350
Savarino et al., [45]	Evaluation of MRI techniques of OCTT assessment towards LHBT in healthy volunteers	28 healthy volunteers were recruited OCTT was assessed by the arrival of the head of the lactulose ingestion (10g/125mL)	OCTT by MRI measurements was [median (IQR)] 135 (120-150)min
Lam et al., [31]	MRI investigation of the effect of PEG electrolyte as a laxative on the colonic environment	24 patients with functional constipation and 24 with IBS-C participated in this study. They has to consume 5 MRI marker pills before the scanning day and 1L of PEG electrolyte after the baseline scan on the study day	WAPS for FC [3.6 (2.5-4.2)] was higher than the IBS-C [2.0 (1.5-3.2)], p = 0.01

Reference	Aims	Methods	Outcomes
Lam et al., [46]	Distinguish subgroups of IBS based on MRI markers	91 volunteers took part (34 healthy, 30 with IBS-D, 16 with IBS-C and 11 IBS-M as mixed. IBS-M and IBS-D were listed as IBS-nonC)	WGT for IBS-C, healthy volunteers and IBS-D was 69 (51-111) h, 34 (4-63) h and 34 (17-78) h respectively and OCTT was 203 (154-266) min, 188 (135-262) min and 165 (116-244) min respectively
Pritchard et al., [47]	Study the ascending colonic transit in healthy and constipated subjects	11 healthy and 11 constipated subjects were scanned fasted and after ingestion of 500 mL of macrogol and consumption MR markers	WAPS between healthy and patients was [median (IQR)] 0.6 (0-1) and 2.6 (1.4-3.6) respectively, $p = 0.0011$
Zhi et al., [48]	Evaluation of the applicability of gadolinium filled MRI capsules towards ROMs on CTT	7 constipated and 9 healthy subjects ingested 5 gadolinium-based capsules as MRI markers and 20 ROMs[5]	MRI measurements revealed that CTTs in healthy and constipated were 30.9 ± 15.9 h and 74.1 ± 7.2 h respectively, $p < 0.05$ Patients had higher CTTs than the healthy ones
Khalaf et al., [49]	Establishment of an MRI technique for bowel motion and transit assessment	Baseline and fed state MRI scanning of 15 healthy subjects Meal: chicken or mushroom soup Each subject consumed 5 MRI capsules of Gadoteric acid the day before the study day	WAPS (24h) = 1.0 (0-3.8) WGT (hours) = 33 hr

Reference	Aims	Methods	Outcomes
Major et al., [34]	Evaluation of psyllium consumption on colonic environment of healthy and constipated volunteers	9 healthy subjects received maltodextrin (placebo) and psyllium 10.5 g and 21 g for 6 days randomly and 20 constipated subjects ingested maltodextrin and 21 g of psyllium in the same way On treatment day 5, each volunteer ingested 5 MRI marker capsules with Gadoteric acid	WGT was higher in healthy than patients ($p < 0.05$) Controls: WAPS24 showed no differences as [median (IQR)] it was 1.0 (0.1-2.2) on maltodextrin, 1.4 (0.2-2.1) on 10.5 g of psyllium and 0.6 (0-1.9) on 21 g of psyllium Patients decreased from 4.2 (3.2-5.3) on maltodextrin to 2.0 (1.5-4.0) on psyllium ($p = 0.067$)
Wilkinson-Smith et al., [32]	Evaluation of intestinal volumes and function on kiwifruit consumption	2 kiwifruits or maltodextrin (control) 2 times per day for 3 days in the fasted and fed state	WGT for kiwifruit was [median (IQR)] 0.8 (0-1.4) and for control 1.0 (0.5-3.1), $p = 0.11$

Abbreviations: ^{1}H: Hydrogen-1; ^{19}F: Fluorine-19; CTT: colon transit times; FC: functional constipation; IQR: interquartile range; IBS-C: Irritable Bowel Syndrome with constipation; IBS-D: Irritable Bowel Syndrome with diarrhoea; IBS-M: Irritable Bowel Syndrome with alternating constipation and diarrhoea; LHBT: lactulose hydrogen breath test; LUBT: lactose ureide breath test; MRI: Magnetic Resonance Imaging; OCTT: oro-caecal transit time; PEG: polyethylene glycol; ROMs: radio-opaque markers; WAPS: median average weighted position score; WGT: whole gut transit.

This dislocation was characterized as forward and backward and took place at the same time and region of the ascending colon (central). Moreover, there was a fast (> 4.8 cm) retrograde central “jet’’ and a decrease in the tag intensity as well. Results from all the scans allowed the observation of higher central motion in the ascending colon rather than peripheral/membrane motion which was weaker but still detectable at t = 120 min mainly in the healthy large intestine [25% (18-360), p = 0.002] and not so much in the constipated large intestine [13% (12-180), p = 0.76]. The researchers concluded that there were significant differences in the coefficient of variation (%COV) and, therefore, in the movement events in each time point between the two conditions [60 min (p = 0.0020), 120 min (p = 0.003), Mann-Whitney rank sum test] [47].

1.4 Drug Delivery to the lower GI tract

The oral route is considered the prevalent administration route of drug formulations [1, 8, 50]. Conditions such as the acidic environment of the stomach, the proteolytic and enzymic activity in the small intestine, the need of administration of macromolecules and vaccinations, the higher efficacy of absorption enhancers in the lower intestine and local pathological conditions introduce the need to control the drug absorption site and target the lower parts of the GI tract with modified release formulations [51-56].

The aim of the CR formulations is to regulate the absorption rate, the plasma concentration and the pharmacodynamics of the integrated drug [57]. CR

drug delivery is applied not only through the oral route, which is the most convenient, but through other routes too e.g. rectal administration [54].

The large bowel is of great importance for oral drug administration under specific circumstances. Specifically, in the cases where the drug has limited solubility or permeability in the small bowel and the colonic environment favours these processes then this is a good candidate for colonic drug delivery. [9].

The advantages of colon-targeted formulations (modified or delayed) compared to the immediate release formulations, are that they can be used not only for colon-related disorders such as Inflammatory Bowel Disease (IBD) which is Crohn's disease and Ulcerative Colitis (UC) but can also achieve unmet therapeutic goals such as oral administration of macromolecules. Due to their prolonged activity they reduce dose frequency when drugs are quickly eliminated and so they increase patient compliance. Their effects last longer but at the same time the side effects are lighter because of the controlled high plasma concentration [57, 58]. The colon may also be suitable for protein and peptide absorption because of the weak proteolytic and enzymic activity and the high residence times. The large intestine is also very favourable for absorption enhancers [54, 58]. Insulin, calcitonin and vasopressin could be suitable for colonic absorption [58].

A drug has to be dissolved in order to be carried in the blood (absorption) and therefore dissolution is crucial for drug delivery [39, 59]. Even though solubility and permeability remain the key points, different physiological,

physicochemical and biopharmaceutical conditions in the colon require colon-specific approaches [56, 57, 60]. The physiological factors that mainly affect dissolution and absorption derive from the composition either from the GI fluid or the intestinal membrane and are listed in Table 1.3. Drug properties as solubility, pKa, diffusion coefficient, particle size and dose are equally important to dissolution and absorption [39, 56].

Table 1.3. Factors affecting dissolution and absorption.

Composition of the GI fluid	pH, buffer capacity, osmolality, surface tension, viscosity, temperature (through diffusion, drug solubility and bulk drug concentration), volume liquid, hydrodynamics, gastric-emptying rate and forces, intestinal transit time and flow rate
Composition of the intestinal membrane	Surface area, shear rate, nature of intestinal membrane and absorption mechanisms: concentration gradient, electrochemical potential difference, and hydrostatic pressure gradient between the lumen and the membrane, physical barrier of the intestinal mucosa, metabolizing enzymes and efflux transporters.

The colon is characterised by a smaller surface and tighter junctions than the small intestine, which does not favour passive permeability. Reduced potential of passive permeability and reduced expression of transporters lead to an overall limited permeability [57]. The colon absorbs water to a great extent and therefore its contents are viscous and cannot be mixed thoroughly [54]. Furthermore, the large intestine has irregular motility and absence of bile salts which all affect negatively drug solubility [54, 57]. The bacteria and

the expression of cytochrome P450 (CYP450) and phase II enzymes can also affect drug bioavailability. All these factors make CR design very challenging [56, 57].

Colon-targeted formulations should be designed to remain intact through their transit in the GI tract and to be triggered exclusively by elements of colonic physiology in order to release the drug timely in the colon. Enzymatic activity, motility and fluids decrease alongside the GI whereas pH gradually increases. These physiological changes are not sharp and therefore cannot serve as clear triggering mechanisms. On the contrary, the dramatic microbiota change (in number and nature,- mostly anaerobic) in the colon has been exploited for drug delivery purposes [58].

The most popular site-specific formulations are presented in Table 1.4 and are based mostly on pH and microbiota changes but prodrugs and time-dependent systems are also used [58].

The first drug designed for colon-targeted delivery was sulfasalazine for the treatment of IBD which served as a prodrug [56]. Sulfasalazine is metabolised by colonic microbiota into 5-aminosalicylic acid (also known as 5-ASA, mesalamine, mesalazine) which is the therapeutic moiety and sulphapyridine which is associated with side effects [61-63]. Due to the associated side effects, more prodrugs of 5-aminosalicylic acid were developed [64, 65].

Drug behaviour in the GI tract is regulated by complex and constantly changing conditions and differs significantly due to inter- and intra-subject variability. Despite the progress in the design and formulation of modified

release drugs, it remains a challenge to prove that their promised efficacy can be achieved [8]. Therefore, there is a need for better biorelevant *in vitro* tools for the early selection and screening of potential CR candidates. Current animal models as well as *in vitro* and *in silico* biorelevant models predict inadequately drug bioavailability because there are still “uncharted waters” in the field of drug absorption in the GI tract [43, 66, 67]. Nowadays, Caco-2 cell lines and regional in situ rat perfusion are mostly for permeability assessment. For solubility, *in vitro* models based on pH simulation are currently used but their design has not taken into account unique characteristics of colonic physiology (volumes, elements and hydrodynamics) [57].

Table 1.4. Colon-targeted formulations**.**

Type of approach	Type of formulation	Onset of action	Comments
Traditional	Prodrugs	Microbial enzymes break the drug into 2 molecules (active substance and carrier) mainly through hydrolysis or reduction	Most commonly used in IBD
	pH-dependent	Polymers that correspond to pH changes alongside the GI tract (become soluble only in high pH values that exist only in the colon)	Its success is subject to inter-/intra- subject variability and similar pH values in the lower small intestine and the colon
	Time-dependent	Formulation is programmed to release the drug in the colonic area	Its success is subject to transit time and motility variability
	Microflora-activated	Drug release happens after non-starch polysaccharides being metabolized by colonic microflora	High exclusivity but time-consuming (over 12 hours)
Modern	Intestinal pressure-controlled colon delivery capsules (PCDCs)	High colonic peristalsis creates high luminal pressure leading to drug release	Water-resistant polymer e.g. ethylcellulose, density and capsule size are crucial

	CODES^{TM} technology	Double system: 1) polysaccharides substrates only for colonic bacteria, 2) pH-sensitive coating	Consistent and reliable
	Applying pectin and galactomannan coating	Traditional oral formulations coated with pectin and galactomannan, each not soluble in the colon	The solubility of their mixture is subject to the pH of the coating solution
	Azo hydrogels	pH-sensitive molecules and azo-cross bonds in a hydrogel formulation which swell as the pH rises. When pH = 7.4 swelling is maximum and cross bonds are degraded colonic enzymes	Swelling properties can be further monitored by adding hydrolysable elements in the hydrogel
	Osmotic Controlled	Single or multiple osmotic parts in a hard gelatine capsule	Can deliver drugs for 4 up to 24 h

Abbreviations: GI: gastrointestinal tract; IBD: Inflammatory bowel disease; PCDCs: Intestinal pressure-controlled colon delivery capsules.

At the moment, there is area of improving the relevance of the *in silico* models for colonic drug absorption evaluation [40, 41]. Overall, the current methodologies are considered as simpler to the real conditions due to lack of biorelevant knowledge which is usually acquired via capsule techniques, intubation and colonoscopy studies [57].

1.5 Imaging the bowel to study to drug delivery to the lower GI

There is a growing need for the *in vivo* investigation of colon-targeted formulations under physiological and undisturbed conditions that represent the real-life administration schemes [40, 56]. Throughout the years, gamma scintigraphy has been predominantly applied for this investigation and, only lately, MRI has been introduced in the field [24, 68-71]. In these studies, the various manufacturing techniques for targeting the lower intestine include single and multi-pellet systems, radiolabelled solids and resins, non-disintegrating capsules and non-disintegrating capsules.

1.5.1 Pellet systems in combination with disintegrating capsules

The influence of multiple-sized radiolabelled formulations on intestinal transit on a lactulose-induced catharsis was studied. Either 100 mg of ^{111}In-labelled 0.2 mm ion-exchange resin particles or 2 enteric coated ^{99m}Tc-labelled 5 mm/8.4 mm non-disintegrating tablets were encapsulated into 000-sized hard gelatin capsules. On the study day, 3 such capsules were administered to 12

healthy volunteers. Catharsis was induced by the administration of a lactulose solution. Lactulose did not affect significantly the overall residual in the colon after 24 h but for the ascending colon residual, this was significantly less by 50%. In conclusion, the non-lactulose co-administration of the particles with either the 5 mm or 8.4 mm tablets, the mean ascending residence time was 11.0 ± 4.0 h suggesting that the ascending colon would be a good candidate for sustained topical or systemic absorption. Under no pathophysiological circumstances, there is no significant difference in the range of 0.2 - 8.4 mm sizes for transit through the ascending colon but lactulose co-administration may cause a separation in the movement of the two sizes. The non-significant difference in transit but the significant difference in the dispersion of multiparticulates in the colon could be useful for the investigation of widespread disease of the area and for delivery of the systemic drugs that need contact with the mucosa, elsewhere less feasible because of the viscous faecal material [72].

The difference in the GI movement between single unit formulations (tablets) of multiple sizes (3 mm, 6 mm, 9 mm and 12 mm) was investigated. For this study, 8 healthy volunteers went under a specific dietary regimen of 28 g of fibre per day. There were 3 study days in total and on each day, each volunteer consumed 5 control tablets (6 mm diameter) radiolabelled with ^{111}In and 5 ^{99m}Tc-radiolabelled tablets sized of either 3, 9 or 12 mm diameter and coated with ethylcellulose. The tablets were consumed on the fasted state and a large intra- and inter-subject variability on GE times was detected.

It is likely that GE took place during the phase III of the MMC. The size of tablets had no effect on GE and no pattern in GE was spotted. No significant differences were observed on the small intestinal transit (SIT) based on tablet sizes. A regrouping of the formulations at the ileo-caecal junction (ICJ) occurred where they stayed 0-99 min. The time spend at the ICJ depended on whether the tablets reached the region before lunch (smaller time spent at the ICJ). Motility at the terminal ileum was small and erratic when on the fasted state but was provoked through the ‘’gastro-colonic response’’ when food was consumed. Tablets entered the large intestine as a bolus and it was concluded that tablet size in the range of 3-12 mm does not affect movement until and through the ICJ. The 3 mm and 6 mm tablets remained at the ascending colon the longest, and bigger sizes left the ascending colon the quickest but differences in the size were more prominent after the exit from the ascending colon. The most apparent difference was spotted between tablet sizes of 6 mm and 9 mm that differ significantly in diameter and depth whereas 9 and 12 only differ in diameter and not depth for swallowing reasons. This led to the observation that tablet volume is equally significant as tablet diameter. Total oro-caecal transit time was unaffected by tablet diameter. Tablets arrived at the colon as a bolus but the 3 mm and 6 mm tablets stayed at the ascending colon for the longest indicating that they could be good candidates for targeting drug delivery at the ascending colon. Tablet movement does not depend only on the tablet diameter but on their volume as well [73].

The research of the possible differences of the gastrointestinal passage of a multiple and single-unit formulation was conducted. The multiple-unit formulation contained 95 mg metoprolol CR/ZOC (Seloken ZOC®, Toprolol XL®, prolonged-release for a time period of 20 h). The second objective of the study was the plasma quantification of metoprolol in correlation with pellet localisation applying gamma scintigraphy techniques. The radiolabelling of the pellets happened with ^{51}Cr and the tablets with ^{99m}Tc. 8 healthy volunteers were co-administered these two formulations alongside with breakfast. For the pellets, the mean gastric emptying and small bowel transit time was similar. The only significant difference was for the GE time. In the large intestine, the pellets spent more time in a more dispersed manner than the tablet which moved intermittently after being stationery. This could be possibly explained by the pellets being retained in the colonic haustra whilst larger objects could move in a more independent way. However, the passage of the formulations was subject to variability which was attributed to diet habits and exercise. Upon colonic entry, the pellets stayed mainly at the ascending colon for 14 h and at the transverse colon for a minimum of 48 h whereas they were spotted just passing through the rest parts of the colon. The tablets exited the body 26 (9.5-42) h post-administration when pellets needed significantly longer time [35 (10-15) h]. In regards to metoprolol plasma quantification, it was concluded that this was irrespective of the position of the pellets. The 50% of the absorbed amount occurred when the pellets were found in the colon at similar rate with other most proximal

locations. The peak concentration was 139 nmol/l 11 h post-administration and mean plasma concentration of 83 nmol/l 24 h post-administration [74].

The movement of a non-disintegrating capsule and a multiparticulate pellet system through the GI tract was studied with gamma scintigraphy in 6 healthy volunteers. Both formulations moved alongside through the stomach and the small intestine until they reached colon on an average of 4 h post-administration. In the large intestine, there was a dispersion of the pellets which moved slower than the capsule. A large inter-subject variability in the large intestinal transit times was identified with an oro-caecal transit time of 17-27 h on a fasted stomach. Colonic arrival times were mainly influenced by GE times both for the tablet and the capsule. Anterograde movement in the colon was not described as a continuous process but was a succession of hours of quiescence and abrupt propulsion. This study suggested that when colonic formulations are administered, they need approximately 5 h to reach the colon when on a fasted stomach and from this point and later, there is variability with solid dispersion in the AC and the TC happening across 10 h with implications to the control of drug levels [75].

In conclusion, the administration of single- or multi- pellet systems *in vivo* has been successful into providing an insight into the gastrointestinal transit times and passage events.

1.5.2 Radiolabelled solids or resins in combination with capsules

The monitoring of the location and quantity of radiolabelled solids in the undisturbed large intestine took place with gamma scintigraphy. ^{111}In-labelled Amberlite pellets (0.5-1.8 mm diameter) were placed in a gelatin capsule which was further coated with a pH-sensitive polymer (methacrylate) and administered to 15 healthy volunteers. All capsules disintegrated in the distal ileum or proximal large intestine in 13 out of 15 volunteers. The scintigraphic assessment of the location of the capsule segments in the large intestine and stool radioactivity showed that at 12 h, radioactivity was mostly in the AC and the TC. At 24 h, radioactivity was equal between the AC and the TC ($p > 005$). At 48 h, half of the radioactivity was out of the body but 30 ± 10% was still in the TC. At 24 and 48 h, the DC and RS had less residuals than the TC or stools ($p < 0.05$). Overall, movement from the AC to the TC happened after a lag period of no movement and continued at a linear fashion. In conclusion, the AC and the TC appear to be residual sites favouring drug delivery, topical or systemic [76].

The variance of the colonic residence and propulsion of dispersed and big single unit formulations based on administration timing (morning or evening) was studied. Eighteen healthy volunteers were administered ^{111}In-labelled resin and a large ^{99m}Tc-labelled non-disintegrating capsule at 8am or 5pm. Resin travelled at a slower pace in night time than day time ($p < 0.02$) and maximum movement was measured just after morning awakening but before food consumption. The non-disintegrating capsule travelled further down than the resin 15 h post administration. The researchers concluded that sleep

causes slower movement in the colon and large items move quicker than dispersed smaller ones. However, there was significant inter-individual variability in targeting regions with either small dispersed of large units [77].

1.5.3 Non-disintegrating tablets and radiotelemetry capsules

The overnight transit of drug formulations through the GI tract was studied in 6 healthy volunteers. Each volunteer consumed 5 radiolabelled non-disintegrating tablets, a radiotelemetry capsule (pressure-sensitive radiotelemetry capsule or RTC), and a radiolabelled meal either at 8.00 am or 11.15 pm. The gastric residence time of tablets and capsules was significantly increased ($p < 0.05$) during the night-time administration with longer gastric emptying time for the 50% of the meal (not statistically significant). No significant difference was identified for the small intestinal transit time depending on day or night-time meal consumption. Regarding colonic arrival times (CA), these were extended mainly because of the extended GE for t50% of the tablets and capsules. The total transit time of the RTC capsules (that was retrieved from the volunteers) had medians of 24 h (12-30 h) and 35 h (15-41 h) for day and night, $p = 0.022$. The researcher concluded that during night-time the gastric motility is less frequent with less effective housekeeper wave emptying. This was associated with the different body posture suggesting that supine position slows the GE whereas exercise enhances the GE [78].

The investigators aimed to study the colonic delivery of tablets in 6 healthy male participants (Figure 1.5). The tablets were radiolabelled with ^{99m}Tc-DTPA and pectin-HPMC was added for the site-specificity of tablet disintegration. All tablets travelled the GI tract intact and were seen to release the contrast agent in the large intestine, half of them in the AC (group B) and half in the TC (group A). Drug release was initiated sooner for group B than A (343 min vs 448 min) mainly because group B tablets resided for a certain amount of time at the ICJ compared to group A. This extra time provided deeper hydration of the hydrogel layer around the core tablet and therefore, tablets showed signs of drug release upon arrival at the AC 1.5 h after food consumption. On the contrary, group A tablets arrived at the AC before or just after food consumption were propelled through the AC to the TC offering minimum contact with the colonic water pockets. Limited prior hydration of the hydrogel and limited fluid presence in the TC inhibited tablet break down and radiolabel signalling [79].

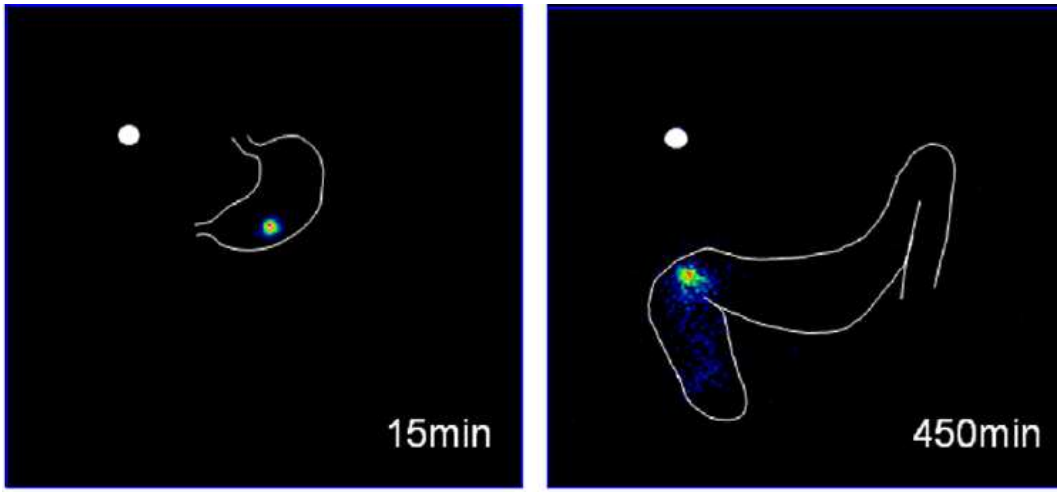

Figure 1.5. Images of the intact tablet in the stomach and the ascending colon 15 and 450 minutes, respectively, acquired by gamma scintigraphy. Taken from [79].

1.5.4 Studies inducing a diarrhoea secretory model

The follow-up of an enteric capsule designed to target the ileo-caecal area was investigated. An experimental model of diarrhoea was created by administering lactulose, three times per day, to 11 healthy volunteers. Then, codeine was administered for its antidiarrhoeal properties. Each volunteer consumed 3 tablets of 5-mm diameter and ^{99m}Tc radiolabelling. The tablets were co-administered with a capsule radiolabelled with ^{111}In-labelled 0.2-mm resin particles and coated with an acid-resistant polymer. Codeine administration delayed transit from mouth to terminal ileum and through the ascending colon ($p < 0.05$). It also reduced whole colon transit mostly in the proximal colon and less in the distal colon and the occurrence of retrograde movement and colonic reaction to food consumption. Overall, the effect of codeine was on the increase of the oro-caecal time. The visual investigation of the gamma scans confirmed that the capsules disintegrated at the ileo-caecal

site and no capsule was seen to leave the mid-ascending intact. In the lactulose regimen, the mean arrival time at the terminal ileum was increased ($p < 0.02$) when codeine was co-administered. Codeine delayed transit through the ascending colon for the 0.2-mm resin particles ($p < 0.05$) and the 5-mm particles ($p < 0.02$), too. This delay was also reflected in the increased percentage of remaining 0.2-mm resin particles at the ascending colon at 24 h from 12.4 ± 8.2% to 23.9 ± 7.3% ($p < 0.05$) [80].

A non-invasive investigation on the effect of lactulose and codeine on luminal water content and whether this effect can affect quinine and ^{51}Cr-EDTA absorption from the proximal large intestine was designed. Therefore, the Pulsincap™ formulation was used to target the ascending colon. Quinine and ^{51}Cr-EDTA were chosen as absorption probes as transcellular and paracellular absorption molecules respectively. Sixteen healthy volunteers were administered the timed-release delivery system Pulsincap™. Water content was assessed in frozen stool samples. Quinine and ^{51}Cr-EDTA absorption was measured with HPLC analysis of plasma and urine samples. On the control days, the initial disintegration happened in the small intestine and the ascending 5 times and in the transverse 6 times. On the lactulose arm of the study, initial drug delivery happened in the small intestine 6 times, in the ascending 7 times and in the stomach, transverse and descending once. Lactulose administration increased ascending colon transit ($p < 0.05$) and stool water content ($p < 0.01$). It also caused bigger dispersion of released material and favoured absorption of transcellular probe quinine ($p < 0.05$)

compared to control measurements. On the codeine arm, there were 5 times of initial drug release in the small intestine, 8 times in the ascending, once in the descending and once no release at all. The codeine arm of the study decreased ascending colon transit ($p < 0.05$) and stool water content ($p < 0.05$) and was unfavourable to absorption ($p = 0.20$). The researchers concluded that in any given region of the lower intestine the factors that enhanced luminal water content favoured quinine absorption (codeine < control < lactulose) but this was of significant difference only in the ascending colon. As far as the delivery site is concerned, the more distal in the large intestine the breakdown, the less the absorption extent (small intestine > ascending > transverse) [81, 82].

1.6 Modified release capsules

Egalet® as a constant-release formulation filled with 50 mg of caffeine and radiolabelled with Sm^2O^3 was used and the release-profile was monitored. Six healthy male volunteers abstained from caffeine for 48 h and swallowed the formulation on a fasted stomach. Blood samples were taken after each imaging acquisition and caffeine blood levels were measured by gas chromatography. All formulations left stomach within 1h. The mean small intestinal transit (SIT) time of the intact Egalet® was around 2h due to the high-intensity sport lifestyle of the majority of the volunteers. Four hours post-administration, the formulation reached the colon but 8-12h were

needed for the movement from the ICJ to the splenic flexure. Caffeine absorption was picked up as early as 15 min post-administration while gamma scintigraphy picked up samarium release 1 h post-administration. This could be explained by caffeine's high water solubility whereas samarium oxide is insoluble in water. Caffeine reached its highest levels 4 h post-administration but caffeine bioavailability differed among the volunteers. It was mainly dependent on the SIT and on the regional residence times. Release was quicker in the small intestine and slower in the distal large intestine. The longer the formulation stayed in the ascending and transverse colon the higher the bioavailability whereas the descending is not friendly to absorption processes [83].

The distal part of the large bowel is not easily accessible to oral drug formulations under normal conditions. The researchers studied whether this part of the gut is even less accessible to drugs in active ulcerative colitis. 32 volunteers (22 healthy volunteers and 10 patients) were recruited for the needs of this study. A gelatin capsule coated with Eudragit® S 100 and filled with ^{111}In-labelled Amberlite resin was administered to the participants for four days in a row. Gamma images acquisition took place on the 4th day. Shorter total, proximal and distal colonic transit was measured against the group of healthy volunteers (all $p < 0.01$ respectively). The resin was unevenly dispersed in the colon of the healthy volunteers which was even more evident in patients. These measurements indicate that less content is located in the distal part of the colon in the state of the ulcerative colitis and normally, the

healthy distal colon has more content. These observations imply that colon-targeted formulations are unevenly found in the distal large intestine irrespective of its state (healthy or active ulcerative colitis). When this is combined with the shorter colonic transit, it leads to the conclusion that distal colon is not accessible to oral formulations with topical use which possibly justifies the inefficacy of these formulations in the active state of the disease compared with the relevant efficacy when administered for the maintenance of the remission state [84].

The enteric polymers Eudragit® L 30 D-55 and Eudragit® FS 30 D for the enteric coating of HPMC capsules for targeting the human colon was investigated. Size 0 capsules were filled with 380 mg paracetamol and 10 mg samarium oxide and administered to 8 healthy volunteers. All capsules left the stomach during the phase III housekeeper wave intact. Capsules coated with Eudragit® L 30 D-55 disintegrated entirely in the small intestine 2.4 h post-administration. Capsules coated with Eudragit® FS 30 D disintegrated entirely until after they reached the distal small bowel and proximal large intestine 6.9 h post-administration [85].

The researchers aimed to apply gamma scintigraphy to confirm that their colonic formulations release the encapsulated drug in the colon. The tested formulations were HPMC capsules size 0 with 0.96 mg of paracetamol as the active ingredient radiolabelled with Sm_2O_3. MCC or hypromellose (HPMC, Methocel K4M) were added for their gel formation properties that provided gradual drug release at a slow rate to the whole large intestine. The capsules

were then dip-coated with Eudragit® S 100 polymer for its site-specificity properties and were administered to 6 healthy male volunteers. Capsules were intact in the stomach and upper GI tract of the volunteers. Their transit through the stomach lasted less than 1 h and the capsules were first seen at the ileo-caecal junction 3-4 h post-administration. The capsule disintegration started at the ileo-caecal junction or the ascending colon. The MCC formulations released the imaging marker instantly at the disintegration site. At the other hand, the HPMC capsules released it slowly throughout the colon and their complete gel disintegration happened after 12-14 h had passed. The researchers pointed out that *in vitro* studies are not enough when evaluating modified-release formulations and concluded in the potential of colonic formulations to release drug at the ileo-caecal junction and further down gradually when enteric coating is combined with hydrophilic polymers [86].

A different study team built non-disintegrating capsules to study the GI transit and luminal fluid presence in 12 healthy participants applying MRI techniques. The team was able to follow-up the capsules' locations in the lumen and concluded that fluid is not evenly distributed in the colon but is rather found in pockets. Water and food were found to be propelled further down in the gastrointestinal tract by food-initiated gastro-ileo-caecal reflux [24].

1.7 Aims and Hypothesis

The brief review of the literature presented above showed that there is a gap in understanding drug delivery from coated capsules and that new imaging methods have the potential to provide new physiological insights into drug performance in the lower intestine. This, in turn, could help the pharmaceutical industry to improve coated capsules design and bio-relevance of models.

Building on the body of literature, the hypotheses underpinning this work were that: (1) MRI will be able to track the transit of a coated capsule and its disintegration in the human lower intestine non-invasively; (2) that this will link to absorption kinetics of an active pharmaceutical ingredient (API), and (3) that MRI can monitor other parameters of gastrointestinal function relevant to capsule transit such as small bowel motility.

Based on these hypotheses, the primary aims of this study were to exploit MRI to monitor the gastrointestinal fate of a coated capsule and to correlate this to the API's absorption kinetic. The secondary aim was to assess the ability of MRI to monitor small bowel motility by correlating MRI and conventional perfused manometry measurements of duodenal motility.

Specifically, this work aimed to:

1. Design and manufacture coated capsules with the potential to reach the lower human intestine and at the same time to be MRI-visible

2. Develop and demonstrate an MRI method to track the transit of the coated capsule and its disintegration in the lower human intestine

3. Load the coated capsule with an active pharmaceutical ingredient (API) and correlate the MRI findings with the API's systemic appearance

4. Compare small bowel motility measurements performed by MRI with those performed by perfused manometry

1.8 Thesis outline

All the work described in this thesis was conducted by the author, except where specifically credited to collaborators, at the Nottingham Digestive Diseases Centre (NDDC), at the School of Medicine and School of Pharmacy and at the Sir Peter Mansfield Imaging Centre of the University of Nottingham, and at the National Institute for Health and Care Research (NIHR) Nottingham Biomedical Research Centre (BRC) from 2018 to 2022.

The research described in this thesis is original, unless otherwise stated.

The layout and content of the thesis chapters are as follows:

Chapter one: Introduction

Chapter two: Coated capsule development

Chapter three: *In vivo* MRI feasibility study of imaging the coated capsules

Chapter four: *In vivo* MRI versus caffeine assay study

Chapter five: Small bowel motility MRI and manometry study

Chapter six: Discussion

Chapter seven: References

2 Coated capsule development

The first part of the experimental work comprised the development of coated capsules with the potential to reach the lower human intestine and at the same time to be MRI-visible. This Chapter details the choice of materials and the protocol for the manufacture of the capsules. After this weight gain was measured for different amounts of coating and *in vitro* disintegration tests were also carried out.

2.1 Introduction

The work started with a non-systematic search of the literature in order to identify the most promising starting point for the design of the capsules. There have been different approaches to the manufacture of oral drug formulations for targeting the lower intestine. Some of the relevant approaches found are reviewed below.

Various approaches have been adopted to navigate drug delivery to the lower GI tract. Most commonly, they have taken advantage of pH and/or time-sensitive polymers in a single- or multiple-coating of solid formulations and technology that takes advantage of the local gut microbiome. pH polymers such as Eudragit® prevent the premature drug release as they are insoluble in the low pH (1.25) of the upper GI tract (stomach and proximal small intestine) and dissolve at higher pH values that are found in the last parts of the small intestine (6.6 ± 0.5) and the large bowel (maximum value of 7.5 ± 0.4 and slight decrease afterwards) [85, 87, 88]. Time dependent polymers such as

HPMC and microcrystalline cellulose (MCC) depend on their swellability properties when they come in contact with water or chyme. These polymers get wet and gradually swell which leads to their gradual dissolution and drug release in the large bowel [55, 86, 89]. Conventionally, formulations that depend on only one type of technology are less likely to be fully successful and therefore, modern approaches usually combine more than one technology.

Capsules size 0 were coated with Eudragit® S polymer in order to deliver sulphapyridine in the lower intestine and the capsules were followed up by X-ray imaging *in vivo* [90]. The Eudragit® polymer is designed to be resistant to the acid conditions such as found in the stomach, but it dissolves at pH above 7.0 as found in the terminal ileum and colon, which makes it a suitable choice to coat capsules for this purpose. The researchers were successful into delivering the capsules in the colon (32 out of 36 capsules arrived there intact).

Similarly, Schroeder et al administered 5-aminosalcylic (5-ASA) acid tablets coated with the pH-triggered polymer Eudragit® S or placebo in 87 patients with mild to moderate active ulcerative colitis (UC) [91]. The 5-ASA moiety was administered in the form of sulfasalazine which is prescribed for the remission of mild to moderate of UC and for log-term maintenance too. Sulfasalazine is a pro-drug for 5-ASA and sulphapyridine and it only breaks down by colonic microbiota. This work set the basis to the drug product ASACOL®.

Similarly, researchers coated rapidly disintegrating tablets with Eudragit® S for protection from dissolution in the upper GI tract and colonic delivery, using gamma scintigraphy for follow-up [92]. The tablets were administered to 7 healthy participants on fasted conditions and food was provided upon emptying from the stomach. *In vivo* break down was not consistent and happened along the terminal ileum and the splenic flexure at various sites. Poor mixing with colonic contents was also observed. Twelve hours post-administration, the tablets were spotted in between ileocecal junction and splenic flexure [92]. Overall, Eudragit® S protected from early disintegration but did not provide sufficient site specificity on its own because of long residence times at ileocecal junction and variability in transit times [55, 88, 92].

Another interesting approach is that to use combination methodologies. For example, in a study pressure-controlled colon delivery capsules (PCDCs) were used and their disintegration *in vivo* was regulated by ethylcellulose (EC) thickness [53]. Specifically, there were 3 types of PCDCs based on 3 types of thickness as the inner surface of the gelatin capsules was coated using 3 different amounts of EC: type 1 had the smaller, type 2 a medium and type 3 the greatest thickness. Type 3 capsules were more likely to reach intact in the colon.

Similarly, PCDCs as gelatin capsules were formed as suppositories and coated in the inside surface with 4 types of coating thickness of water-insoluble ethanolic 5% w/v EC. Their oral administration, ingestion and exposure to

body temperature caused the suppository base to melt and form a balloon-like form with the drug inside. The upper GI tract has enough liquid to protect the EC balloon from GI pressures but in the colon, where water reabsorption happens, there is higher viscosity of contents and disintegration happens. The study had 2 healthy participants volunteering and in both the capsules arrived at the colon 4h post-administration [93, 94].

Another type of colon-targeted capsules were manufactured by using size 2 hard gelatin capsules and a combination of pH- and time-dependent colonic delivery approach. The capsules were coated from inside to outside with an acid-soluble layer of Eudragit® E, then a hydrophilic layer of HPMC- and last an enteric layer of Eudragit ® L. Capsule disintegration was observed under both fasted and fed conditions and in both occasions in most cases [95].

In order to determine the role of morning or evening administration of drug formulations on their colonic residence time and behaviour, small particulates and a large capsule were tested. Eighteen healthy participants were given ^{111In}-labeled resin inside a gelatin capsule size 0 and a large ^{99m}Tc-labelled non-disintegrating gelatin capsule coated with ethylcellulose and Eudragit® S100 [77]. Overall, sleep significantly delayed the transit of drug formulations but large capsules moved faster. However, there was high inter-subject variability that challenged colon-targeted drug delivery with both types suggesting that colon-targeted drug delivery based just on one mechanism may not be favourable. One more attempt of colonic delivery included HPMC capsules size 0 coated with 2 types of polymers: Eudragit® L 30 D-55

(designed to dissolve at pH 5.5) and 6 mg cm^{-2} Eudragit® FS 30 D (designed to dissolve at pH 7 and higher) for enteric and colonic targeting respectively. *In vivo* the L 30 D broke down primarily in the small bowel at 2.4 h (mean) post administration compared to the FS 30 D which disintegrated in the distal small bowel or further down in the proximal colon at 6.9 h (mean) [85]. Another approach to deliver aminosalicylic acid to the colon used HPMC capsules coated with amylose and EC and compared them to uncoated capsules. Amylose is polysaccharide that disintegrates by colonic enzymes that are produced by local bacteria. The uncoated capsules disintegrated in the stomach within 10 min but the coated ones arrived in the colon intact in 6 out of 7 cases [96].

Another example of the exploitation of the colonic microbiota along with the pH changes along the GI tract saw the use of Eudragit® S in combination with lactose in tablets. Eight healthy participants consumed these capsules and disintegration point was mainly the ileo-caecal junction or large intestine regardless of the feeding status [55].

Similarly, capsule size 0 were used with either microcrystalline cellulose (MCC) or hypromellose (HPMC K4M) along with Eudragit® S for colon-targeted delivery. Overall, Eudragit® was more likely to succeed in preventing drug release before the ileo-caecal junction [86].

Double-coated tablets were also used with Eudragit® S and compared to single-coating tablets. *In vivo*, the disintegration of the single coated tablets in large bowel was inconsistent compared to the double-coated that had less

variable disintegration sites which was the ileo-caecal junction or terminal ileum. The authors concluded that the double-coated may be favourable compared to the single/conventional colon-targeted [87].

The literature briefly reviewed above indicated that a combination of a HPMC capsule and Eudragit® multiple coating could be satisfactory for the purpose of this work. The selection of HPMC as the capsule shell took into consideration that HPMC is often used as a pre-coating material in gastro-resistant/enteric coated formulations as gelatin capsules do not appear to have good adhesion properties when directly coated with Eudragit® polymers [85, 97]. The polymer Eudragit® S 100 was chosen based on literature findings. The main advantage considered was its pH-responsiveness (the pKa value of Eudragit® S is approximately 6). The presence of the weakly acidic carboxyl groups in its chemical structure are in protonated state at acidic pHs (as found in the stomach). Further down in the GI tract, these groups start to get disorganised as the pH goes up and the charged carboxylate groups favour disentanglement. That way, the polymer transforms into a form of solution [98, 99].

It was essential to choose capsule filling materials that would lead to MRI visibility of the capsule inside the body. The HPMC capsules would not be able to contain a water-based material (with or without a contrast agent in it) as this would dissolve the HPMC very quickly. Gadolinium, commonly used in MRI as an imaging marker, has however been associated with brain

deposition [100] and therefore was not considered for this study. Other oral agents with magnetic properties have limited market application or have been discontinued [101]. Interestingly, an oil filling would be less prone to destabilise the HPMC shell whilst provide a unique signal for MRI fat/water imaging as the distal bowel does not usually contain fat. A relatively large capsule size would make MRI detection easier and also allow to determine its shape in three dimensions.

Based on these considerations the work presented here started moving towards designing a capsule with a HPMC shell with a large size, coated with an Eudragit® polymer for gastro-resistance, and containing an oil filling for MRI detection.

2.2 Materials and Methods

2.2.1 Capsule development

The first attempts of capsule development involved sourcing suitable Size 0 HPMC capsules, (Your Supplements, Stockport, UK). There came as separate capsule caps and bodies, they were colourless, and when assembled the capsules had a length of 21 mm and a diameter of 7 mm.

Secondly, contact was made with the manufacturer of Eudragit®, the company Evonik Operations GmbH via personal contacts of the supervisory team. Drs Nina Hauschildt and George-William Smith at Evonik provided precious advice on how to manufacture and coat the capsules and also kindly gifted a supply of Eudragit® S 100 (Figure 2.1) which was indicated as the best candidate for this work from their range of products.

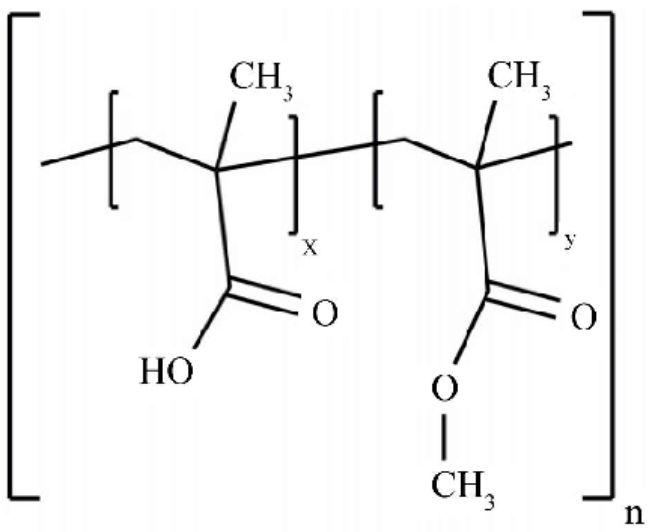

Figure 2.1. Chemical structure of Eudragit® S 100. Taken from [102]

The coating solution was prepared following the manufacturer's protocol. A 20:1 w/w stock mixture of ethanol (96% Reag. Ph Eur, Sigma-Aldrich®) and water was prepared as the solvent mixture for the coating process. The Eudragit® S 100 polymer powder (Evonik Operations GmbH, Essen, Germany) was added into the solvent mixture while stirring, until the formation of a clear solution. A concentration of 16.7% Eudragit® S 100 solution was chosen

based on literature. The coating solution was then stored at room temperature for 24 h to cool down to be ready for use the next day. The HPMC capsule caps and bodies were dip-coated separately into the solution 3 times in total in consecutive dipping (coating) cycles, leaving 3 min drying time in between each dipping. The idea was that the capsules caps and bodies could be coated first and then filled with oil and assembled. However, brittles and cracks appeared immediately (Figure 2.2) and the capsules could not be assembled.

Figure 2.2. Brittles and cracks on the HPMC capsule shells upon dip-coating in the 16.7% Eudragit® S 100 solution.

These tests led to revise the plan and hypothesise that the HPMC capsules could be filled with olive oil and assembled first as a whole capsule, which could then be more resistant to cracking upon dip-coating. Olive oil and HPMC were compatible as predicted, but the HPMC capsules' shell quickly

spoiled when in contact with the coating polymer and olive oil came out of the capsules (Figure 2.3).

Figure 2.3. Cracking of the pre-assembled and pre-filled HPMC capsule upon dip-coating.

This observation led to questioning the first hypothesis that HPMC would be compatible with the Eudragit® polymer coating. For this purpose, commercially available cod liver oil gelatin capsules were sourced and tested with the Eudragit® coating, and few cracks appeared in these capsules too. Upon revisiting the coating protocol, with further Evonik company help, the addition of a plasticizer to the coating solution was considered.

Triethyl citrate (TEC) was then used as a plasticizer and added to the Eudragit® solution. TEC (Sigma-Aldrich®) (3.56 % w/w) was added as a plasticizer into a separate, equal amount of the ethanol and water solvent mixture while stirring. The plasticizer solution was mixed with the Eudragit®

solution under stirring conditions. The final coating solution was again stored at room temperature for 24 h to cool down to be ready for use the next day.

The addition of the plasticizer was successful as no brittling or cracks appeared in the capsules' body and cap. Also, during this initial experience it was noted that the two capsule parts could not be assembled well after the coating has been carried out, and it was decided that they will be best coated as a single entity.

Initially, the capsules were filled with olive oil (Tesco Stores Ltd, Welwyn Garden City, Hertfordshire, UK) upon completion of the coating with the help of a needle and syringe. The filling volume was 0.65 mL of olive oil. The choice of olive oil was made as it is easily sourced and food grade, therefore suitable for human experiments. However, the capsules could not be sealed well after the filling and eventually olive oil would come out of the capsule upon application of some pressure (Figure 2.4).

Figure 2.4. Pre-filled HPMC capsule dip-coated into the Eudragit® S and TEC solution.

To address the issue of oil leaks after filling, the drying time in between each coating cycle had to be optimised. It was also decided to apply a glue around the connection point of the capsule cap and body. Methocel™ K4M (Colorcon) glue was used to seal the capsules and to prevent oil leaking from the capsule.

The drying time in between the coating cycles was initially set to 3 minutes following the initial Evonik company's recommendations. In this case, this proved to be inadequate, possibly because the capsules here were not sprayed but dipped into the coating solution. For this reason, a longer 5 minute window was allowed for drying between cycles of dipping. This gave better results in terms of capsules' hardness but there was lack of shape uniformity among different capsules. Experiments were performed with drying time windows of 10, 20, 30, 40 and 50 min. The 10 and 20 min drying windows still lead to soft capsules but the 30, 40 and 50 min drying windows produced capsules equally strong and more uniform.

In the interest of the time-efficiency, the shorter 30 min window was chosen.

Another improvement to shape uniformity came from increasing the speed of removing the capsules from the solution after dipping, so that any excess amount of coating solution was removed. A visual inspection of the shape was performed as the application of more sophisticate methods such as scanning

electron microscopy (SEM) was beyond the scope of this thesis. The capsules were then left to dry on a drying rack (Figure 2.5).

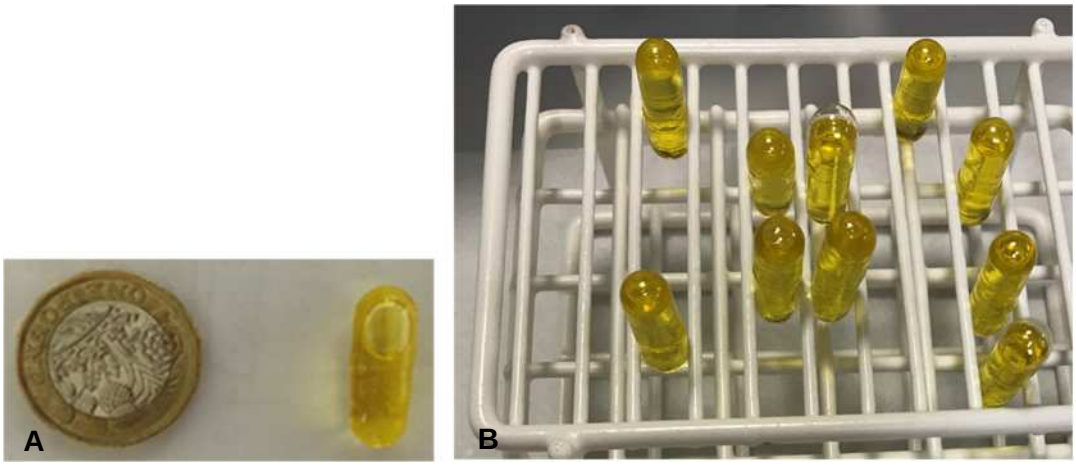

Figure 2.5. A) Physical comparison of the capsule next to a one-pound coin, and B) Drying capsules on the rack.

To monitor coating uniformity, measurements of capsule diameter and length were attempted with the use of a manual calliper (RS PRO, 914-0485) at the end of the coating day and also on the next day. However, the variability of these measurements was fairly high, possibly depending on the inherent precision of the calliper and also possibly to variability in the strength and pressure the polymer was exerting on the capsules. For this reason, the calliper measurements were abandoned and capsule weight gain was recorded as a more accurate measure of amount of coating applied.

Once the coating procedure was completed, each capsule was stored individually to avoid tacking and allowed to dry overnight. Weight gain was monitored throughout the coating process and at 24 hours.

At this point, a range of concentrations of Eudragit® S 100 coating solution with plasticizer and increasing number of dipping cycles were chosen based on literature data and preliminary *in vitro* observations. Coating solutions concentrations of 2.3%, 4.6%, 6.7%, 8.8%, 10.7% and 13.0% of Eudragit® S 100 were prepared in order to investigate dependence of capsule weight gain on the coating polymer solution concentration. Weight gain was measured throughout the manual dip-coating in triplicate to quantify the amount of coating placed on each capsule. The surface area of a capsule was calculated using the sphero-cylinder area formula, knowing the length and diameter of the capsule.

2.2.2 *In vitro* disintegration study

The disintegration behaviour of the uncoated and coated capsules was tested in the USP compatible basket apparatus (ZT 120 light, ERWEKA GmbH, Langen, Germany) based on the United States Pharmacopeia (USP) guidelines for disintegration tests of oral formulations. In this protocol 700 mL of 0.1 M hydrochloric acid was used for the 'acid stage', simulating the gastric fluid, and the capsules were exposed for 1 hour. The capsules were then immersed into 700 mL of phosphate buffer pH 6.8, termed here the 'buffer stage', simulating the intestinal fluids. The experiments were performed at 37 ± 2^{o}C and a stirring speed of 30 ± 1 strokes/min as per the USP guidelines [103, 104]. Triplicates of un-coated and capsules coated by 1, 2 or 3 dipping cycles in 10.7% Eudragit® S 100 and TEC coating solution were tested. Time to loss of

capsules integrity, as well as to complete disintegration of capsules were recorded. Loss of integrity was intended as apparent deformation of the capsules' shape and/or release of some or all the oil filling and was determined by the PhD student and the lab technician assisting the experiments.

2.3 Results

2.3.1 Capsule coating

A representative example of the coated capsules ready for use is shown in Figure 2.6A. Figure 2.6B plots the weight gained by the HPMC capsules upon coating with solution of Eudragit® S 100 at different concentrations. The amount of coating deposited on the capsules increased with increasing concentration of Eudragit® S 100 solution and with the number of dipping (consecutive coating) cycles. Weight gain variability also increased with higher polymer concentrations and number of dipping cycles.

2.3.2 Capsule disintegration

The data from the disintegration tests in acid (stomach) and buffer (intestinal) conditions are reported in Table 2.1. In the disintegration tests (in triplicates)

the uncoated capsules lost their integrity and released their first drop of oil in 6.2 ± 2.2 min in the simulated stomach (acid) stage. The uncoated capsules had disintegrated entirely within 11.5 ± 2.9 min in the acid stage. All the coated capsules remained intact in the acid stage. The capsules manufactured using the lowest amount of coating (9.2 mg, 1.9%) released their first drop of oil in 15.5 ± 3.2 min during the intestinal (buffer) stage. The capsules manufactured using 18.2 mg (2.9%) of coating lost their shape and released the first drop of oil after 116.9 ± 20.4 min in the buffer stage whereas the capsules manufactured using the higher 25.9 mg (4.6 mg) coating maintained their integrity in the buffer stage for over 6 hours, when the disintegration experiment was stopped, with no signs of loss of shape or oil release.

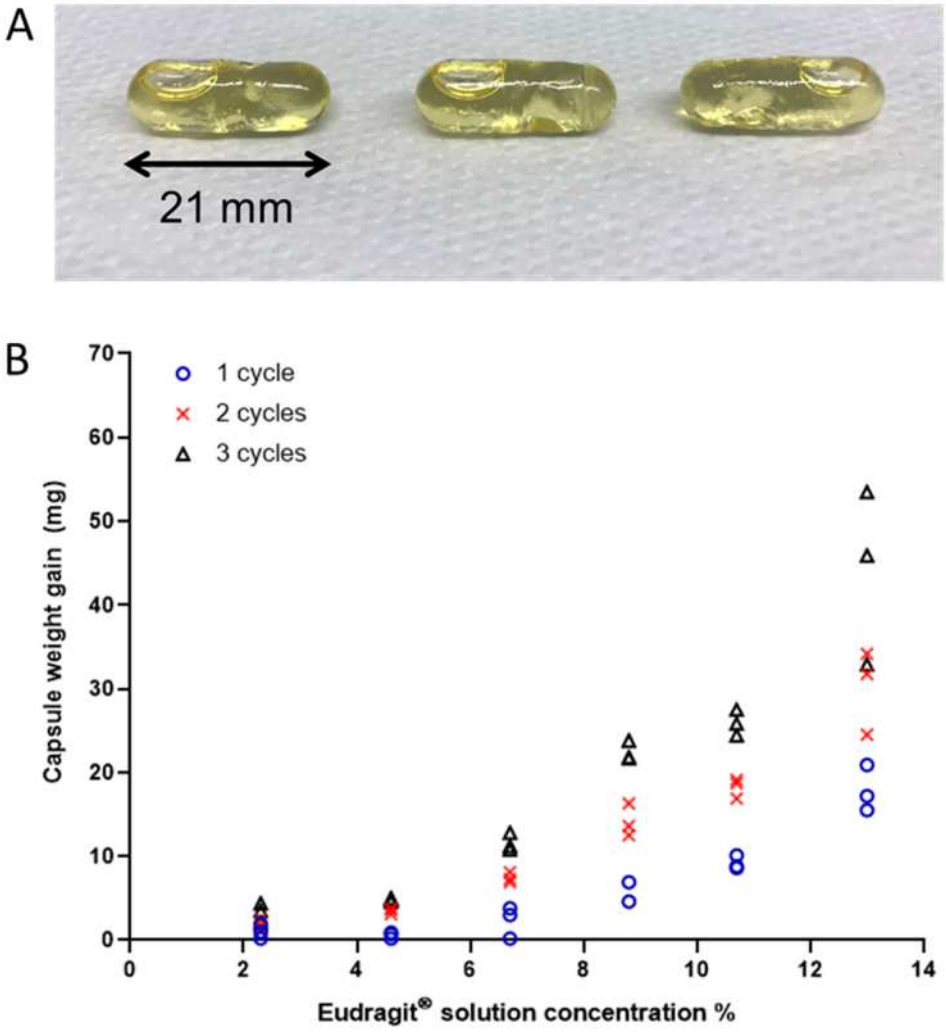

Figure 2.6. (A) A representative example of HPMC capsules filled with olive oil and coated with Eudragit® S 100. The capsule measures 21 mm length by 7 mm diameter. (B) Capsule weight gain measured in triplicate at 24 hours after one, two and three dipping (coating) cycles for different concentrations of Eudragit® S 100 solution.

Table 2.1. Disintegration tests of capsules with different amount of coating in acid (simulated stomach) and buffer (simulated intestinal) conditions.

	Acid (simulated stomach) stage [a]							
	Time to loss of capsule integrity (min)				Time to complete capsule disintegration (min)			
Weight gain (mg, %)	Capsule 1	Capsule 2	Capsule 3	Mean±STD	Capsule 1	Capsule 2	Capsule 3	Mean±STD
0 (uncoated)	5.3	8.7	4.5	6.2±2.2	9.1	14.7	10.7	11.5±2.9
9.2±0.8; 1.9	Intact	Intact	Intact	-	Intact	Intact	Intact	-
18.2±1.2; 2.9	Intact	Intact	Intact	-	Intact	Intact	Intact	-
25.9±1.5; 4.6	Intact	Intact	Intact	-	Intact	Intact	Intact	-
	Buffer (simulated intestinal) stage [b]							
	Time to loss of capsule integrity (min)				Time to complete capsule disintegration (min)			
Weight gain (mg, %)	Capsule 1	Capsule 2	Capsule 3	Mean±STD	Capsule 1	Capsule 2	Capsule 3	Mean±STD
0 (uncoated)	N/A	N/A	N/A	-	N/A	N/A	N/A	-
9.2±0.8; 1.9	17.8	11.8	16.8	15.5±3.2	>60 [c]	>60 [c]	>60 [c]	-
18.2±1.2; 2.9	139.3	99.4	112.0	116.9±20.4	>375 [d]	>375 [d]	>375 [d]	-
25.9±1.5; 4.6	Intact	Intact	Intact	-	-	-	-	-

[a] 700 mL 0.1M hydrochloric acid at 37.4°C

[b] 700 mL pH = 6.8 phosphate buffer at 37.4°C

[c] The capsule had disintegrated entirely but some capsule debris was still visible.

[d] Up to this time the capsule had shown minor, observable coating changes but without oil release.

N/A, capsule had already lost its integrity at the acid (stomach) stage

2.4 Discussion

This initial part of the experimental work was successful. It was possible to design a coated capsule containing olive oil which is a fluid that can be imaged well by MRI exploiting the water and fat imaging capabilities. The idea of using olive oil as a capsule filling to monitor the capsule's intestinal fate is novel.

The capsule resisted stomach acid condition in a standard disintegration test and subsequently disintegrated in a time proportional to the amount of coating applied, as one would have predicted. The capsules without coating disintegrated in the acid stomach conditions, but all the coated capsule remained intact for the entire acid test. In intestinal conditions, the capsules with less coating material lost their integrity and then disintegrated entirely within 20 minutes. Capsules with more coating applied resisted the intestinal buffer stage for up to 6 hours for the more heavily coated ones, confirming a proportionality between capsule integrity and coating weight gain.

The design of the gastro-resistant, polymer coated capsule used in this study, the choice of specific Eudragit® polymer and the range of concentrations of the coating solution was based on the literature [77, 85-89, 95, 97, 105-112] and interactions with the manufacturer of the Eudragit® polymer were very valuable to refine the protocol. . In addition, HPMC properties seem to favour the gradual drug release in the colon [86].

Of particular relevance, the materials used for the capsule, its filling and for its coating were all safe for use in human studies and not expected to raise and issues with obtaining Ethical approval.

Limitations of this initial phase of the work included the lack of a more sophisticated method to monitor capsule surface as the coating with a polymeric material may result in a creation of an uneven layer, particularly if adhesion forces between two materials are low, as for gelatin capsules, and this supported the choice of HPMC capsules. In future studies and optimizations, one would aim to measure the layer thickness and its uniformity at the capsule shell. Furthermore, future studies could evaluate the bioavailability of active pharmaceutical compounds incorporated within the capsule.

2.5 Conclusions

Based on this work, it was concluded that the manufacturing protocol and *in vitro* characteristics of the coated capsules were appropriate to bring the capsule into an *in vivo* feasibility MRI study, which is the subject of the following Chapter.

3 *In vivo* MRI feasibility study of imaging the coated capsules

This Chapter describes the feasibility study aiming to develop and demonstrate the MRI *in vivo* tracking of the coated capsuled manufactured in Chapter 2. Data from 10 healthy adult participants showed that it was possible to track the capsules and also image its loss of integrity using combinations of MRI fat and water imaging.

3.1 Introduction

The aim of targeted oral formulations, including delayed release dosage forms, is to deliver the active agent at the intended site in the gastrointestinal tract and in that way regulate the absorption rate, the plasma concentration-time profile and the pharmacodynamics of the formulated drug [57]. Despite the importance of colon-targeted formulations, the knowledge of formulation transit and release is still limited. Whilst knowledge of formulation behavior in the upper gastrointestinal (GI) tract is improving, the lower GI tract remains much less explored, partly because of the difficulty of accessing the anatomical areas under physiological (unprepared and undisturbed) conditions [113]. Much of the available information derives from gamma scintigraphy studies conducted initially in the 1980s and 1990s. Whilst pioneering and very informative, nuclear medicine methods have limited spatial resolution and provide limited anatomical or functional information on

the surrounding organs [77, 78, 81, 82, 114-116]. Other innovative methods such as Magnetic Marker Monitoring (MMM) have been used. These techniques use a magnetic detector to follow the fate of solid formulations along the GI tract [117-122] providing good temporal resolution, but again limited anatomical information.

Imaging techniques such as Magnetic Resonance Imaging (MRI) have the potential to enrich current knowledge by providing new non-invasive and non-ionizing insights on the undisturbed gastrointestinal (GI) tract, with the real-time assessment of the physiological environment surrounding drug products including water content, chyme properties, and mixing by the intestinal wall contractions [34, 43, 123]. MRI has been gaining increasing attention in the pharmaceutical field to inform understanding of the environment that drug products will be experiencing and the development of pharmaceutical products [24, 26, 28, 32-34, 124-126].

The MRI phenomenon exploits fundamental properties of nuclear physics and requires the use of strong magnets that create a strong and homogeneous magnetic field, where the sample is placed. The most common nucleus used for MRI imaging is the hydrogen proton. Protons are abundant in the human body as they are present in water and also in fat. When a participant is positioned in the magnet, the magnetic field makes protons in the body align with the magnetic field. This alignment creates an overall magnetisation vector that is parallel to the axis of the MRI scanner. A radiofrequency pulse then used to transmit energy to the sample, which in turn tilts the magnetization vector away from its position of equilibrium. This process is

dependent on the nuclei themselves, the environment that the nuclei are immersed in and the strength of the applied magnetic field. When the additional radiofrequency pulse is switched off, the magnetic vector returns to its initial state while emitting a signal that can be received by an aerial placed on the body. The use of additional magnetic field gradients during this process encodes the radiofrequency signal spatially, which then allows to reconstruct the MRI images [127].

One of the first studies, conducted by Schiller *et al*, applied MRI to investigate the simultaneous passage of non-disintegrating oral formulations and quantify the fluid presence in the intestines in the fasted and the fed state [24]. The study concluded that fluid presence remains mainly unchanged in the colon in both fasted and fed states and introduced the concept of gastrointestinal tract fluid pockets, which increase in numbers after food administration. The study was able to locate the oral formulation tested (non-disintegrating gel capsules with 16.8 mm length and 4.6 mm diameter) and link movement of these capsules to food intake [24]. Sager at al., took advantage of the superparamagnetic properties of incorporated iron oxide to visualize the transfer of immediate-release hard gelatin capsules in the GI tract [128]. Grimm et al. encapsulated dried pineapple and used MRI to monitor the behavior of acid-resistant capsules *in vivo* exploiting the MRI contrast agent properties of the fruit on T1-weighted water imaging [129]. MRI has also been used in other studies to image formulations, but primarily in the upper GI tract, including non-disintegrating oral formulations, release

of MRI contrast agents from capsules, multi-particulate surrogates and gadolinium-labelled liposomes [130-139].

Building on this work, our study aims to test the hypothesis that it would be possible to use MRI to track the location of a fat-filled oral coated capsule throughout the GI tract and to image their loss of integrity by taking advantage of the ability of MRI to image fat and water separately, and in combination. We report here the use of enteric coated oral capsules in a range of coating concentration to overcome variability in physiology and the feasibility of their *in vivo* MRI imaging following oral administration to healthy human participants

3.2 Materials and Methods

3.2.1 *In vivo* study design and participants

The experiment was an open-label, one arm, feasibility study. The study protocol was approved by the University of Nottingham's Faculty of Medicine and Health Sciences Research Ethics Committee, Nottingham; approval number 402-1910. All participants gave written informed consent, and had no contraindications to MRI.

Inclusion criteria were:

- Aged 18-45
- Body mass index (BMI) ≥ 18.5 and ≤ 30 kg/m^2
- Able to give informed consent

- Apparently healthy

Exclusion criteria were:

- Any history of serious, unstable medical condition, unstable/uncontrolled diabetes mellitus, and/ or major psychiatric diagnosis such as attention deficit hyperactivity disorder, obsessive compulsive disorder, panic attacks and generalized anxiety disorder.
- Any reported history of gastrointestinal disease
- Any conditions requiring daily intake of any prescription and/or over-the-counter medications
- Any reported history of surgery that could affect gastrointestinal function (e.g. colectomy, small bowel resection)
- Reported alcohol dependence
- Pregnancy
- Contraindications for MRI scanning i.e. metallic implants, pacemakers, history of metallic foreign body in eye(s) and penetrating eye injury
- Inability to lie flat
- Poor understanding of English language
- Any conditions causing fidgeting
- Claustrophobia
- Participation of any medical trials for the past 3 months
- Known allergy to one of the capsule ingredients or drugs used in the study

All ten participants (4 male and 6 female) were healthy participants aged 22-41 years with no history of underlying cardiac or gastro-intestinal disorders or symptoms. All participants had a normal range body mass index (BMI) between 20.5 and 24.4 kg/m^2, and reported no food intolerances or allergies. The participants were asked to fast from 8.00 pm the evening prior to the MRI study day. They were asked to skip breakfast and to report to the imaging facilities fasted. Prior to the study process, all participants underwent an initial fasted baseline MRI scan to check that the stomach was fasted, determine anatomy and to plan upcoming scans. Following that, the participants were administered in a standing position a coated capsule with the standard FDA oral dose of water (240 mL) that is used in drug trials of solid oral dosage forms [140] . Capsules coated with the Eudragit® S 100 and TEC solution in a range of amount of coating weight gain ranging from 9.2 mg to 52.6 mg were prepared and administered to participants, as summarized in Table 3.1. The weight gain for each of the 10 capsules manufactured for the human study is reported in the Table 3.1 both in terms of absolute weight gain and estimated weight gain (mass) *per* capsule unit surface area at 24 hours after preparation.

Participants were scanned at predetermined time intervals, with the images acquired every 45 minutes post-administration of the capsule. This choice of interval was due to the need to alternate scanning with periods of rest for the participants, in what was anyway expected to be a slow process of transit and loss of integrity. Image data was acquired until the investigators were confident that the capsule could no longer be detected for loss of filling or up

to 8 hours post ingestion. The 8 hours limit was chosen for practical reasons including building opening times, presence of first aid cover and reported OCTT in bibliography to include small bowel transit [44-46]. The participants were provided with a meal only when the coated capsule exited the stomach so that the capsule would first be emptied from the stomach in the fasted state, without interference or delays caused by a meal. Also, a meal provided after the capsule left the stomach would promote fed state GI transit whilst at the same time interrupting the fasting that the participants had been keeping up to that point. This consisted of a cheddar and ham sandwich, a 25 g pack of salted crisps, a butter croissant, and 500 mL of water (total energy content 670 Kcal).

At each time point, for each participant, the gastrointestinal tract location of the capsule was noted from the image data. Also, the capsule's intact appearance or loss of integrity, intended as apparent deformation of the capsules' shape and/or release of some or all the oil filling, was noted. This was determined by two investigators, the student conducting the study and the MRI radiographer or PhD supervisor in a non-standardized way. When the capsule presence in the image stacks could not be detected, this was labelled in Table 3.1 NO or Not Observed.

3.2.2 MRI acquisition

The participants were scanned in the supine position in a 3 Tesla Philips Achieva MRI scanner (Philips, Best, The Netherlands). They lay supine on the

scanner table with a 16-channel receiver placed around the abdomen. A multiple-echo, mDIXON [141] sequence was used with echo time 1 = 1.32 ms, echo time 2 = 2.2 ms, flip angle = 20°, repetition time = 10 ms, field of view = 250x350 mm^3 and acquired resolution = 1.8 × 1.8 × 4.4 mm^3. Coronal views of the abdomen were acquired, divided into short breath hold stacks. The reconstructed mDIXON sequence yielded 4 image types (water, fat, water and fat in phase, water and fat out of phase). At each time point the MRI procedure took approximately 15 minutes including set up, scout imaging and calibrations.

The time taken by a capsule to go from the stomach to the colon was taken as the small bowel transit time, calculated as time of first detected appearance in any colonic region minus time of last detection in the stomach. The anatomical regions of the colon were identified and determined by the investigators and MRI radiographer.

The data are presented as mean ± standard deviation (STD).

3.3 Results

All 10 participants swallowed the capsules without problems and tolerated the serial MRI scanning procedures, and the relatively long study day, well.

Figure 3.1 shows an example of MRI tracking of an intact capsule inside the body of one participant, from the stomach through the small bowel until the capsule is seen as completely empty at the end of the distal ascending colon, having released the oil 'payload'. In this case the release of the oil happened in between the imaging time points and was not captured. By contrast Figure 3.2 shows a partially filled and deformed capsule at the hepatic flexure region of colon in a different participant 180 minutes post-administration. Figure 3.2A displays the whole body section with the anatomy (the fat and water out of phase image plane) to pinpoint the location of the capsule. Figure 3.2B displays the fat only imaging mode and depicts not only the partial filling remaining in the capsule, but also the oil released from the capsule, present in the colon chyme and close to the colon wall. Similar results obtained from another participant are shown in Figure 3.3. This time the capsules was imaged at the bottom of the ascending colon 135-180 minutes post-administration with some oil filling released and distributed along the colon wall.

Table 3.1 summarizes details of the capsule detection in all 10 participants. All capsules were detected intact in the stomach at t = 45 minutes after ingestion. After this time the capsule's transit through the GI tract varied across participants. In 9 participants the capsules were detected in the small intestine. Only in 1 participant the capsule was imaged losing integrity in the stomach. This was the capsule with the lowest weight gain of 9.2±0.8 mg or 0.02 mg/mm^2. All other capsules reached the small intestine apparently intact. Eight capsules reached the terminal ileum and 4 the colon. Loss of

integrity was imaged directly in 8 of the capsules at various locations as detailed in Table 3.1.

From the timing of the images it was also possible to calculate small bowel transit time as the time taken from the stomach to the appearance in the colon which was 169 ± 22 min (n = 4, mean ± STD).

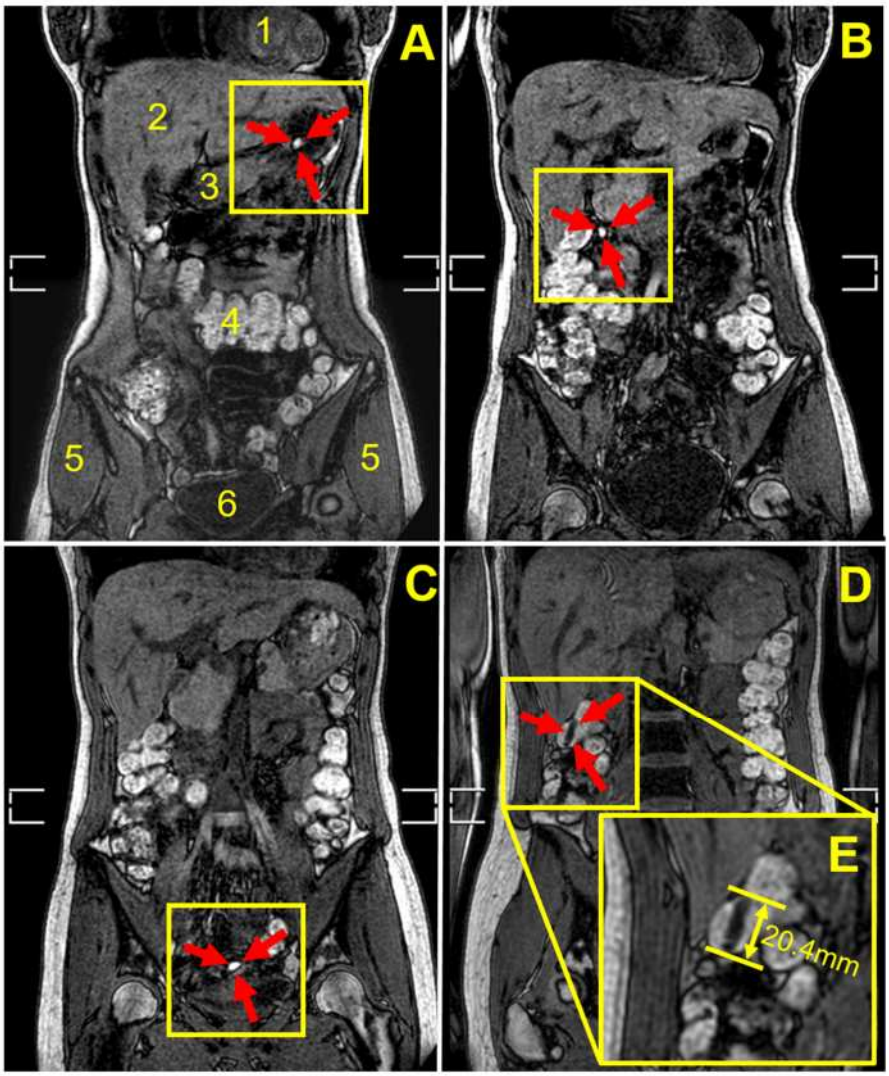

Figure 3.1. Coronal, fat and water out of phase MRI images of the abdomen of participant number 2 after consumption of the coated capsule co-administered with 240 mL of water. Anatomical landmarks are indicated in (A) by numbered labels as heart (1), liver (2), stomach antrum (3), transverse colon (4), gluteus medius muscle (5) and bladder (6). The white brackets at the side of the body derive from the fusion of the two separate breath-hold image stacks acquired. The filled capsule appears bright. It was located intact and floating in the body of the stomach 45 min after consumption as shown in panel (A) indicated by the red arrows inside the yellow box. The capsule was detected later in the small bowel in the duodenum 90 min (B) and ileum (C) 135 min after consumption. Finally, the capsule was located in the large intestine in the ascending colon, near the hepatic flexure, 180 min after consumption (D). By this time the capsule appeared to be empty of oil but still with an almost complete capsule shape, visible in (D) as a dark spherocylindrical object that measured 20.4 mm length (inset E). The white brackets at the side of the body derive from the fusion of the two separate breath-hold image stacks acquired.

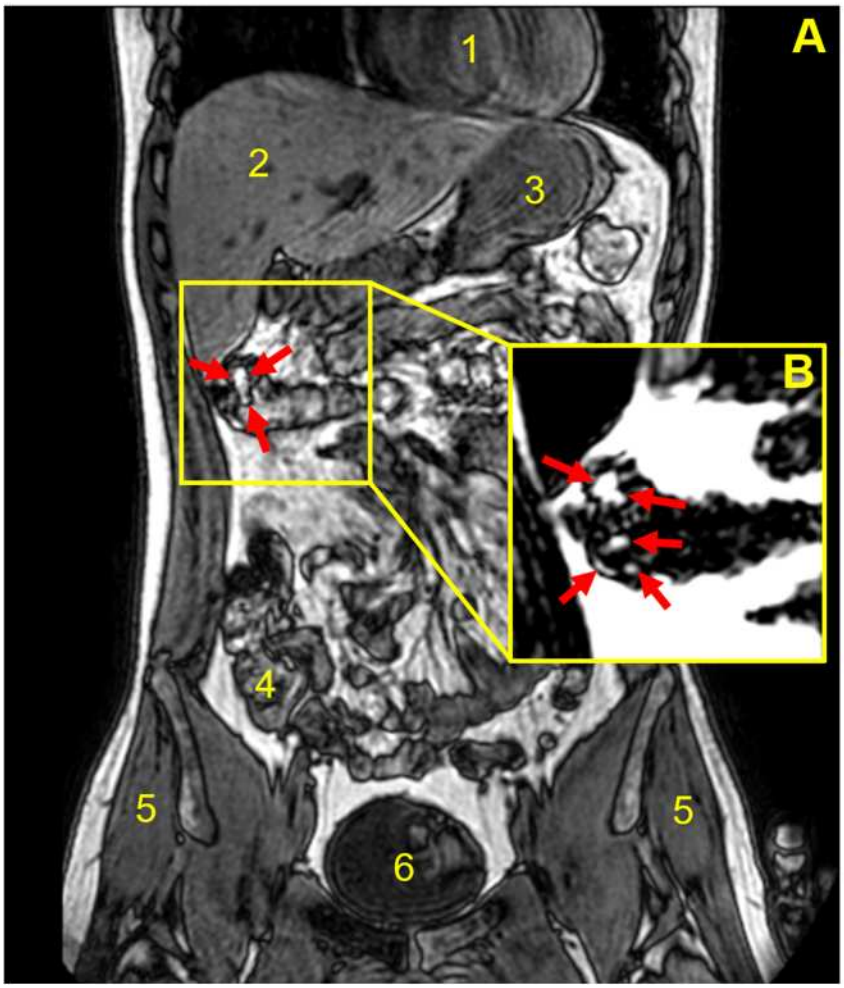

Figure 3.2. Coronal, fat and water out of phase MRI image of the abdomen of participant number 3, acquired 180 min after consumption of the coated capsule with 240 mL of water. Anatomical landmarks are indicated in by numbered labels: heart (1), liver (2), stomach fundus (3), transverse colon (4), gluteus medius muscle (5) and bladder (6). (A) The filled capsule appears bright and is located in the ascending colon/hepatic flexure of the large intestine. The capsule here appeared deformed and unevenly filled. The inset (B) is from the corresponding fat only MRI image, capturing oil leaks out of the capsule into the colon indicated by the red arrows.

Table 3.1. Summary of the specifications of the capsules administered to the healthy human participants and their location and integrity in the gastrointestinal tract at different time points post ingestion.

Participant/ Sex	Weight gain (mg; %)[a]	Weight gain per surface area (mg/mm²)	Gastrointestinal location and integrity of the capsule at the different imaging time points (min)							
			45	90	135	180	225	270	315	360
1/M	9.2±0.8; 1.9	0.02	Stomach	Stomach	*Stomach*[b]	NO[c]	NO	NO	NO	NO
2/M	18.2±1.2; 2.9	0.04	Stomach	Stomach	Duodenum	Duodenum	Term ileum	NO	NO	[d]
3/M	18.2±1.2; 2.9	0.04	Stomach	Stomach	Term ileum	*Asc colon*	*Hep flexure*	*Hep flexure*	*Hep flexure*	*Hep flexure*
4/F	18.2±1.2; 2.9	0.04	Stomach	Jejunum	Jejunum	Jejunum	*Term ileum*	*Term ileum*	*Term ileum*	NO
5/F	18.2±1.2; 2.9	0.04	Stomach	Jejunum	*Caecum*	*Caecum*	*Asc colon*	*Asc colon*	NO	*Hep flexure*
6/F	18.2±1.2; 2.9	0.04	Stomach	Stomach	Term ileum	*Term ileum*	NO	NO	NO	NO
7/F	25.9±1.6; 4.6	0.06	Stomach	Jejunum	Jejunum	*Term ileum*	*Term ileum*	NO	NO	NO
8/F	36.0±5.2; 11.2	0.08	Stomach	Jejunum	Term ileum	*Caecum*	NO	NO		
9/F	52.6±9.7; 20.2	0.11	Stomach	Duodenum	Term ileum	Hep flexure	Hep flexure	Trans colon	Trans colon	
10/F	52.6±9.7; 20.2	0.11	Stomach	Stomach	Duodenum	*Duodenum*	NO	NO		

[a] Mean±Standard Deviation of triplicate measures measured 24 hours after coating.

[b] When loss of integrity of the capsule (deformation of the capsules and/or release of some or all the oil filling) was detected in the images, this is indicated by italic font.

[c] NO, Not Observed, indicates when it was not possible to observe the capsule in the MRI images.

[d] Grayed out cells indicate no imaging was performed at that time point.

Abbreviations: F: female; M: male; Asc: ascending; Hep: hepatic; Term: terminal; Trans: transverse.

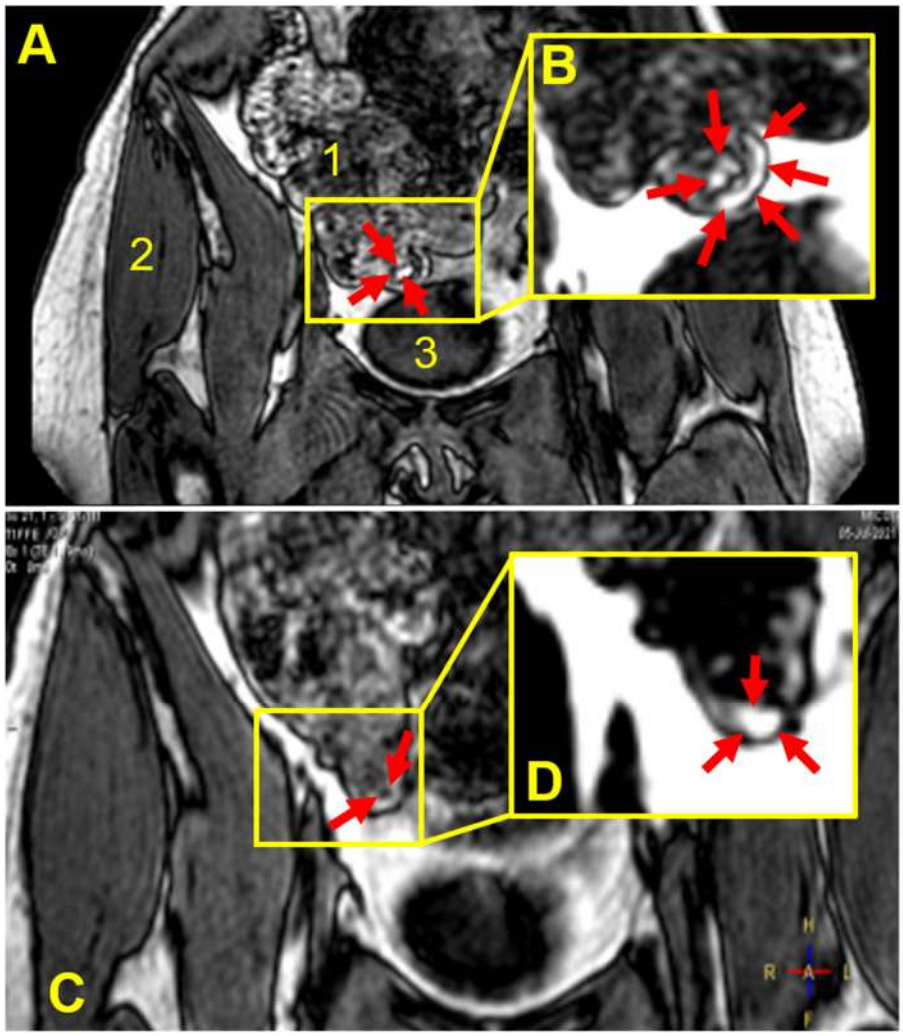

Figure 3.3. Coronal, fat and water out of phase MRI images of the abdomen of participant number 5 acquired 135 min (A) and 180 min (C) after consumption of the coated capsule with 240 mL of water. Anatomical landmarks are indicated in by numbered labels: ascending colon/caecum (1), gluteus medius muscle (2) and bladder (3). The filled capsule appears bright and is located in the caecum/ascending colon of the large intestine and appeared to be deformed and partially filled (A), the capsule being indicated by the red arrows inside the yellow box. The corresponding fat only image (inset B) captured oil leaks out of the capsule into the colon, indicated by the red arrows. At the later time point (C) the capsule, indicated by the red arrows inside the yellow box, appeared to have emptied further and provided some water signal component as well, possibly due to hydration/mixing. The corresponding fat only image (inset D) captured a cloud of oil filling that leaked out of the capsule into the colon, indicated by the red arrows.

3.4 Discussion

This is the first study to assess the feasibility of using MRI to locate an oil-filled, gastro-resistant (enteric) polymer coated capsule throughout the gastrointestinal tract and evaluate its integrity. Olive oil was chosen as an MRI-visible marker fluid filling for the capsules for two principal reasons. The first one is that conventional MRI scanners have the unique ability to capture and image signal from fat separately from the water signal and to produce different algebraic combinations of fat and water in phase or out of phase from each other, a method known as Dixon imaging. The olive oil contained in the coated capsules provides high MRI fat signal and virtually no MRI water signal allowing to image the intact capsule as well as oil released from a capsule that has lost its integrity. Gadolinium is a traditional MRI marker but has been associated with brain accumulation and other oral MRI markers with superparamagnetic properties for the detection of solid formulations have been discontinued from the market.

Here, as illustrated in the MRI images in Figures 3.1 to 3.3, the fat and water out of phase imaging combination was able to clearly visualize the capsule, whilst providing good anatomical detail, enabling assessment of the capsule's spatial location within the gastrointestinal tract. Furthermore, considering imaging of oil-containing formulations in the distal intestinal tract, one would not expect to find much fluid fat in the chyme in the colon and therefore the signal from the oil in the capsule should be clearly visible. The second reason is that olive oil is an inexpensive, safe, food-grade material, and there are no

ethical issues arising from the capsules disintegrating and releasing oil in the bowel of healthy human participants.

The disintegration test undertaken on Eudragit® S 100 coated HPMC capsules illustrates dependence of the capsules disintegration on weight gain due to coating. Uncoated capsules disintegrated in acidic environment (simulated stomach conditions), whilst all tested coated capsule remained intact for the duration of the acidic environment test (1 hour). In pH 6.8 buffer, simulating intestinal conditions, capsules with 9.2 mg of coating material lost their integrity to release the encapsulated oil, and then disintegrated entirely in less than 20 minutes. On the other hand, the capsules with 18.2 and 25.9 mg of coating layer maintained their integrity in the intestinal buffer stage for approximately 2 and 6 hours respectively, until the release of oil was observed, indicating that the intestinal capsule integrity is proportional to the coating weight gain. These *in vitro* findings corroborate the *in vivo* MRI imaging findings. More specifically, the capsule with 9.2 mg weight gain (administered to participant No 1) showed loss of integrity while still present in the stomach. In the participants that were administered capsules with the weight gain of 18.2 mg and higher, the capsules were emptied from the stomach intact and travelled further down the gastrointestinal tract. The MRI data obtained initially guided iteratively the selection of coating, so that the performance of the capsule with 18.2 mg coating during *in vitro* as well as *in vivo* studies meant that these were predominantly used in the study. In three participants we tested capsules with much higher coating gain (36.0 and 52.5 mg) and resistance to disintegration, the latter shown in the *in vitro*

disintegration test, and observed loss of their integrity in two participants, with intact capsule observed in transverse colon region of one participant.

It should be noted that coating of a surface (e.g. capsule shell) with a polymeric material may results in a creation of an uneven layer, particularly if adhesion forces between two materials are low and this was the reason this study used HPMC capsules. We have visually inspected all capsules tested and used in the MRI study for any unevenness and selected only those with even, smooth coating. In further studies and optimizations, one would aim to measure the layer thickness and its uniformity at the capsule shell. Furthermore, future studies could evaluate the bioavailability of active pharmaceutical compounds incorporated within the capsule.

One limitation of this study was the relatively prolonged interval between consecutive imaging time points. The participants were scanned every 45 minutes and, once the imaging was completed, asked to sit upright in an adjacent room until the following scan time point. This imaging protocol was adopted to make the study day more comfortable for the participants. However, in this way events that may have occurred between scans could not be recorded.

In Table 3.1, when the capsule presence in the image stacks could not be detected, this was labeled as 'Not Observed'. In most cases this has occurred after the capsule was at the previous time point observed to be losing its shape and integrity, or release of encapsulated oil was noticed (text in *italic* in Table 3.1), therefore losing the capsule's imaging signal. In some cases (for example in participant No 5) this might also have meant that at the time of

data acquisition physiological motion could have blurred the capsule signal, effectively masking the visual identification of the capsule's presence. The three-dimensional image acquisition scheme used in this study can be particularly sensitive to motion, and one could in future deploy two-dimensional, multi-slice acquisition sequences to minimize the effect of motion on the images.

The study indicates that Eudragit S 100 coating higher than 0.02 mg/mm^2 of polymer would be needed to ensure capsule's gastro-resistance *in vivo,* based on the data for participant No 1 *versus* those from participants administered capsules with coating equal or higher than 0.04 mg/mm^2. The latter coating resulted in capsules that, in all but two of the participants, reached, and were imaged in, more distal gastrointestinal regions. In this study we have been able to image the presence of coated capsules in the colon in three participants, as illustrated in Figures 3.1 to 3.3, and showed direct imaging of colon delivery and spread of the oil 'payload' inside the colon.

This type of non-invasive imaging studies could assist in understanding distribution of formulations and pharmacologically active ingredients in the colon. Increased knowledge of colon-targeted formulation location and disintegration timing could also inform advanced *in silico* approaches.

3.5 Conclusions

This feasibility study demonstrates that a combination of MRI imaging and fat-filled, coated capsules can extend the reach of current MRI methods to

image more distally along the bowel. This can provide information on the formulation transit, as well as information on the release of the payload in the colon. This method could be used in the future to assess performance of delayed release formulations in an un-disturbed gastrointestinal environment, without using ionizing radiation. This approach could also be used to deliver active pharmaceutical ingredients whilst monitoring the transit and actual arrival in the colon. Further work needs to be done to demonstrate the use of the MRI monitoring of the capsule in conjunction with an active drug marker and its absorption. This is the subject of the following Chapter.

4 *In vivo* MRI versus caffeine assay study

This Chapter builds on the previous work one by adding caffeine as drug marker inside the coated capsules. Nine healthy participants were administered capsules manufactured with varying amounts of Eudragit® coating and caffeine absorption was measured from serial saliva samples using an optimised high-performance liquid chromatography (HPLC) assay. Good correlation was shown between the MRI observations on loss of integrity and appearance of caffeine in the saliva assays.

4.1 Introduction

Linking oral dosage form disintegration and pharmacokinetic parameters such as the time of systemic drug appearance is key to the design of a dosage form and this is particularly important for coated formulations. Having developed the methods to manufacture and image in the body the coated capsules, the next logical step for this project was to add a drug marker that could be assayed, so that correlation of MRI imaging data and drug absorption data could be investigated.

In the literature there are a few examples to consider. They will be noted here to link with the choice of API and discussed further at the end of this Chapter.

One study used caffeine encapsulated in an ice capsule and focused on the stomach and gastric emptying [128]. The investigators then assessed the use of MRI in conjunction with a caffeine saliva assays and showed that the technique is feasible. In another study, caffeine was encapsulated in hard gelatin capsules along with iron oxide as the MRI marker [142]. Timing of capsule disintegration was successfully identified by MRI imaging and salivary caffeine increase concentration. MRI was again used with saliva analysis of caffeine to study the co-administration of small (size 3) and large (size 00) hard capsules as vehicles to study the when and where oral drug release occurred in the GI tract [52]. The different capsule shells used were commercially available, based on HPMC and gelatin and used as singles or capsule-in-capsule vehicles. The capsules contained iron oxide, hibiscus tea powder and caffeine which was evaluated successfully in saliva. MRI and caffeine saliva analysis were also combined to investigate a commercial ready-to-use gastro-resistant capsules in 8 healthy participants [51]. Correlation of MRI measurements with caffeine results was strong for the capsules that broke down in the small bowel where these two techniques gave similar results. Gastric residence time and disintegration upon gastric emptying could not be correlated which showed that these capsules had their enteric properties designed properly and further showed that gastric residence did not affect the capsule disintegration in the small bowel.

The development of an MRI-visible HPMC coated capsule and the possibility to use MRI to track its disintegration in the distal gastrointestinal tract in human healthy participants was discussed in Chapters 2 and 3.

The aim of this study was to incorporate a model active pharmaceutical ingredient (API) inside the coated capsules and test the hypothesis that systemic drug appearance will correlate with the MRI observation of the loss of integrity of the capsules in the GI tract of healthy participants.

4.2 Materials and Methods

4.2.1 Choice of the active pharmaceutical ingredient (API)

There was careful consideration on the selection of the API to be encapsulated and used as a drug absorption marker. In the literature, a range of drugs have been investigated and associated with absorption from the distal bowel. These included, mesalazine and sulphasalazine for their use in UC and oxprenolol, metoprolol, theophylline, verapamil, diltiazem, budesonide, nifedipine, acetaminophen (paracetamol), quinine and caffeine [53, 82, 90, 143-153].

For this work, the choice of possible drug absorption marker fell on caffeine, quinine and acetaminophen as they are relatively safe in small amounts in single acute doses, they can be absorbed through the colonic wall and their absorption can be measured from non-invasive saliva sampling and subsequent assays [53, 82, 152]. Ethical approval by the University of

Nottingham's Faculty of Medicine and Health Sciences Research Ethics Committee (approval number 402-1910) was obtained for the use of either caffeine, quinine and, acetaminophen. Ultimately, caffeine was chosen for the study, the primary reason for this being the existence of an HPLC assay protocol in our Pharmacy laboratory. This would be much quicker to build on rather than developing and validating completely new assays for the other drugs, as pressure on the timelines of the project from the Covid-19 pandemic aftermath was mounting.

Other considerations for the choice of caffeine is that it is a safe API to use and a typical cup of coffee provides 150 mg of caffeine [53]. There has been also sufficient evidence for its determination in saliva samples. Saliva samples were produced in an unstimulated manner as it has been found that stimulated saliva production can have different physicochemical characteristics [154]. Studies have shown that caffeine is absorbed from the colon with the mechanism of passive transport. Its appearance in saliva reflects the plasma caffeine appearance on a first-order excretion process and its oral bioavailability is 100% [53].

4.2.2 Caffeine assay optimisation

The basic HPLC analysis protocol to detect caffeine in saliva samples had been developed previously by the team [155]. After an initial familiarisation with the previous protocol, for this study additional work was carried out to optimise the conditions, peak shapes and run time for the injections. This work consisted of trials of different combinations of the mobile phase and

reconstitution solution, pH of the buffer solution, column temperature and the use of a guard column or not. This work led to optimise the mobile phase combination to 92% of 10 mM ammonium acetate at pH 4.5 and 8% ACN as the mobile phase. This optimisation was based on results of retention time, total run time, peak shape and overlap and machine background pressure.

Next, the assay was validated in terms of the Lower Limit of Quantification (LOQ) to establish the sensitivity of the assay to quantify low traces of caffeine. Concentrations of 10, 15 and 20 ng/ml were tested. The concentration of 15 ng/ml was chosen as the LOQ as it was the lowest concentration that had met the criteria of both the mean of the Relative error (RE) and Coefficient of variation (RSD) < 20%.

HPLC – Final Chromatographic conditions

Separation of the extracted caffeine samples were achieved with Phenomenex Luna C8 (2) 2 x 150 mm, 3 µm particle size column, and pre-column filter including a 0.5 µm stainless steel frit maintained at 50 °C. Mobile phase was 92% 10 mM ammonium acetate at pH 4.5, and 8% ACN, eluted at isocratic conditions at 0.22 ml/min. Caffeine and antipyrine were detected at 273 nm and 241 nm at 9 and 23 minutes respectively.

Caffeine concentration in unknown samples was evaluated by the construction of a calibration curve of peak height ratios of caffeine and antipyrine versus respective caffeine concentrations (15–10,000 ng/ml) with

the use of linear regression. Calibration curves all had correlation coefficient (R) values of > 0.99.

4.2.3 Coated capsules manufacture

Coated capsules were manufactured according to the methods described in Chapter 2. The capsules were manually filled with 0.5 ml olive oil (Tesco Stores Ltd, Welwyn Garden City, Hertfordshire, UK) as the MRI-visible agent and 75 mg of caffeine (Sigma-Aldrich®), suspended, as the absorption API marker. Next, the capsules were sealed with Methocel™ K4M glue (Colorcon) and manually dip-coated. A 10.7% solution of Eudragit® S 100 was selected, TEC was added as a plasticizer and a range of different coating cycles was applied to the capsules. No coating and 1,2 or 3 coating cycles were applied in order to study capsules with a range weight gains.

4.2.4 Saliva samples preparation

For caffeine analysis, 100 µl saliva sample was used. The internal standard used for caffeine detection was 10 µl of 50 µg/ml antipyrine (Sigma-Aldrich, UK).

Protein precipitation was carried out with the addition of 400 µl of 50:50 acetonitrile, methanol mixture (stored at -20 °C). The samples were then vortex mixed in a multi-tube vortexer (VWR VX-2500,VWR, UK) for 2 minutes for protein precipitation.

Some representative examples of the chromatograms (Figures 4.1 to 4.3) are included below.

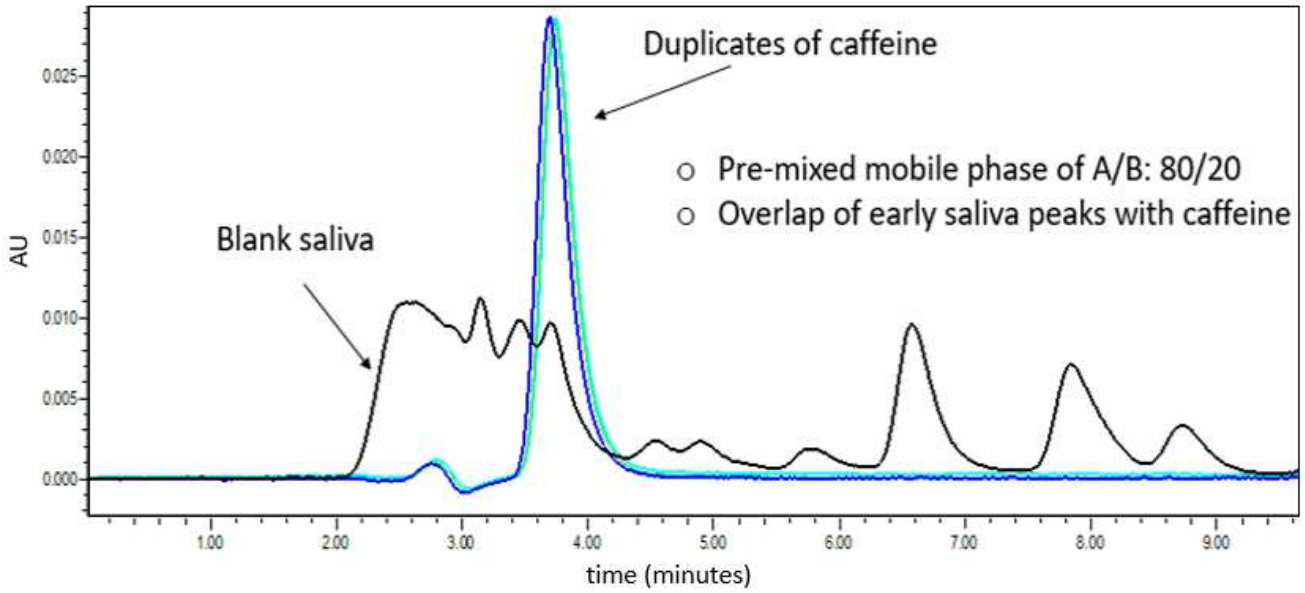

Figure 4.1. Example of high performance liquid chromatography (HPLC) chromatogram of caffeine C = 1000 ng/ml (blue and green) and blank saliva (black) injections with mobile phase of 80% 10 mM ammonium acetate at pH 4.5 and 20% ACN. There was significant overlap of early saliva peaks with caffeine peaks.

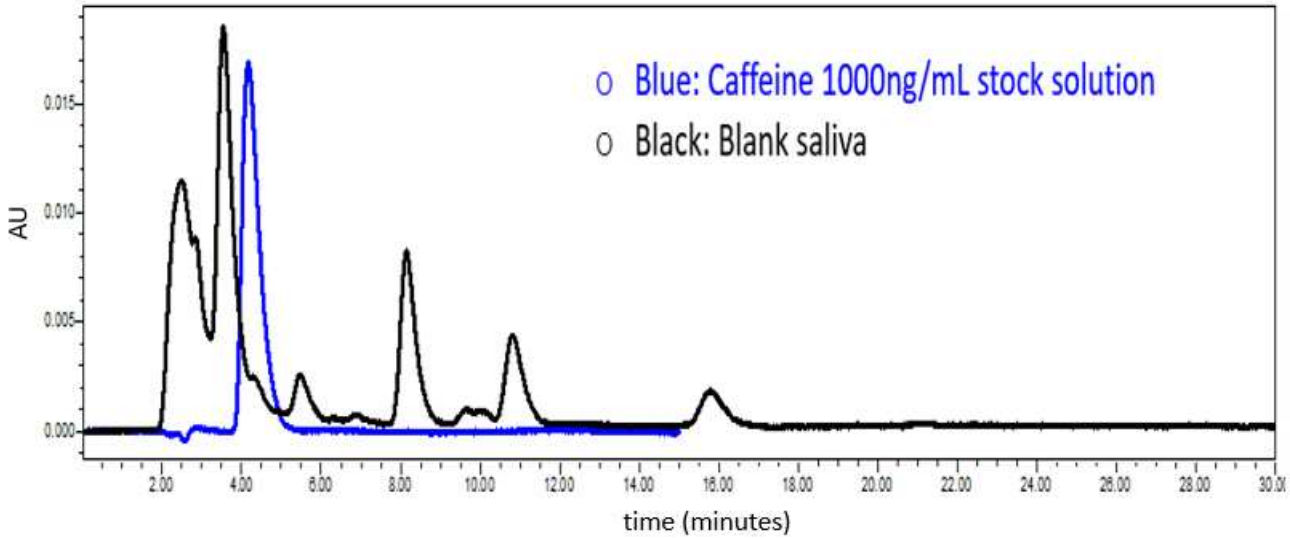

Figure 4.2. Example of high performance liquid chromatography (HPLC) chromatogram of caffeine C = 1000 ng/ml (blue) and blank saliva (black) injections with mobile phase of 86% 10 mM ammonium acetate at pH 4.5 and 14% ACN. There was significant overlap of early saliva peaks with caffeine peaks.

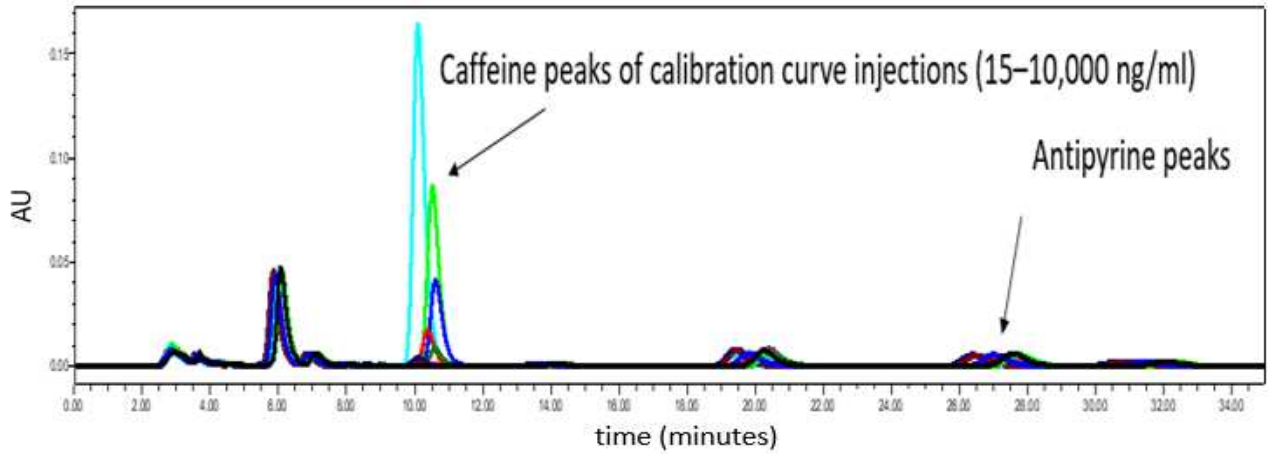

Figure 4.3. Example of high performance liquid chromatography (HPLC) chromatogram of injections of caffeine C = 15-10,000 ng/ml, blank saliva and internal standard of antipyrine with the mobile phase of 92% 10 mM ammonium acetate at pH 4.5 and 8% ACN.

Next, 4 ml of methyl-tert-butyl ether (MTBE) was added to each test tube as the organic solvent for liquid-liquid extraction. After the addition of MTBE, the tubes were vortexed for 10 minutes, and then they were centrifuged at 1690 × g for 10 minutes. Following centrifugation, the organic layer was transferred and evaporated to dryness under nitrogen. The dry residue was then reconstituted with 100 µl of 92% water, 8% ACN.

Reconstituted samples were then vortex mixed and centrifuged at 10,000 rpm for 3 min, before filtering using Costar Spin-X centrifuge tubes with 0.22 µm pore CA filters (Corning B.V. Life Sciences, UK) and then the contents were transferred to HPLC vials.

4.2.5 Study design

The clinical study was an open-label, one arm, feasibility study in healthy adult participants. Ethical approval was obtained as mentioned above. All participants gave written informed consent, and had no contraindications to MRI. Inclusion and exclusion criteria were presented in Chapter 3.2.1. Further exclusion criterion for that study was consumption of caffeine and/or caffeinated products within 48 hours of the MRI study day. They were asked to fast from 8:00 pm the evening prior to the MRI study day. They were also asked to skip breakfast and to report to the imaging facilities fasted. Prior to the study process, all participants underwent an initial fasted baseline MRI scan to check that the stomach reflected fasting state, determine anatomy and to plan upcoming scans.

Following that, the participants were administered in a standing position a coated or uncoated capsule with the standard FDA oral dose of water (240 mL) that is used in drug trials of solid oral dosage forms [140].

Participants were then scanned at predetermined time intervals, with the images acquired every 45 min post-administration of the capsule. At baseline and at intervals throughout the study day the participants were asked to provide a sample of saliva, using a disposable straw, into a cryotube which was immediately frozen in liquid nitrogen and later transferred to a -80°C freezer for subsequent analysis.

Image data were acquired until the capsule could no longer be detected due to release of content or up to 8 h post ingestion, whichever was longer. When the coated capsule exited the stomach, a meal consisting of a cheddar and ham sandwich, a 25 g pack of salted crisps, a butter croissant, and 500 ml of water (total energy content 670 Kcal) was provided to the participants. The timing of meal administration was chosen so that the capsule would first be emptied from the stomach in the fasted state, without interference or delays caused by a meal. Also, a meal provided after the capsule left the stomach would promote fed state GI transit whilst at the same time interrupting the fasting that the participants had been keeping up to that point. At each time point, for each participant, the gastrointestinal tract location of the capsule was noted from the image data. Additionally, the capsule's intact appearance or loss of integrity, intended as apparent deformation of the capsules and/or release of some or all the oil filling, was noted and determined by the PhD

student and the MRI radiographer. When the capsule presence in the image stacks could not be detected, this was labelled as Not Observed (NO).

4.2.6 MRI Acquisition

The MRI parameters established in Chapter 3 were used again here. Namely, the participants were scanned in a supine position in a 3 Tesla Philips Achieva MRI scanner (Philips, Best, The Netherlands). They lay supine on the scanner table with a 16-channel receiver placed around the abdomen. Coronal views of the abdomen were acquired, divided into short breath hold stacks. At each time point, the MRI procedure took approximately 15 min including set up, scout imaging and calibrations.

4.2.7 Time of onset of caffeine absorption

From the HPLC data, the time of onset of caffeine absorption was determined as the time at which the concentration of caffeine in the saliva assays raised from baseline by more than a LOQ and this was termed Tlag.

When the HPLC assay time courses provided not only the rise and peak caffeine concentration but also sufficient elimination time course data points to allow meaningful pharmacokinetic modelling, the time of onset of caffeine absorption was also modelled using Phoenix WinNonlin software Version 6.4 (Pharsight, Mountain View, USA). The modelling software considered the LOQ as well. The modelled parameter was termed Tlag(model) to distinguish it from the previous Tlag parameter described above.

4.2.8 Statistics

Linear regression was used to assess the relationship between the MRI timing of the loss of capsule integrity and Tlag (both experimental and calculated from pharmacokinetic modelling) and also between the Tlag parameters derived from experiment and from pharmacokinetic modelling. R-Squared was used as as measure of the variance between variables, and a p value <0.05 was used to reject the null hypothesis that the variables had no correlation.

4.3 Results

Nine healthy adults (6 male and 3 female) participated. They were 19-34 years old with no history of underlying cardiac or gastrointestinal disorders or symptoms. All participants had a normal-range body mass index (BMI) between 21.9 and 23.5 kg/m^2, and reported no food intolerances or allergies. All participants tolerated well the study procedures: they were all able to swallow the capsules easily, tolerated the serial MRI scanning procedures and the relatively long study day well and there were no adverse events related to the study procedures.

It was possible to visualise the coated capsule intact and the loss of integrity using MRI.

Figure 4.4 shows a representative example of MRI tracking of a capsule inside the body of one participant. The intact capsule is visualised in the terminal

ileum of the participant (Figure 4.4A and enlarged fat-only MRI inset (in Figure 4.4B). At time 135 minutes, the capsule was propelled further down to the terminal ileum (Figure 4.4C) where it was possible to identify on the MRI images the initial deformation (loss of original shape) of the capsule and the start of the release of the oil on the fat only MRI images. The spatial extent of the release of oil could be seen in the multi-slice fat-only MRI scans (Figure 4.4D, E, F and G). In these image slices the capsule was depicted partially filled, embedded in the colon chyme and close to the colon wall.

For each participant the time of loss of integrity of the capsule after consumption was noted, together with the gastrointestinal site of loss of integrity as shown in Table 4.1. For each participant the time of onset of absorption of caffeine Tlag was also reported in Table 4.1.

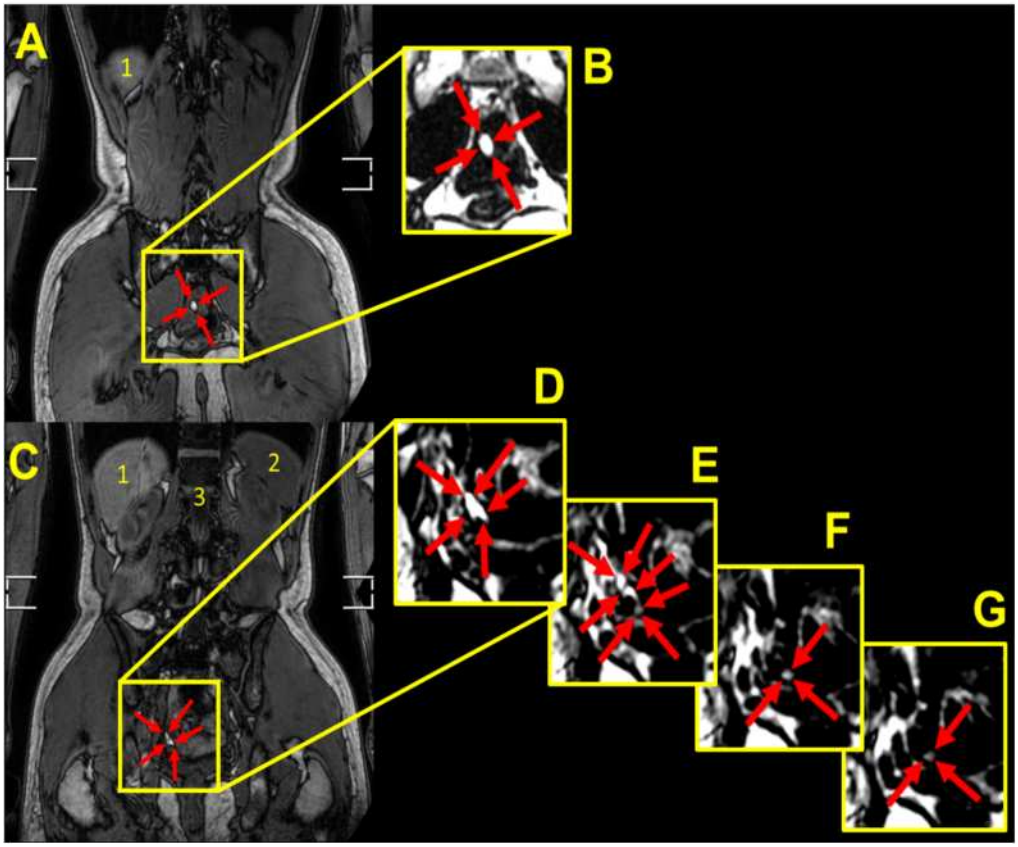

Figure 4.4. (**A**) Coronal, fat and water out of phase MRI image of the abdomen of a representative participant (participant number 8), 90 minutes after consumption of a 36 mg weight gain coated capsule. The filled capsule, indicated by the red arrows inside the yellow box, appeared bright and intact in the terminal ileum. Inset (**B**) shows an enlarged fat-only coronal MRI image of the capsule. (**C**) At time 135 minutes the capsule was detected more distally in the terminal ileum. By this time the capsule appeared to have lost integrity, deformed and unevenly filled. The inset (**D**) shows an enlarged fat-only MRI image, confirming loss of integrity. Insets **E**, **F** and **G** show contiguous fat-only coronal MRI image planes respectively going more posteriorly from inset **D**. They capture the deformed end of the capsule (**E**) and oil leaked out of the capsule into the terminal ileum (**F** and **G**) indicated by the red arrows. Anatomical landmarks are indicated in **A** and **C** by numbered labels as liver (1), spleen (2) and spine (3).

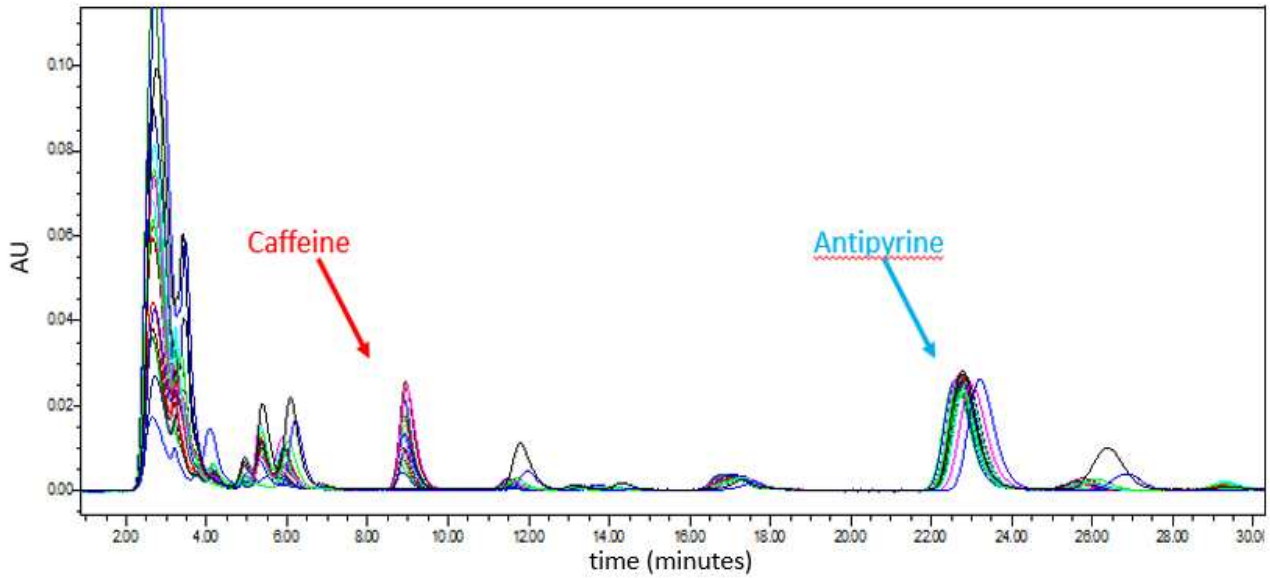

Figure 4.5. Example of high performance liquid chromatography (HPLC) chromatogram of the saliva samples from participant No 2 who ingested a 9.2 ± 0.8 mg weight gain capsule.

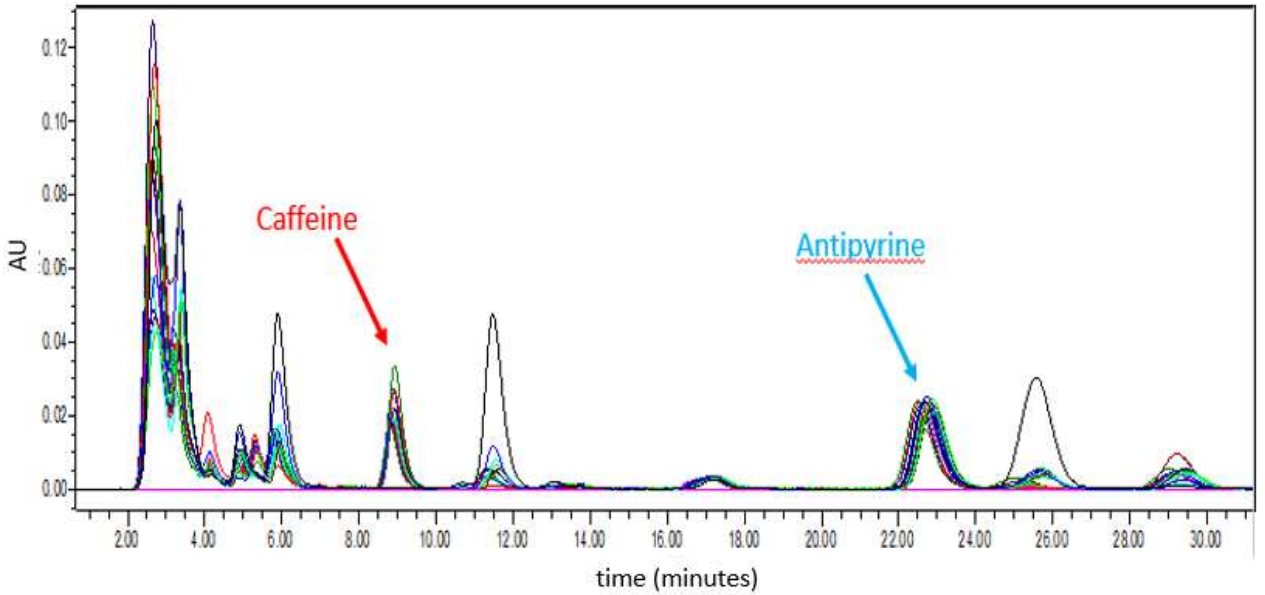

Figure 4.6. Example of high performance liquid chromatography (HPLC) chromatogram of the saliva samples of participant No 3 who ingested a 18.2 ± 1.2 mg weight gain capsule.

Table 4.1. Summary of the specifications of the coated capsules administered to the healthy human participants. The time and site of loss of integrity in the gastrointestinal tract as evaluated by MRI and the time of onset of caffeine absorption Tlag as evaluated by saliva high performance liquid chromatography (HPLC) are also indicated.

IDs/Sex	Capsule coating cycles	Capsule weight gain (mg; %)	MRI time of loss of integrity of capsule following administration (min)	Site of loss of integrity	Onset of absorption of caffeine following administration Tlag (min)	Phoenix WinNonlin Tlag(model) (min)
1/M	None	0	5	Stomach	20	0
2/M	1	9.2; 1.9	45	Stomach	105	60
3/M	2	18.2; 2.9	150	Term ileum	150	60
4/F	2	18.2; 2.9	145	Term ileum	190	n.a.
5/F	2	18.2; 2.9	155	Term ileum	170	n.a.
6/F	2	18.2; 2.9	95	Caecum	65	n.a.
7/M	2	18.2; 2.9	90	Term ileum	150	n.a.
8/M	3	36.0; 11.2	180	Term ileum	190	145
9/M	3	36.0; 11.2	150	Asc colon	160	n.a.

Abbreviations: F: female; M: male; Asc: ascending; Term: terminal; n.a.: not applicable.

The MRI timing of the loss of capsule integrity correlated well with Tlag ($R^2 = 0.76$, $p = 0.0022$).

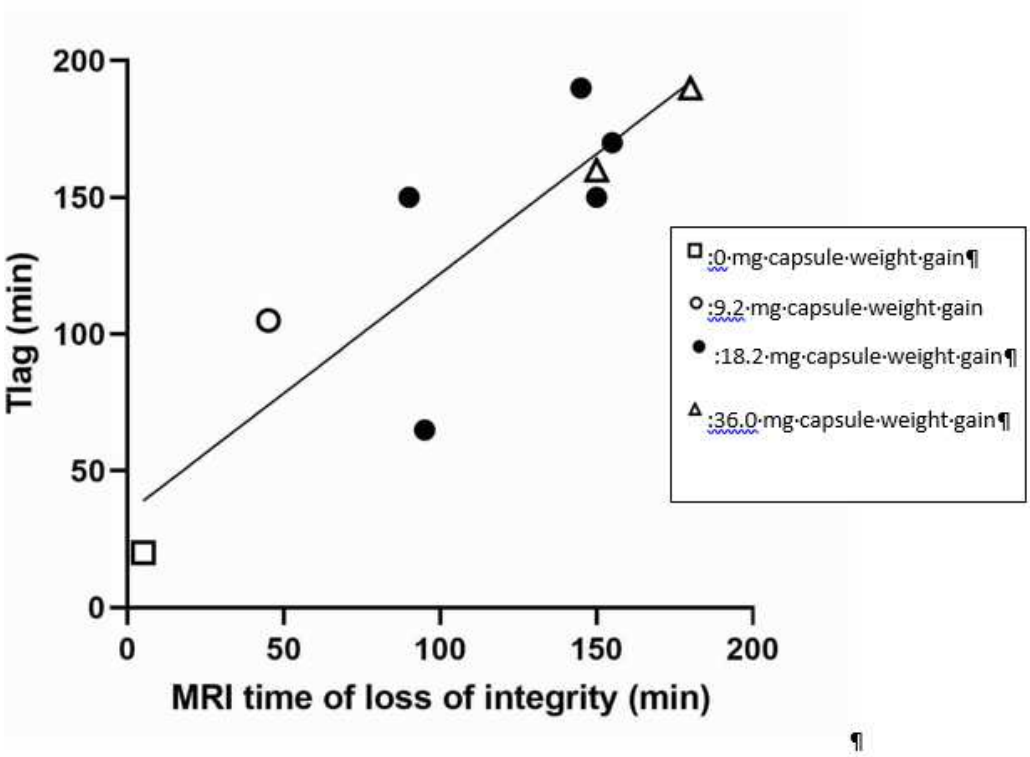

Figure 4.7: Correlation of the MRI timing of the loss of capsule integrity with Tlag defined as the time of the onset of caffeine absorption in the saliva assays). The participants (n = 9) swallowed one capsule each. There were 4 different types of capsules administered with different weight gain characteristics and they are represented here with different symbols (□ for 0 mg, ○ for 9.2 mg, ● for 18.2 mg and Δ for 36.0 mg capsule weight gain).

In 4 participants the time courses of the HPLC assay showed not only the rise and peak caffeine concentration but also sufficient elimination time course to allow meaningful pharmacokinetic modelling (Figure 4.8). For these participants the Tlag(model) parameter was calculated using Phoenix WinNonlin software and listed in Table 4.1.

Tlag(model) as expected correlated strongly with Tlag (R^2 = 0.85) and with the MRI timing of the loss of capsule integrity (R^2 = 0.72), though these correlations were not significant (p = 0.0773 and p = 0.1535 respectively).

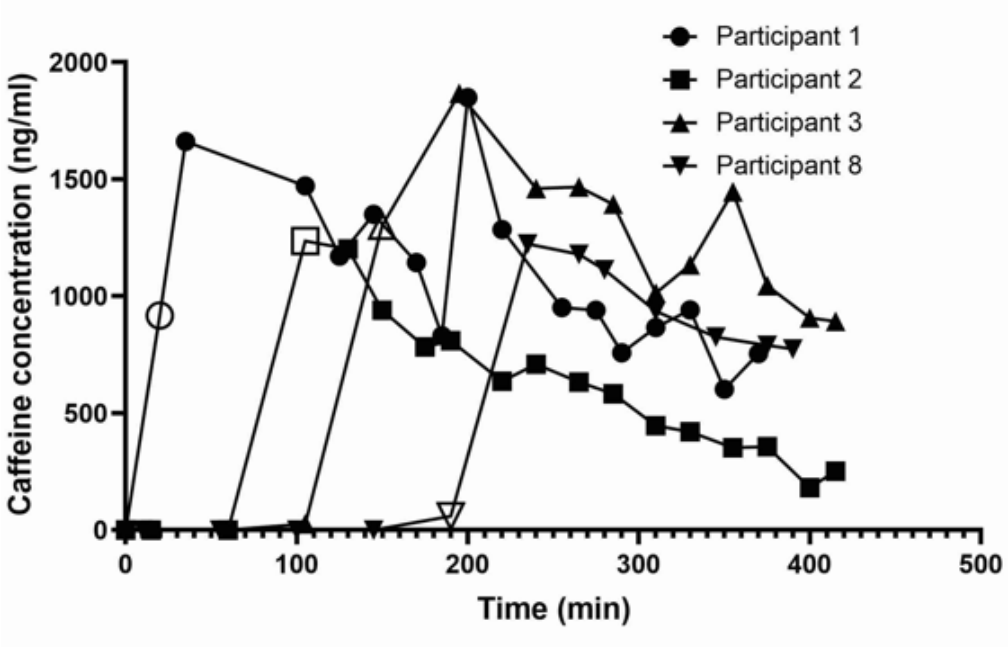

Figure 4.8: Time courses of the concentration of caffeine in saliva for participants 1, 2, 3 and 8 as measured by saliva high performance liquid chromatography (HPLC) assay. For each participant, the open symbol indicates the time of the onset of caffeine increase in saliva Tlag.

4.4 Discussion

The study presented here built on the previous chapter and added caffeine as API marker inside the capsules to investigate whether MRI monitoring of the fate of the coated capsules would correlate with drug absorption. The study was successful and the MRI data on timing of loss of integrity correlated well

with systemic appearance of the chosen model API and also with key pharmacokinetic modelling parameters.

Caffeine is known as the world's most widely consumed drug [156]. It was chosen for this work based on its safety profile, known determination methods from saliva, its high solubility, dissolution rate and rapid absorption when it becomes available in the gastrointestinal tract [51, 53, 93, 155, 157].

The MRI timing of the loss of capsule integrity correlated well with Tlag (R^2 = 0.76, p = 0.0022). This implies that MRI has the potential to identify, real-time and *in vivo,* the time point when a coated capsule loses its integrity and releases an API that it expected to be absorbed instantly. This observation is further strengthened by the strong correlation of Tlag(model) with Tlag (R^2 = 0.85) and with the MRI timing of the loss of capsule integrity (R^2 = 0.72), although not significant (p = 0.0773 and p = 0.1535 respectively). However, it has to be noted that the data available for this analysis was limited and this could explain the non-significance of the correlations.

Studies in the literature show that, caffeine was administered in form of tablets or capsules, but is also commercially available in energy drinks, gels, bars and gums [156, 157].

The caffeine API on the capsule went through sequential steps before being detectable in the saliva of the participants. Firstly, caffeine had to come out of the formulation vehicle (capsule). Then dissolution, absorption and transport of caffeine had to happen from the gastrointestinal tract into the systemic circulation. Lastly, caffeine had to transfer into the saliva [53]. Because

caffeine is rapidly dissolved and absorbed rapidly and extensively from the whole GI tract, the principal controlling factor for its availability in this study was its release from the capsule.

In this study caffeine absorption varied markedly among the participants. This could be linked to different gastrointestinal motility and transit patterns. For instance, different transit times could have led to higher exposure to the fluid pockets and/or bowel contraction forces (particularly gastric antral contractions) could have started an early loss of integrity of some capsules.

Some participants showed more than one high caffeine peak. Drug fluctuations in body fluids, which can be also further enhanced by meal consumption, are usually associated with enterohepatic circulation such as with 5-aminosalicylic acid (5-ASA). For example this drug was administered three times per dosing scheme and it was found to lead to a plasma peak 10 h after the last dosing in the next morning following breakfast consumption [158]. Since caffeine is not subject to enterohepatic circulation, multiple peaks can be indicative of initial leak from the capsules, followed by another release due to progressive failure of the capsules.

Using MRI here localized the capsules inside the GI tract and allowed to draw initial correlations of the imaging findings with caffeine absorption kinetics.

In our study, initial MRI scans ensured that participants were fasted and the same meal was provided after the capsule had left the stomach, thereby

reducing some variability. However, motility, gastric residence times and gastric emptying can vary between individuals and this should be taken into account in light of the different times of loss of integrity and location for capsules with the same amount of coating. Calculation of the MRI time of loss of integrity of capsule as the time from the capsule exit from the stomach to its arrival in the loss of integrity site should eliminate the impact of the variability of gastric emptying times. Other factors increasing variability could be inhomogeneous distribution of fluid pockets in the GI tract and different motility phases in the intestine which could exert different amounts of pressure on the capsules.

As mentioned in Section 4.1, there are a few previous studies in the literature that need to be discussed in relation to this work. One study used the interesting concept of freezing the 35 mg of caffeine as an API into an ice capsule, which was expected to melt quickly into the stomach with an 'immediate' release. The encapsulated caffeine was co-administered with 240 mL of tap water on a fasted or fed state (964 kcal meal: two strips of bacon, two slices of toast with butter, two eggs fried with butter, 113 g of hash brown potatoes, and 240 mL of full-fat milk). This study therefore focused on the stomach and gastric emptying rather than on the distal bowel. MRI showed the quick emptying of the 240 mL water co-administered with the ice capsule in 10-50 min both in fasted and fed state. Determination of caffeine levels in saliva proved as a useful methodology to correlate the water gastric emptying as a non-caloric liquid in both fasted and fed state and it was able to

be performed because caffeine dissolves instantly. The authors observed the phenomenon of the ''Magenstrasse'', whereby non-caloric liquids can find a preferential route to exit the stomach rapidly [128]. It is worth noting that caffeine itself may affect gastric emptying, secretion and oesophageal sphincter pressure which may in turn affect drug absorption and their variability [128].

Another study used, hard gelatin capsules to deliver caffeine, encapsulated together with iron oxide aimed to provide the MRI marker. Saliva assays were again used. The time difference between the MRI and saliva assay data was 4 min as the saliva peak appeared 4 min later. This was attributed to the fact that capsule broke in the stomach and then gastric mixing and emptying took place along with the processes of dissolution of the capsule shell, absorption and distribution which were also affected by the gastric motility processes. These could have possibly led to a delay of caffeine loading to the GI environment [142]. In the present study, the caffeine was suspended in olive oil. Although caffeine is insoluble in olive oil, the oily component may have somehow inhibited the immediate availability of caffeine to the absorption site.

A further study compared different size vehicles in order to assess the site and timing of caffeine (assayed in saliva again). Small (size 3) and large (size 00) hard capsules were used. These were HPMC and gelatin based, and available on the market as singles (Drcaps® and Vcaps®, 25 mg caffeine each) or capsule-in-capsule (DUOCAP®, 50 mg caffeine) vehicles. The capsules were

loaded with caffeine and with iron oxide and hibiscus tea powder, both for their strong signal when they are placed in a magnetic field. The timing and site of capsule disintegration was dependent on the combination of capsule shells but the authors noted a high inter-subject variability in the 6 participants. However, there was less variability for the DUOCAP® system (Drcaps® as release formulation in the Drcaps® capsule shell) with the inner one consistently opening after the ileum. The researchers then concluded that the combined formulation scheme is most promising for ileum-targeted drug delivery. For the administration of single formulations, the Vcaps® Plus HPMC capsules had the fastest and most reliable (less variability) disintegration (8.8 ± 3.0 min as assessed by MRI and 12.5 ± 4.5 min by saliva analysis) [52].

Another study used Lonza Capsugel® Next Generation Enteric as ready-to-use gastro-resistant capsules in 8 healthy participants. MRI imaging and caffeine API with saliva assays were also used. The gastric residence times were found to be variable (7.5-82.5 min) but no drug release/capsule break down was noted in the stomach. 7 capsules broke down distally in the small bowel and one in the colon due to unusually brief intestinal transit time (15 min). For this particular capsule, Gastric residence time and disintegration upon gastric emptying could not be correlated which showed that these capsules had their enteric properties designed properly and further showed that gastric residence did not affect the capsule disintegration in the small bowel [51]. In the present study, the coated capsules were expected to maintain their

integrity through the proximal GI tract and to be subject to more mechanical stress/movement and higher pH in the small intestine rather than in the colon where highly viscous environment exists.

4.5 Conclusions

This feasibility study built on the previous work shown in Chapters 2 and 3 and showed that MRI can localise the coated capsule in conjunction with PK analysis of the absorption of caffeine as an API marker. The MRI data correlated well with traditional HPLC techniques linking the loss of capsule integrity, intestinal location and appearance of caffeine in the saliva. This was done in an un-disturbed gastrointestinal environment. Such studies assessing drug formulations in the distal intestine can help our understanding of bioavailability differences in relation to gastrointestinal function and build more biorelevant predictive *in vitro* tools.

5 Small bowel motility MRI and manometry study

The final piece of experimental work explored the ability of MRI to monitor small bowel motility as another parameter of gastrointestinal function relevant to the passage of a dosage form through the small bowel. In this Chapter the analysis of a retrospective large data set of MRI motility dynamic images is described and the results compared to standard perfused manometry endpoints.

5.1 Introduction

The GI transit time of drug formulations has been found variable and dependent on their size and pre-existing motility activity [140]. GI motility has a determining role on transit times, GE and intestinal residence times which in turn can affect drug bioavailability. These processes and their temporal variability are associated with changes in bioavailability. Furthermore, when motility and content propulsion is studied alongside with fluid movement and the presence of intestinal water pockets the impact on drug absorption is substantial [33, 159]. The presence or absence of meals, as well as their caloric content, can affect motility and drug behaviour as well [160]. Transit time of solid elements such as food and drugs are also affected by gastric emptying rate, bowel motility and gastro-ileal reflex [24, 161]. Drugs are likely to be absorbed from a specific part of the GI tract (absorption window) and variations in GI motility can affect transit and local residence time which in turn can cause variability in their expected bioavailability [159, 161]. The

effect of GI motility on oral drug delivery is of greater importance in populations with motility disorders such as extended periods of stagnation and gastroparesis [162], and this can be predicted to be particularly relevant for drugs that have characteristics of low permeability or limited absorption from the lower intestine [163]. GI motility's consequences on drug absorption can impact bioequivalence studies for drugs that get absorbed and eliminated fast and for low absorption drugs as well [159].

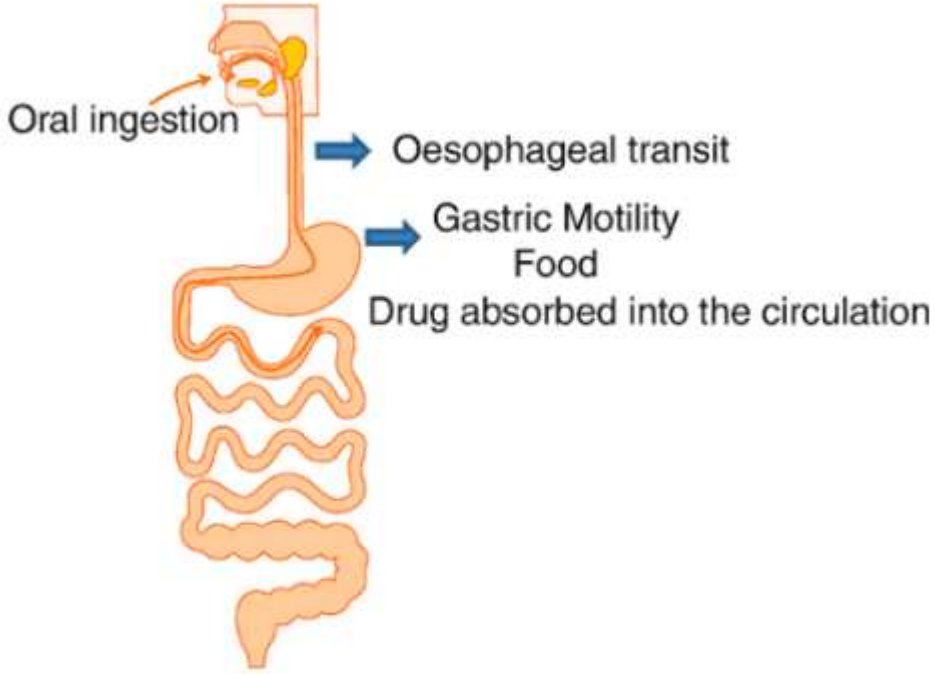

Figure 5.1. Oral drug absorption is dependent on gastrointestinal transit and motility patterns. Taken from [164].

The Migrating Motor Complex (MMC) is the main motility pattern found in the stomach and small bowel. It is a system of electrical waves driving patterns of movement (contractions) that originate in the stomach or upper duodenum and become stronger while travelling to the small intestine

(proximal to distal direction). This inter-digestive pattern starts approximately 2 to 3 hours post meal-consumption. The pace of the movement gradually decreases as it travels and once it reaches the ileum, a new activity font may start again proximally. Peristalsis is achieved when the activity front travels from its starting point to a lower point and successive peristalsis fronts can progress through the small bowel, moving the contents of the GI lumen. The activity front consists of waves (electrical slow waves, action potentials and contractions) that travel faster than the front itself. Each wave, with the associated action potentials and contractions, is one propulsive event in the activity front [13].

The MMC is divided into 4 successive periods. Phase I is quiescent, without contractions, Phase II has irregular contractile behaviour and represents the leading and trailing traces of the travelling activity front and Phase III has regular, strong, propulsive contractions which last 8-15 min and have a frequency of about 8-10/min. Phase IV is a transition phase back to the quiescence. The MMC's speed in the duodenum is around 3-6cm/min which slows down to about 1-2 cm/min in the ileum [13, 165].

Meal administration can interrupt an MMC that was progressing [165]. A duodeno-jejunal complex (DJC) motor pattern had also been described and may represent a motor transition in the distal duodenum where non-propagating pressure events were recorded at a frequency of 9-12/min. This suggested that local motility could be sub-divided into two physiologically different points, the point before the transition point was named duodenal

loop (DL) and after duodeno-jejunal (DJ) loop which was less intense in the fasted state and characterised by a sharp change of pressure/motility (duodeno-jejunal complex or DJC). This complex may help to retain food components in the DL region, which could act like a brake (duodenal brake) for further propagation of the chyme [166].

The contractile activity is usually studied with pressure sensors into the lumen or electrodes onto the GI surface [13, 140]. Manometry is the gold standard for measurement of GI contractions by measuring luminal pressure [140]. Recently, MRI has been used along with manometry for the measurement of GI pressure and motility [140, 167, 168]. High-resolution fibre-optic manometry has been introduced to investigate bowel motility under fed conditions previously hard to study due to limitations of traditional manometry techniques [140, 166].

In a previous study from our laboratory, Heissam et al. used MRI and simultaneous water perfused manometry in 18 participants in order to correlate these techniques for motility measurements. They analysed the MRI data relating to the antral motility using automated methods to determine the calibre of the stomach from dynamic MRI imaging and compared that analysis against the antral perfused manometry data. They concluded that there was a good correlation ($r = 0.860$) when plotting the area under the curve of the MRI antral measurements against the relevant manometry AUC [140]. However, all the data from that study relating to the small bowel motility remained to be analysed.

The current work shown in Chapters 3 and 4 imaged the HPMC coated capsule's journey through the small bowel and showed that in some cases the loss of integrity of the capsule could start in the upper small bowel too. This opened up the question of whether MRI could monitor also small bowel motility in order to provide more information on other bowel physiological events that the capsules can be subject to, beyond transit. Such data could be found in the small bowel MRI and manometric data sets from the Heissam study [140] that had not been analysed thus far.

Therefore, the primary aim of this retrospective study was to assess the ability of MRI to monitor small bowel motility by correlating MRI and conventional perfused manometry measurements of duodenal motility.

5.2 Materials and Methods

5.2.1 Subjects and study design

Eighteen healthy participants with no history of gastrointestinal disease (9 male; 9 female; age 29 ± 10 years old (mean ± SEM); body mass index (BMI) 24 ± 2 kg/m^2) participated in an MRI study investigating gastrointestinal fluid and motility responses to the standard FDA oral dose of water (240 mL) that is used in drug trials of solid oral dosage forms [140]. The study was approved by the University of Nottingham Faculty of Medicine and Health Sciences Research Ethics Committee (A14112016) and by the US Food and Drug Administration Research Involving Human Participants Committee (16-073D).

All participants gave writing informed consent for the study. The study was registered with ClinicalTrials.gov with identifier NCT03191045. Inclusion and exclusion criteria were presented in Chapter 3.2.1.

This study was single-centre and open-label requiring 2 same study visits of at least 4 weeks in-between of normal diet. They were asked to attend a first study day that lasted approximately 8 hours, and to return a week later when the whole study day was repeated. Inclusion criteria were to be healthy and in the age range from 18 to 60 years old. Exclusion criteria comprised the use of medication affecting gastrointestinal function, major surgery, working night shifts, habitual strenuous exercise, alcohol dependency and the standard contraindications for MRI scanning.

Each study day lasted approximately 8 hours and was divided in 5 parts. The participants were asked to fast overnight before each MRI study day. On arrival at the study unit the participants were intubated naso-duodenally by a designated clinical specialist (Dr Khaled Heissam). The first part was the naso-duodenal intubation and rest to allow the GI system to re-adjust to the manometer (up to 2 h). Local anaesthesia was performed with the administration of Xylocaine® spray (AstraZeneca Ltd, UK) and a water-soluble lubricant (Optilube 5 g sachets, Optimum Medical Solutions, Leeds UK) in order to move the intubation catheter through the nose. The second part had the application of MRI and manometry measurements (1 hour) and the third part was a rest break for the participant (1 hour). The third part was followed by administration of 240 mL of water and then the fourth part which had MRI

and manometry measurements again (3 hours). The last part of 1 hour was mainly for tube removal and participant discharge (Figure 5.2).

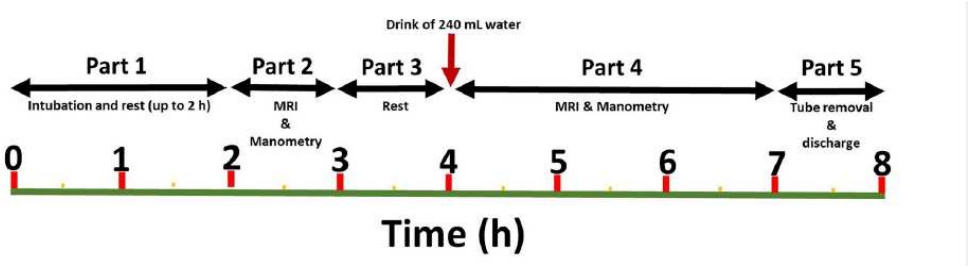

Figure 5.2. Diagram of the study day timeline. Taken from [140].

The custom-made water-perfused catheter (Mui Scientific, Mississauga, ON, Canada) had 16 channels and was MRI compatible. It had external diameter of 4.0 mm, luminal diameter of 0.3 mm, core of 1.0 mm with side holes at 5-cm intervals, total length of 180 cm with additional pigtails of 100 cm. Water was perfused at a rate of 1 mL/min and system pressure was set at 1 bar. The tube has a small balloon which can be inflated with water and is introduced in the body for MRI site localization. The catheter was connected to the manometry system (Biomedical Engineering Department, The Royal Melbourne Hospital, Melbourne, Australia).

Figure 5.3. The MRI compatible, 16 channel perfused manometry system used in this study is shown on the left. The computer and medical air pressure cylinder shown on the right remained in the scanner control room with cables and tubing to the MRI-compatible system in the scanner room passed through a wave guide in the wall.

The pressure recordings were made by converting the manometer measurements to electrical signal outside the scanner bore via the pigtail sensors and the attached electric cables and pipes. The manometry machine was calibrated manually before and after every study part and records were kept. The pressure recordings were kept in a digital format data logger (Trace 1.3, Biomedical Engineering Department, The Royal Melbourne Hospital, Melbourne, Australia) extracted to be analysed with a common software (MMS, Medical Measurement Systems B.V., Enschede, The Netherlands).

A break was then permitted, when the participants were allowed to step outside the scanner room having disconnected the catheter. Once the participants were back in the scanner, the system was reconnected and the 240 mL water administration followed as per standard recommendation of

the US Food and Drug Administration for bioavailability/bioequivalence (BA/BE) studies in the fasted state [169, 170].

At the final 3-hour part of the study, data was recorded with an optional 20 min comfort break and/or other comfort breaks if needed. During the study, the location of the catheter was occasionally checked by inflation of the balloon. Upon completion of the data collection, the catheter was removed and refreshments were provided.

5.2.2 MRI imaging of small bowel motility

MRI imaging was carried out on a 1.5T General Electric HDxt MRI scanner (General Electric Healthcare, Little Chalfont, Buckinghamshire, UK), shown in Figure 5.4.

Figure 5.4. The 1.5T XDxt MRI scanner at the Sir Peter Mansfield Imaging Centre at the University of Nottingham. The full body coil used for this study is visible on the scanner bed.

Bowel motility was assessed at intervals using a cine-MRI acquisition set at coronal oblique planes through the abdomen. Each dynamic motility MRI

scan acquired 33 sets of 4 slices over a time window of approximately 3.5 min. This was chosen to remain below the limit of the old scanner reconstruction hardware for a single cine-acquisition. During the cine-MRI scanning the participants were asked to breathe gently. The data were acquired using a FIESTA (TrueFISP) sequence (repetition time TR = 3s, echo time TE = 0.9s, Flip angle = 45°, Slice thickness = 8 mm, field of view = 400 mm x 400 mm, matrix size = 256x256, and image resolution in plan e= 1.56 mm × 1.56 mm with a slice thickness = 8 mm). Throughout each part of the study, the cine-MRI acquisition blocks were interleaved with other T2-weighted MRI scans carried out for secondary outcomes (not relevant to the thesis work) and also to visualise periodically catheter positioning by inflating temporarily the tip balloon with a small volume of fluid.

5.2.3 Water-perfused manometry analysis

The manometry data was retrieved from the system and loaded onto a different computer to be analysed using common commercial software (MMS, Laborie, Mississauga, ON). Expert GI physiologist Dr Jeff Wright from the Nottingham GI Surgery department was the researcher who carried out the manometry analysis, identified contractions and recognised motility events and patterns. Respiratory artefacts were removed from the pressure traces. The manometry traces were inspected visually for quality and then segmented in 10 minutes epochs. For each epoch the software yielded the area under pressure versus time curve or AUC in mmHg × second and also the Motility Index or MI in cmH_2O as in Ln((Number of peaks * (Number of peaks * Average amplitude))+1).

The presence and timing of any MMC III was also recorded in the manometry traces for each participant by the same specialist GI physiologist. Duodenal MMC phase III was defined as a propagated burst of contractions with a frequency of 10-12 per minute lasting for at least 2 minutes and followed by a period of motor quiescence.

5.2.4 MRI data analysis

Each study visit (either Study Visit 1 or Study Visit 2) was organised into 1 folder which was then loaded in Matlab and contained a dynamic motility MRI series of scans (motility sequence of 2D MRI images).The scans were registered with a previously validated optic-flow-based registration technique [171, 172]. Each dynamic motility MRI series acquired up to 33 sets of 4 slices, each set being acquired over a time window of approximately 3.5 min. Each set needed approximately 2 min to load in Matlab and then its 4 slices became available for analysis.

The boundaries of the small intestine (duodenum and proximal jejunum) were identified and regions of interest (ROIs) manually drawn in the images. The same boundaries were drawn across the different time points of the corresponding data set images of each participant. The ROIs drawn were automatically transformed into the standard deviation of the Jacobian (STDJac) by Matlab. The respiratory motion was corrected using the Dual Registration of Abdominal Motion (DRAM) GIQuant (Motilent, London, UK) [173].

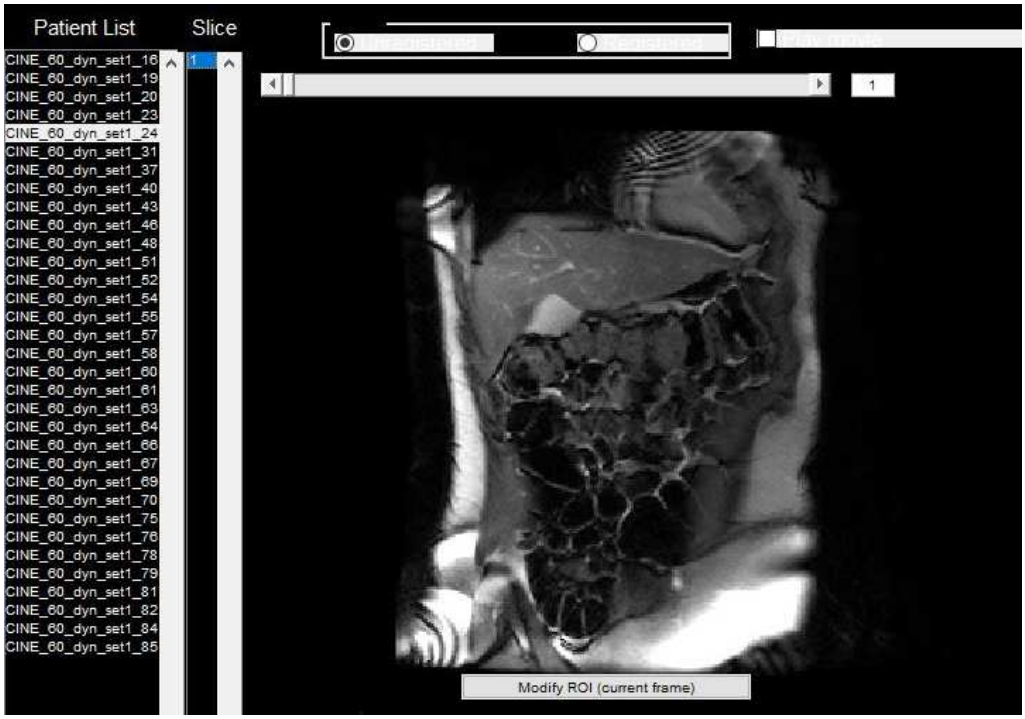

Figure 5.5. An example of a specific MRI set selected when its folder is loaded on Matlab.

Next, a visual check browse of each of the 4 slices was performed in order to establish image quality and organ visibility and determine which slice(s) were most appropriate for drawing ROIs. On average, approximately 16 slices of each dynamic MRI motility scan were suitable for this image analysis. Then, ROIs of the duodenum and proximal jejunum were drawn alongside the intestinal borders.

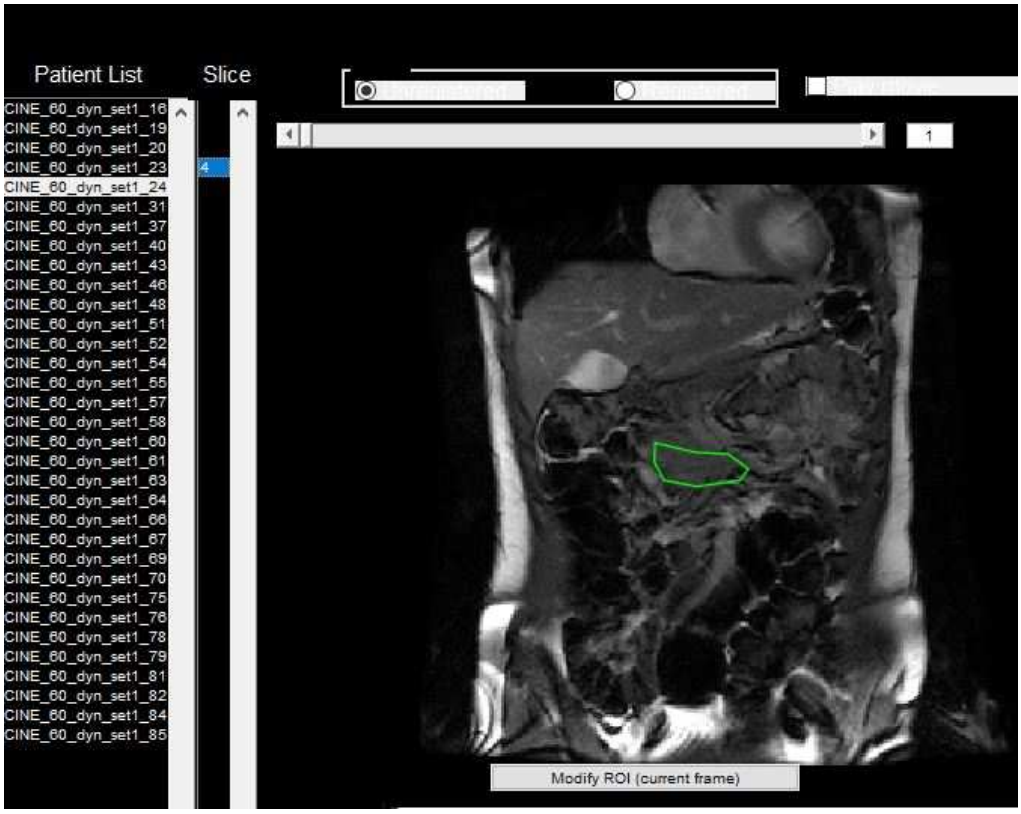

Figure 5.6. The ROI of the duodenum was drawn manually in slice 4 of set 24.

When more than one slice per set offered good image quality and a view of the duodenum, additional ROIs were drawn on the other slices too.

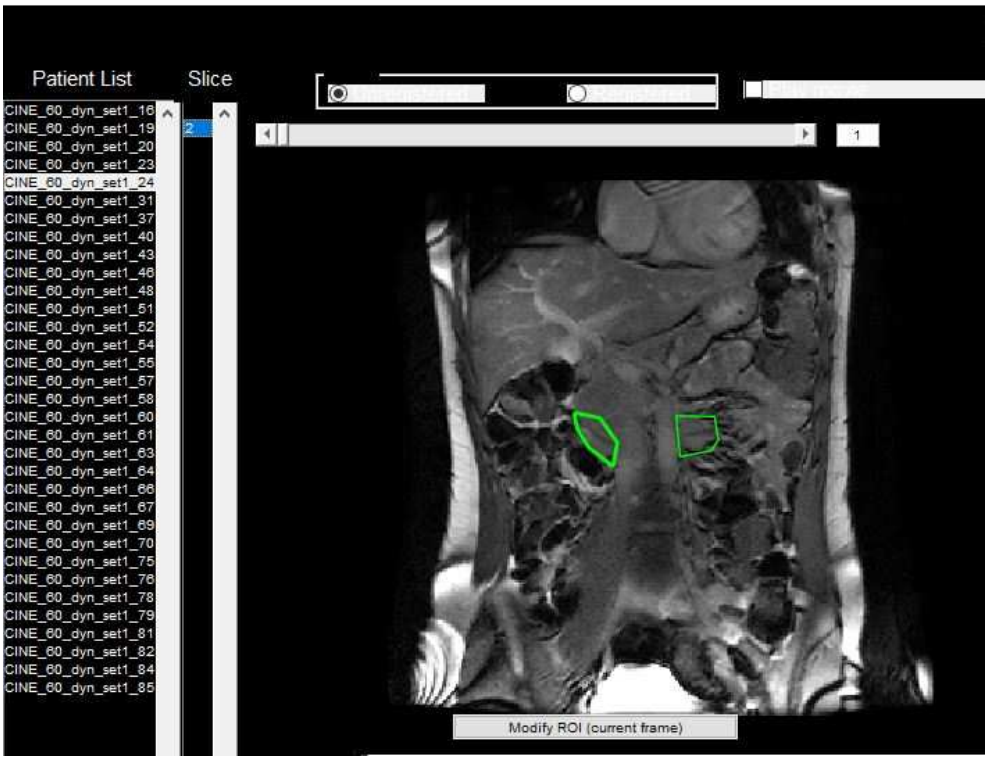

Figure 5.7. Manual drawing ROIs of the duodenum and proximal jejunum in slice 2 of set 24.

The ROIs drawn were then processed by the software throughout the dynamic MRI series. The algorithm calculated a series of deformation fields which were then transformed into a motility index. The motility index was calculated by taking the standard deviation of each deformation field's Jacobian determinant per pixel (standard deviation of the Jacobian) by Matlab [171, 172]. In the case of more than one ROI for the same region in the 4 different slices under the same set, then the mean standard deviation across that region was calculated.

5.2.5 Comparison of MRI and manometric data

The MRI scanner console and the perfused manometry system in this study were separated systems with no trigger signalling between them. The manometry recorder was started in the morning before calibration of the pressure and never stopped until the end, it recorded the signal from the transducers continuously, regardless of the catheter being connected or not. Conversely, the MRI data sets were acquired serially, with acquisition time varying slightly between experiments, depending also on actual start and length of the breaks taken by the participants. As such, the time stamps on the manometry traces and the ones on the MRI data sets needed first to be synchronised at post-processing stage.

Having realigned the MRI and manometry data sets, firstly the MRI motility index values were plotted against the manometry MI and AUC values respectively. Linear correlation was used to assess the agreement between MRI motility index and corresponding manometry parameters MI and AUC.

Secondly, visual inspection of the time courses of the different motility indexes indicated the presence of multiple peaks of high activity for both MRI and manometry indexes. Some were clearly coincident in time for both techniques and some weren't. The question arose of how to compare them in a more quantitative way. It was therefore decided to develop a standard definition of what constituted a 'peak' above the noise presence so that

peaks of motility indexes could be counted and compared in time to see if both MRI and manometry had an association in recording the same motility events and how significant that association was.

The method developed was as follows:

A) Firstly, any gaps in the time courses of the participants due to study breaks were removed.

B) The time courses for a given study day were then normalised (STDJac, MI and AUC values respectively) using Graphpad Prism. The normalisation process took the data for each column and normalised it between 0% and 100%, by defining zero as the smallest value in each data set, and 100 as the largest value in each data set, and then it expressing the results as percentages. This normalisation process made it easier to compare the three traces for STDJac, MI and AUC on the same scale.

C) The standard deviation for each of the data sets was then calculated. This was done to define objectively a 'noise' threshold in the data.

D) At this point a motility index 'peak' was defined as a point in the time course whose y -value was larger than the neighbouring y -values by at least one STD. This is not dissimilar from the classic perfused manometry automated analysis that defines a noise threshold (5mmHg or 10 mmHg) and counts as a peak a rise and fall in pressure above the noise threshold.

E) Having identified all MRI, and manometry MI and manometry AUC peaks, the operator identifies peaks as happening in coincidence if they were

occurring within one time point of each other. This was done to allow a margin of error in the data realignment process descried above.

F) At the point the process in E) included noting also the MMC III events and whether they occurred in coincidence with the MRI motility peaks.

G) contingency tables were then built in to investigate associations of MRI motility index peaks and manomety MI peaks, manometry AUC peaks , and MMC III events respectively, using Fisher's exact test in GraphPad Prism.

5.3 Results

MRI and manometry data were collected from the 18 participants that entered this study. However, 4 participants had to be excluded because of intubation problems, reconnection problems post-drink consumption and manometry traces affected by too much electrical noise at the end of the process. Twenty-four study days from 14 participants were available for data analysis.

5.3.1 Results MRI

Ideal image quality was not established in every MRI image acquired and duodenum and proximal jejunum were not clearly visible in every dataset. Therefore, fewer data points were eventually paired with the corresponding manometry data points.

Eventually, the MRI analysis resulted in 24 individual time courses comprising 420 data points and approximately 600 ROIs and the manometry analysis in 432 data points and relevant measurements. The MRI and manometry data points paired in the final correlation analysis were 393 from the 24 study days.

5.3.2 Results manometry

The manometry analysis resulted in 432 data points for each of the different manometry parameters (AUC, motility index, peaks and peaks/min). For this study, MRI data was paired with the corresponding AUC and motility index values.

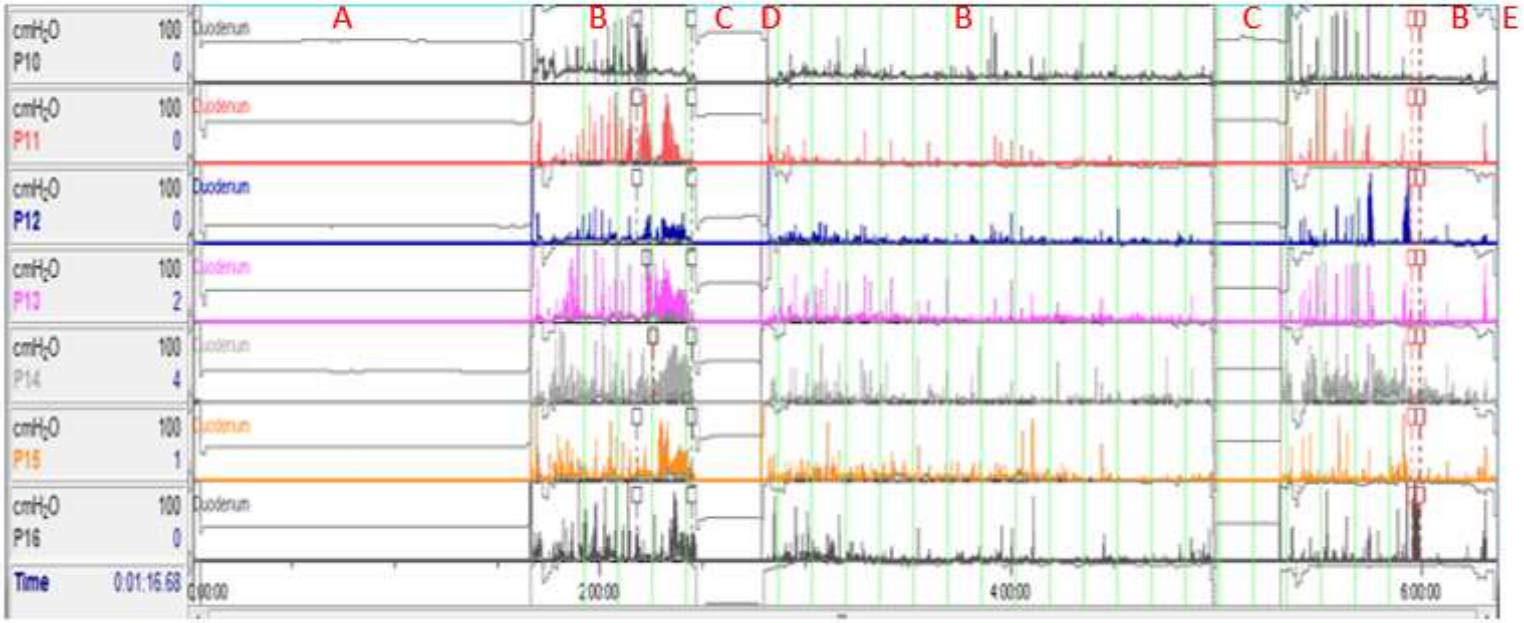

Figure 5.8. An example of the manometry spectrum as generated from the channels located in the duodenum of the participant. A) Intubation and rest (up to 2h), B) MRI & Manometry, C) Rest, D) Drink of 240 mL water, E) Tube removal & discharge.

5.3.3 Combined results and correlations

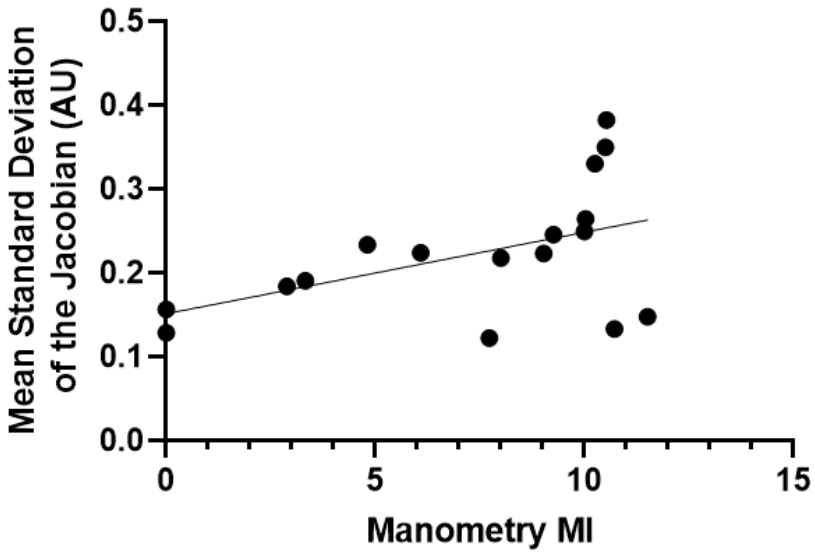

Figure 5.9. Linear correlation of the mean standard deviation of the Jacobian and the corresponding manometry motility index (MI) for participant No 11 (Visit 2).

MRI and manometry AUC participant No 11 (Visit 2) correlated positively (R^2 = 0.2275) but not significantly (p = 0.0529).

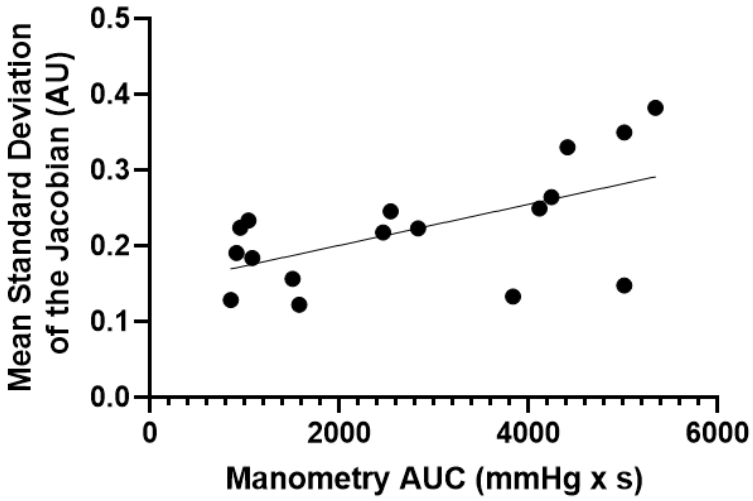

Figure 5.10. Linear correlation of the mean standard deviation of the Jacobian and the corresponding manometry area under the curve (AUC) for participant No 11 (Visit 2).

MRI and manometry AUC participant No 11 (Visit 2) correlated positively ($R^2 = 0.3364$) and significantly ($p = 0.0147$).

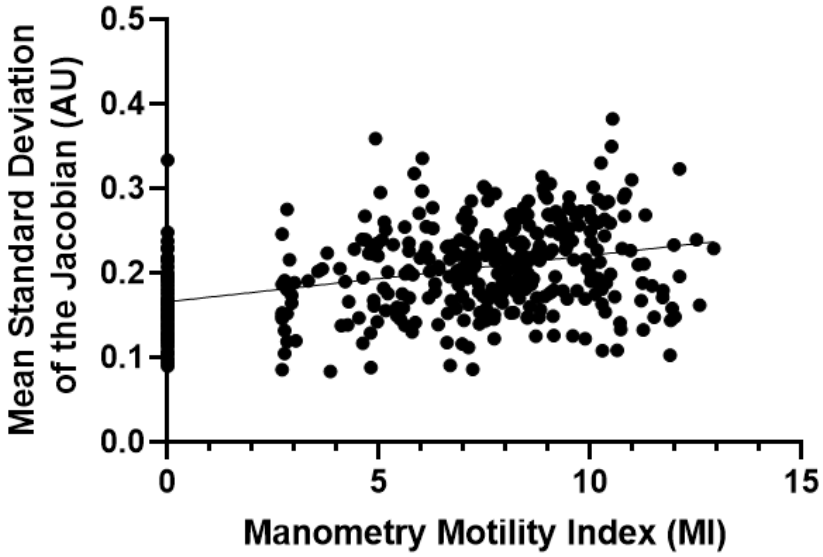

Figure 5.11. Linear correlation of the mean standard deviation of the Jacobian and the corresponding manometry motility index (MI) for all participants.

MRI and manometry MI of all participants correlated positively ($R^2 = 0.1214$) and significantly ($p < 0.0001$).

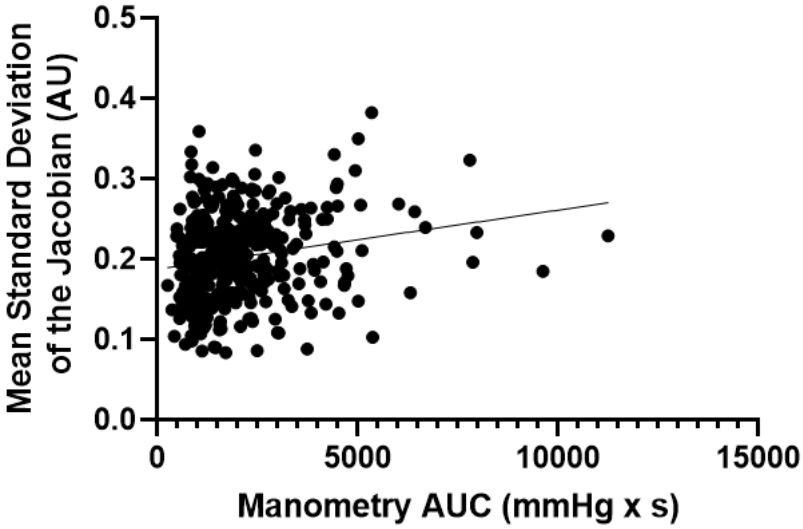

Figure 5.12. Linear correlation of the mean standard deviation of the Jacobian and the corresponding manometry area under the curve (AUC) for all participants.

MRI and manometry AUC of all participants correlated positively ($R^2 = 0.03583$) and significantly ($p = 0.0002$).

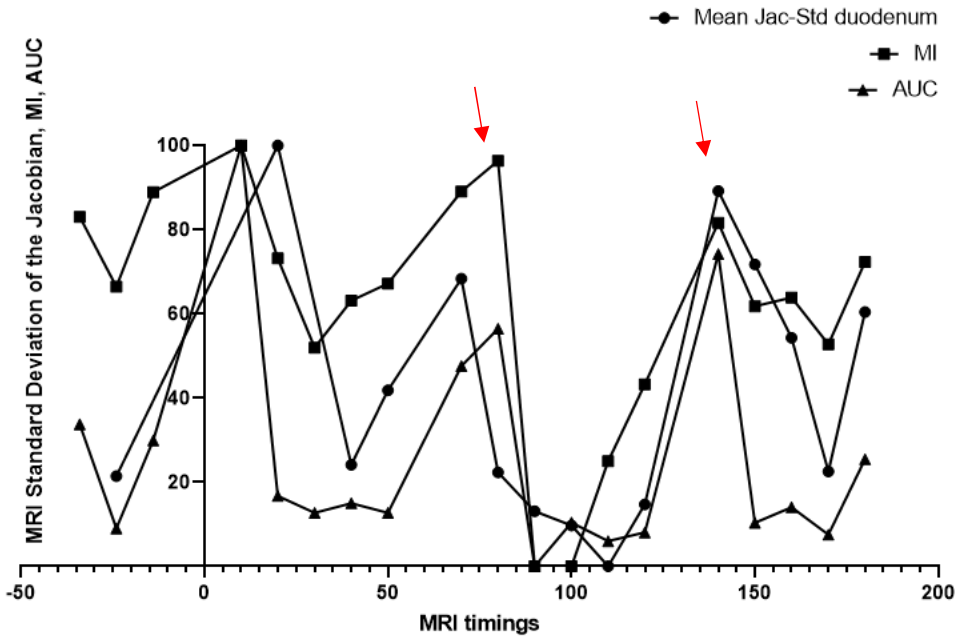

Figure 5.13. Normalised values of MRI standard deviation of the Jacobian, motility index (MI) and area under the curve (AUC) acquired from participant No 20 (Visit 2). Red arrows indicate the MMC III events.

MRI standard deviation of the Jacobian, MI and AUC resulted in their highest values in the same timings during the second visit of participant number 20. The timings of these high values correspond with the record of MMC phase III twice as it derives from the movement travel in the manometry spectrum.

Table 5.1. Number of motility peaks summed from all n=24 data sets

MRI peaks	83
Manometry MI peaks	91
Manometry AUC peaks	82
Coincident MRI and MI peaks	58
Coincident MRI and AUC peaks	52
Coincident MRI and MI and AUC peaks	50
MMC III events in the manometry traces	41
Coincident MRI and MMC III events	25

Abbreviations: AUC = area under the curve; MI = motility index; MMC = migrating motor complex

The number of motility peaks observed in the time courses are shown in Table 5.1. The table also lists how many of the MRI peaks occurred in coincidence with a perfused manometry peak for MI, AUC or both indexes. Overall, 64% of MRI and MI peaks occurred at the same time (as defines in Methods section) and 63% of MRI and AUC peaks occurred at the same time. Out of the 41 MMC III events recorded in the manometry spectrum, 25 were recorded by MRI too (61%).

The association of these events is best characterised using contingency tables as shown in Tables 5.1, 5.2 and 5.3. Fisher's exact test (two-tailed) showed no significant association between MRI and manometry MI peaks (P=0.2808) or between MRI and manometry AUC peaks (P=0.0563). However the association between MRI peaks and MMC III events was stronger and statistically significant (P<0.0001).

Table 5.2. Contingency table of number of MRI index peaks and number of manometry MI peaks. Y indicates motility peaks occurring at the same time in the time courses and N indicates motility peaks that did not occur at the same time in the time courses for both techniques.

		MRI peaks		
		Y	N	Row total
Manometry MI peaks	Y	58	33	91
	N	25	8	33
	Column total	83	41	124

Table 5.3. Contingency table of number of MRI index peaks and number of manometry AUC peaks. Y indicates motility peaks occurring at the same time in the time courses and N indicates motility peaks that did not occur at the same time in the time courses for both techniques.

		MRI peaks		
		Y	N	Row total
Manometry AUC peaks	Y	52	30	82
	N	31	7	38
	Column total	83	37	120

Table 5.4. Contingency table of number of MRI index peaks and number of MMC III events. Y indicates motility peaks and MMC III events occurring at the same time in the time courses and N indicates motility peaks or MMC IIIs that did not occur at the same time in the time courses.

		MRI peaks		
		Y	N	Row total
MMC III	Y	25	16	41
	N	58	0	58
	Column total	83	16	99

5.4 Discussion

The main aim of this retrospective study was to evaluate the ability of MRI to carry out non-invasive monitoring of small bowel motility by comparing MRI motility measurements against simultaneous water perfused manometry data. To do so, a *de novo* analysis of an existing large amount of data was carried out.

The data analysis required lengthy temporal realignment between serial MRI and manometry data and hundreds of ROIs were manually drawn on every slice that imaged the duodenum. This was successful and the data between the two techniques could be compared.

The degree of correlation found between MRI and manometry in terms of motility indexes values was low albeit significant.

A second part of the analysis aimed at comparing the ability of MRI to identify main small bowel motility peaks, as bursts of activity can apply more stress to coated capsules during their journey. Again, the association of MRI motility index peaks with perfused manometry motility indexes peaks was low, the one against manometry AUC index being very close to the significance threshold of $P<0.05$. Interestingly when considering the main MMC III manometry events, MRI motility index peaks associated with the MMC III events significantly ($P<0.0001$).

High-resolution manometry has long been used as the gold standard to describe motility events. MRI has only more recently been applied in the investigation of bowel motility using the standard deviation of the Jacobian as the primary motility metric [49, 171, 172, 174, 175].

Previously, Khalaf et al., assessed the small bowel motility in unprepared physiological conditions of healthy volunteers upon food consumption with MRI scans at intervals using total power ($AUC_{power\ spectrum}$) and the standard deviation of the Jacobian. They followed-up the effect of food consumption on both metrics and concluded that both reflect changes in bowel motility with the standard deviation of the Jacobian being less sensitive to changes (31.8% ± 20.7%) than the $AUC_{power\ spectrum}$ (122.4% ± 98.7%) for that kind of feeding intervention [49]. Another study aimed to assess the clinical significance of bowel motility in healthy volunteers and patients with Crohn's disease, ulcerative colitis and irritable bowel syndrome by using the standard deviation of the Jacobian index metric and MRI. This motility metric was able

to identify reduced motility in the terminal ileum of CD compared to the healthy subjects ($p = 0.002$). The metric tool also identified that motility further reduced with age ($p = 0.021$) and the presence of C-reactive protein ($p = 0.031$) [175]. Similarly, Gollifer et al., correlated this metric with the presence of CD symptoms stating that higher CD symptoms associated with larger changes in small bowel motility [171].

MRI and manometry were co-applied to study gastric motility during gastric emptying and its association firstly with intra-duodenal nutrient infusion and then with simultaneous intravenous erythromycin. This study was primarily focused on antral motility in the stomach not on the small bowel but interestingly the researchers suggested that manometry identified approximately 80% of the contractile activity compared to MRI [167].

Another team co-applied MRI and manometry on the measurement of antro-duodenal motility in order to validate the MRI technique of echo planar imaging against manometry. Ten healthy participants were under fed or fasted conditions. MRI was able to detect bigger propagating activity in both states (fasted $p = 0.03$ and fed $p = 0.02$) but manometry identified more isolated duodenal pressure waves ($p = 0.005$). It was suggested that manometry is less likely to identify all propagating activity. MRI recorded occlusive and non-occlusive events but could not distinguish them in the proximal antrum. Manometry is thought to be less sensitive to non-occlusive events and their associated mild pressure changes. These two techniques were overall in 93% agreement [168].

One possible reason for differences between MRI and manometry recordings could be that they measure physically different aspects of small bowel physiology. The MRI motility technique used in this Chapter captures the variations in time of signal intensities resulting from motion and local expansion and contraction on a pixel by pixel basis, with high values of the index representing more intense motility [171]. The water-perfused manometer on the other hand captures the pressure applied from the fluid (water perfusion) directly to the mucosal surface of the small bowel (contact pressure) or indirectly by the pressure applied to an element which in turn is in direct contact with the mucosal surface area of the small bowel (intra-bolus hydrodynamic pressure) [140]. When pressure is more than 15-35 mmHg, the manometer is more likely to pick up contact pressure whereas when pressure is lower it is more likely to capture hydrodynamic pressure [176].

The changes in MRI signal arise from changes in geometry and fluid motion in time, but MRI cannot distinguish pressure changes caused by muscle activity. For example, occlusive small bowel contractions that get stronger in time will generate an increasing amount of luminal pressure on a manometer port and, in turn, higher MIs and AUCs but not much change on the MRI images. Conversely, MRI is more likely to observe changes relating to non-occlusive contractions which would not affect greatly pressure ports on a catheter. So the two techniques can be at times disconnected by the physical nature of the phenomenon they measure, and this could be the explanation for the only modest correlations observed here.

The two techniques have inherent limitations and advantages.

Manometry's main disadvantages are that the procedure is invasive and uncomfortable and could disturb GI physiology through mechanical stimulation of the bowel wall by the catheter itself and the continuous perfusion of water in the lumen. Manometry catheters can hardly access the most distal parts of the small bowel.

On the other hand, MRI is a non-invasive technique without radiation and it offers the simultaneous acquisition of different parameters such as motility and water volumes. It also provides direct soft tissue imaging of the walls of the bowel. However, MRI is expensive and time-limiting as participants get uncomfortable when laying on the MRI bed for a prolonged time-period and they need to take breaks outside the scanner room (intermittent motility recordings), whilst manometric catheters can record continuously for hours. A simple MRI scanning session provides a large amount of data and its analysis is often time-consuming. Furthermore, the manual drawing of ROIs around the bowel regions and their processing is time-consuming and not entirely standardized yet. At times image quality is sub-optimal due to motion. However, the MRI technique can study the bowel in an undisturbed, physiological state and assess its motility, volumes, transit and movement of chyme in health and disease [171, 172, 177-179].

5.5 Conclusion

This final experimental part of the work aimed to explore how MRI could be used to add information on other aspects of bowel physiology that are relevant to the fate of coated capsules, such as small bowel motility, during future human studies like those described in Charters 3 and 4. Such an extensive appraisal is unprecedented. The results shown here are however mixed. MRI detection of peaks of motility activity was significantly associated with MMC IIIs but other correlations tested were only modest. The most likely explanation is that the MRI and manometric techniques used measured different physical quantities and a head-to-head comparison does not necessarily yield direct correlations between motility indexes. The MRI technique is non-invasive and clearly observed large motility events. As such it may be a useful addition to future studies imaging coated capsules in the small bowel.

6 Discussion

6.1 Summary

This work aimed to use MRI imaging as a real-time, non-invasive and safe way to monitor the gastrointestinal fate of a coated capsule, particularly in the distal GI tract (terminal ileum and the proximal large intestine) and to correlate the capsule's fate to the absorption kinetic of a model API.

These aims were successfully met. Capsules were designed and manufactured in-house, using coating able to withstand the conditions of the upper GI tract. The capsules were able to reach the lower intestine and be MRI-visible. MRI enabled tracking of the transit of the coated capsules and their loss of integrity in the human intestine. The capsules were then loaded with caffeine as an absorption API marker. An HPLC assay was optimised and used to measure caffeine absorption in saliva. The assay showed that the MRI findings correlated with the API's absorption kinetic.

As a final piece of work, since intestinal motility can contribute to the fate of drug formulations and particularly the fate of those targeting the distal GI tract, a comparison was carried out between MRI measurements of small bowel motility and well-established water perfused manometry, considering also the ability to identify important motility events such as MMC events.

6.2 Discussion

The design of these gastro-resistant capsules for intestinal drug targeting was based on the literature, including the choice of an HPMC capsule shell and specific Eudragit® polymer coating, and the range its concentrations in the coating solution [77, 83, 85-87, 95, 97, 107]. The HPMC capsule shells served their purpose as HPMC is commonly selected as pre-coating material in gastro-resistant/enteric coated formulations and seems to provide gradual drug release in the lower intestine [86, 87, 97].

Building on the available literature, this work introduced for the first time the novel method of using olive oil as an MRI-visible marker and exploiting fat-water DIXON imaging techniques to follow-up gastro-resistant (enteric) polymer-coated capsule throughout the gastrointestinal tract. The capsules were monitored throughout the intestine and evaluate their integrity was evaluated. Conventional MRI techniques can separate and image fat and water based on the water and fat chemical shift. Significant work has been conducted in the investigation of oily formulations and their intra-gastric distribution in relation to food [132, 134, 135, 180]. The encapsulated olive oil provided high MRI signal which allowed clear visualisation of the capsule along the bowel. It also allowed to identify the capsule's loss of integrity and to detect capsule oil release spatially. The distal bowel does not usually contain much luminal fat which further helped identifying the presence of the capsule in the MRI images.

The first study that followed-up oral drug formulations in the distal GI tract with MRI techniques intended to investigate fluid volumes and transit [24]. For this purpose, non-disintegrating capsules were administered to healthy participants in fasted and fed conditions. The capsules and their transit were successfully imaged exploiting MRI imaging. Notably, this study was pioneering to describe that colonic fluid is located in pockets and discussed its variability in relation to food and the possible effects on drug absorption [24]. However, since then, MRI techniques have been applied for the understanding of oral drug behaviour in the upper GI tract. These studies have mainly used acid-resistant or gastric-retentive tablets and capsules to study their disintegration time upon exiting the stomach, transit and overall performance [52, 129, 132, 135, 142, 180]. Lately, MRI investigation of drug performance in the upper GI tract has been combined with the caffeine salivary tracer technique [142]. This work adds to the field by successfully imaging enteric coated capsules filled with olive oil in the distal intestine and correlating the MRI site of loss of capsule integrity with the onset of caffeine absorption.

Having determined that it was possible to visualise the capsules and their loss of integrity in the bowel, the next logical step was to add an API to the fat filling of the capsule and to explore how MRI findings would correlate with drug absorption. Caffeine was chosen as a safe drug marker that could be monitored in saliva and it was thought that saliva collection would be much easier than cannulating a forearm vein of the participants and taking blood

samples. The arrival of the pandemic overturned these expectations, and ironically made the risk assessment and handling of saliva samples much more difficult that taking and handling blood, because the procedure of taking saliva could be generating some aerosol. This was eventually solved using careful procedures and personal protective equipment.

Caffeine salivary determination with HPLC analysis had been used previously in our laboratory in the School of Pharmacy [155]. For this work, the caffeine HPLC method of this work was further optimised and the lower limit of quantification (LOQ) determined to establish how low the levels of caffeine could be detected with confidence.

Most commonly studies that have exploited the caffeine salivary analysis with HPLC were designed for the upper gastrointestinal tract and have used a range of caffeine concentrations of 25-50 mg [51, 52, 128, 138, 181] so no direct comparison of expected salivary caffeine levels could take place. This work has encapsulated 75 mg of caffeine and was expected to be adequate for absorption from the lower intestine as reported in the literature [53, 93] in which only the caffeine excretion rate was reported. Up to 400 mg of caffeine per day is thought to be safely tolerated by adults and in this study only 75 mg were used.

Bioavailability observations that derive only from *in vitro* (blood or saliva) testing of drug characteristics are limited because they do not offer insight on the gastrointestinal fate of the drugs [132, 180]. MRI and drug assays are two techniques that complement each other and together could be more

informative, for example in the case that a capsule disintegrated in the colon but drug release had been initiated prior to reaching the colon [51].

Recent work has used MRI and pharmacokinetic analysis of caffeine in saliva, mainly in order to further understand the effect of the upper GI transit and motility on disintegration and absorption from immediate-release formulations in undisturbed physiological conditions [51-53, 93, 128, 129, 142, 181, 182]. The work presented in this thesis adds to the field as it developed original MRI methods for the investigation of absorption kinetics in the lower intestine. In fact, MRI imaging was able to follow-up the capsules and the site of their loss of integrity and correlated significantly with saliva analysis for the investigation of caffeine absorption.

The final part of the thesis is related to gastrointestinal motility as this can have a profound effect on dosage forms [159, 160, 183]. Indeed, individual motility, gastric residence times and gastric emptying variability should be taken into account if the same type of capsules exit the stomach and arrive in the intestine on different timings. MRI offers an insight on motility patterns as the MMC is mainly responsible for the exiting of monolithic drug formulations in-between meals which is characterized by high inter-subject variability and is affected by the timing and contents of the last meal and individual motility characteristics [52].

High-resolution manometry has been used as the gold standard to describe motility events. These include more commonly the MMC events as well as newer findings such as pan-colonic pressurizations [20]. Traditionally, MRI

and manometry have been co-applied principally for the study mostly of gastric motility, gastric emptying and their association with or without food presence [134, 168, 171]. More recent work, has used MRI imaging to study the bowel motility using automated image analysis algorithms and the standard deviation of the Jacobian as the motility metric [49, 171, 172, 174, 175].

This study was built on the research of Heissam et al. [140] of the upper GI motility patterns and it went one step further evaluate motility events in the small bowel.

These techniques are physically different as MRI provides information on changes in geometry or signal intensity but does not capture pressure changes caused by muscle activity. MRI is a non-invasive and non-ionizing radiation technique which can acquire simultaneously different parameters such as motility, water volumes and flow. It also provides insight on luminal contractions and occlusions with good anatomical information as well. MRI has been used against manometry to investigate and validate motility events in the upper GI tract [167, 168]. This work is the only study carried out to date to compare simultaneous MRI and perfused manometry of the small bowel on this scale.

The results are mixed. MRI can assess motility in more inaccessible parts of the bowel, although continuous MRI monitoring for many hours in the magnet is not possible and the participants need breaks which could miss out detection of motility events.

6.3 Impact

Exploiting all the information that MRI can provide, GI physiological processes should be taken into account when designing coated drug formulations. This will help understand further the variability in drug administration in the lower intestine. Exploiting MRI's ability to follow-up the fate of oral drug formulations *in vivo* in the lower GI tract in a biorelevant way can help to build more biorelevant tools for the *in vitro* evaluation of oral drug formulations.

Further understanding of the impact of the environment of the lower gastrointestinal tract will help the design of intestinal drug formulations with consistent and reproducible site targeting and absorption rates. The work presented here indicates a simple, safe and biorelevant way to follow-up the administration of intestinal formulation in the lower intestine.

This work also opens up the possibility to study oil-based formulations along with pharmacologically active ingredients in the undisturbed lower intestine with a non-invasive imaging method. Deeper understanding of the impact of the colonic environment on the drug release and absorption can inform advanced *in silico* approaches.

6.4 Limitations

This work had some limitations. One of the limitations of the coated capsules MRI studies was the interval between consecutive imaging time points. Forty-

five minutes between time points was a relatively long interval and the lack of more frequent imaging missed the determination of the capsules' loss of integrity in some participants. This choice of interval was due to the need to alternate scanning with periods of rest for the participants, in what was anyway expected to be a slow process of transit and loss of integrity. It would be interesting in the future to scan the participants at shorter intervals whilst taking serial saliva samples. This would allow to follow-up the capsule's journey and disintegration events more closely and accurately. This closer follow-up could be enhanced by the arrangement of a next-morning follow-up scanning session in order to investigate whether any intact, more heavily coated capsule might have remained for longer in the distal large intestine.

Adding a simultaneous investigation of GI parameters such as gastric emptying of the dose of water given with the capsule, small bowel water content and gastrointestinal motility would be very valuable. MRI imaging of motility as described in the last experimental Chapter would be of particular interest as it may be possible to link the onset of loss of integrity with larger (MMC III) motility events. However, this would still require a study design compromise as more MRI sequences imply more time spent in the magnet for the participants. In this work, the main focus was on the monitoring of capsule and its loss of integrity.

As far as the absorption marker use of caffeine is concerned, its use requires the abstinence of participants from caffeine and caffeinated products. Regular caffeine consumers may have caffeine detected in their body fluids

even on days when caffeine is not consumed. In this study, participants were asked to abstain from caffeine and chocolate containing products for 48 days prior to the MRI study day to minimise caffeine traces in body fluids as much as possible, which may be unpopular for recruitment. Recently, researchers have replaced the food abundant isotope of 12C with the 13C isotope on the caffeine and studied its absorption from the upper GI tract [181]. They found that these two isotopes have similar characteristics and this could lead to wider use of caffeine in human volunteer studies. This study can be extended to the investigation of the absorption and kinetics of this isotope from the distal intestine as well.

Posture could be a limitation too as the participants were scanned while lying on the scanning bed which may not represent entirely the real-life drug consumption conditions where oral drug products are normally consumed in the sitting or standing position. The time spent in the magnet was however relatively short as the participants were taken out of the magnet and asked to sit upright in an adjacent room until the next scanning session.

However, it should be noted that the Covid-19 pandemic affected the original planning of the study and led to significant delays of study implementation. Initial plans included the administration of more than one colon-absorbed drugs with the simultaneous administration of agents that affect the physiological conditions of the large intestine e.g. laxatives. Eventually, due to University closure and therefore time-pressure, only caffeine was encapsulated. Additionally, Covid-19 University and Hospital regulations

required the submission of complex risk assessments and safe operating procedures, which was time-consuming and delayed re-starting of the study. Interestingly, the unexpected lockdown that led to sudden shut-off of HPLC equipment had a negative impact on their functionality. This required several company engineer visits and delayed establishment of the needed experimental conditions.

6.5 Future Directions

This work has demonstrated new methods to study the fate of coated capsules. In the future it can evolve in various directions.

The first possible application is the study of *in vivo* performance of new coated capsule products. *In vitro* disintegration studies can be very informative but may not entirely represent the *in vivo* situation.

The UK start-up Motilent® has now transformed the platform used for the analysis of gut motility into a medical image analysis product with regulatory approvals in both the US and EU. It would be possible to add to that platform an automated detection algorithm to detect and track the fate of the capsules in the bowel from MRI imaging. This has been discussed with company and it would speed up analysis and remove some operator dependency.

Another interesting development for this work could be the imaging of coated capsules inside dynamic gut models. During the time course of this PhD studentship (but beyond the scope of this thesis), the author has participated in the successful MRI validation of the Dynamic Colon Model (DCM), an

anatomically representative *in vitro* model of the human ascending colon with the ability to reproduce motility patterns dynamically [184-186]. Specifically, pre-existing MRI data of the human colonic wall motion were used to inform the implementation of biorelevant motility patterns in the DCM to study dynamically, *in vitro* the interaction of wall motion, volume, viscosity, fluid, and motion of particles in the lumen. This can enhance the understanding of flow motion and behaviour which, in turn, may ameliorate the design of drug formulations [185, 186]. Biorelevant *in vitro* dynamic models will play an important part when considering dissolution test methodologies for colon-targeted formulations beyond the standard compendial methodology.

Gastrointestinal discomfort, such as constipation and diarrhoea, and pathophysiological conditions such as IBD are under-diagnosed and often un-diagnosed and self-treated. Often, people affected by the abovementioned conditions self-treat with over-the-counter (OTC) drugs that affect and change the gastrointestinal physiology and this has a profound effect on drug performance *in vivo* and potentially drug bioavailability inhibiting ideal/expected drug absorption/partly responsible for drug variability in performance [25, 187, 188]

Another possible development for this work lies in the studying of the impact of other factors that can affect coated capsules, such as consideration of the effect of diet and microbiota, and effects of co-administration of other agents (such as laxatives) and presence of gut disease (such as Crohn's). Diet is responsible for around 30% of colonic volume in a rapid way and this has a.

dynamic character as the 1/3 of colonic content is exited and replaced [189]. Opioid treatment is closely related to gastrointestinal alterations such as prolonged transit time and induced constipation and gastric reflux [190]. Different meals have various effects on GI physiology and through their osmotic effect can affect volume or they can change the secretion/absorption balance in the small intestine [36]. Therefore, further MRI analysis of food and disease state and drug interaction with GI physiology is needed. This work has demonstrated new methods to study the fate of coated capsules. In the future it can evolve in various directions.

6.6 Conclusions

Intestinal drug targeting has been gaining scientific interest mainly for its potential of enhanced drug bioavailability and lower enzymatic activity. However, successful and consistent controlling of the timings and sites of drug targeting remains challenging, also due to an incomplete knowledge of the physiological conditions in the distal gastrointestinal tract. The main reason for this incomplete understanding lies in the difficulty of studying the distal intestine in physiological and undisturbed conditions.

It has recently been shown that MRI imaging can provide new information on the fate of some test dosage forms in the human gastrointestinal tract, primarily the upper GI tract. Building on these initial reports this work has successfully developed and tested *in vivo* a coated capsule using a new

concept for the MRI-visible filling. MRI was able to determine location and disintegration times of these coated capsules in the distal intestine, and this correlated well with absorption kinetics of a model active pharmaceutical ingredient, caffeine in this case.

This work adds to the field new methods to study performance of coated capsules *in vivo* in an undisturbed bowel. The new data and techniques will in turn help to make *in vitro* pharmacopoieial tests and kinetic and bench dynamic modelling more *in vivo* relevant. MRI has also the potential to assess other parameters of gastrointestinal function which are relevant for dosage form transit and disintegration such as small bowel motility. However more work to incorporate such measures with the MRI tracking of coated capsules remains to be done.

7 References

1. Helander, H.F. and L. Fändriks, *Surface area of the digestive tract – revisited.* Scandinavian Journal of Gastroenterology, 2014. **49**(6): p. 681-689.
2. Sellers, R.S. and D. Morton, *The colon: from banal to brilliant.* Toxicol Pathol, 2014. **42**(1): p. 67-81.
3. Greenwood-Van Meerveld, B., A.C. Johnson, and D. Grundy, *Gastrointestinal Physiology and Function.* Handb Exp Pharmacol, 2017. **239**: p. 1-16.
4. Hansson, G.C., *Role of mucus layers in gut infection and inflammation.* Current opinion in microbiology, 2012. **15**(1): p. 57-62.
5. Surgeons, A.S.o.C.a.R. *The Colon: What it is, What it Does*. [cited 2019 10/07]; Available from: https://www.fascrs.org/patients/disease-condition/colon-what-it-what-it-does.
6. Liu, L., A. Hila, and S. Towfighian, *A Review of Locomotion Systems for Capsule Endoscopy*. Vol. 8. 2015. 138-151.
7. Kararli, T.T., *Comparison of the gastrointestinal anatomy, physiology, and biochemistry of humans and commonly used laboratory animals.* Biopharmaceutics & Drug Disposition, 1995. **16**(5): p. 351-380.

8. Senekowitsch, S., et al., *Application of In Vivo Imaging Techniques and Diagnostic Tools in Oral Drug Delivery Research.* Pharmaceutics, 2022. **14**(4).
9. Vertzoni, M., et al., *Biorelevant Media to Simulate Fluids in the Ascending Colon of Humans and Their Usefulness in Predicting Intracolonic Drug Solubility.* Pharmaceutical Research, 2010. **27**(10): p. 2187-2196.
10. Ma, Z.F. and Y.Y. Lee, *Chapter 7 - Small intestine anatomy and physiology*, in *Clinical and Basic Neurogastroenterology and Motility*. 2020, Academic Press. p. 101-111.
11. Deloose, E. and J. Tack, *Redefining the functional roles of the gastrointestinal migrating motor complex and motilin in small bacterial overgrowth and hunger signaling.* Am J Physiol Gastrointest Liver Physiol, 2016. **310**(4): p. G228-33.
12. Deloose, E., et al., *The migrating motor complex: control mechanisms and its role in health and disease.* Nat Rev Gastroenterol Hepatol, 2012. **9**(5): p. 271-85.
13. Wood, J.D., *Migrating Motor Complex*, in *Encyclopedia of Gastroenterology*, L.R. Johnson, Editor. 2004, Elsevier: New York. p. 650-652.
14. Dooley, C.P., C. Di Lorenzo, and J.E. Valenzuela, *Variability of migrating motor complex in humans.* Digestive Diseases and Sciences, 1992. **37**(5): p. 723-728.

15. *Your Digestive System & How it Works*. 2017 [cited 2019 10/07]; Available from: https://www.niddk.nih.gov/health-information/digestive-diseases/digestive-system-how-it-works.
16. Arkwright, J.W., et al., *In-vivo demonstration of a high resolution optical fiber manometry catheter for diagnosis of gastrointestinal motility disorders.* Opt Express, 2009. **17**(6): p. 4500-8.
17. Arkwright, J.W., et al., *A fibre optic catheter for simultaneous measurement of longitudinal and circumferential muscular activity in the gastrointestinal tract.* J Biophotonics, 2011. **4**(4): p. 244-51.
18. Arkwright, J.W., et al., *The effect of luminal content and rate of occlusion on the interpretation of colonic manometry.* Neurogastroenterol Motil, 2013. **25**(1): p. e52-9.
19. Vather, R., et al., *Hyperactive cyclic motor activity in the distal colon after colonic surgery as defined by high-resolution colonic manometry.* Br J Surg, 2018. **105**(7): p. 907-917.
20. Corsetti, M., et al., *Pan-Colonic Pressurizations Associated With Relaxation of the Anal Sphincter in Health and Disease: A New Colonic Motor Pattern Identified Using High-Resolution Manometry.* Am J Gastroenterol, 2017. **112**(3): p. 479-489.
21. Corsetti, M., et al., *High-resolution manometry reveals different effect of polyethylene glycol, bisacodyl, and prucalopride on colonic motility in healthy subjects: An acute, open label, randomized, crossover, reader-blinded study with potential*

clinical implications. Neurogastroenterol Motil, 2021. **33**(5): p. e14040.

22. Dinning, P.G., et al., *Quantification of in vivo colonic motor patterns in healthy humans before and after a meal revealed by high-resolution fiber-optic manometry.* Neurogastroenterology and motility : the official journal of the European Gastrointestinal Motility Society, 2014. **26**(10): p. 1443-1457.
23. Corsetti, M., et al., *Pan-Colonic Pressurizations Associated With Relaxation of the Anal Sphincter in Health and Disease: A New Colonic Motor Pattern Identified Using High-Resolution Manometry*. Vol. 112. 2016.
24. Schiller, C., et al., *Intestinal fluid volumes and transit of dosage forms as assessed by magnetic resonance imaging.* Aliment Pharmacol Ther, 2005. **22**(10): p. 971-9.
25. Placidi, E., et al., *The effects of loperamide, or loperamide plus simethicone, on the distribution of gut water as assessed by MRI in a mannitol model of secretory diarrhoea.* Aliment Pharmacol Ther, 2012. **36**(1): p. 64-73.
26. Marciani, L., et al., *Stimulation of colonic motility by oral PEG electrolyte bowel preparation assessed by MRI: comparison of split vs single dose.* Neurogastroenterol Motil, 2014. **26**(10): p. 1426-36.
27. Pritchard, S.E., et al., *Fasting and postprandial volumes of the undisturbed colon: normal values and changes in diarrhea-*

predominant irritable bowel syndrome measured using serial MRI. Neurogastroenterol Motil, 2014. **26**(1): p. 124-30.

28. Pritchard, S.E., et al., *Effect of experimental stress on the small bowel and colon in healthy humans.* Neurogastroenterol Motil, 2015. **27**(4): p. 542-9.
29. Sandberg, T.H., et al., *A novel semi-automatic segmentation method for volumetric assessment of the colon based on magnetic resonance imaging.* Abdom Imaging, 2015. **40**(7): p. 2232-41.
30. Coletta, M., et al., *Effect of bread gluten content on gastrointestinal function: a crossover MRI study on healthy humans.* Br J Nutr, 2016. **115**(1): p. 55-61.
31. Lam, C., et al., *Colonic response to laxative ingestion as assessed by MRI differs in constipated irritable bowel syndrome compared to functional constipation.* Neurogastroenterol Motil, 2016. **28**(6): p. 861-70.
32. Wilkinson-Smith, V., et al., *Mechanisms underlying effects of kiwifruit on intestinal function shown by MRI in healthy volunteers.* Alimentary Pharmacology & Therapeutics, 2019. **0**(0).
33. Murray, K., et al., *Magnetic Resonance Imaging Quantification of Fasted State Colonic Liquid Pockets in Healthy Humans.* Mol Pharm, 2017. **14**(8): p. 2629-2638.
34. Major, G., et al., *Demonstration of differences in colonic volumes, transit, chyme consistency, and response to psyllium*

between healthy and constipated subjects using magnetic resonance imaging. Neurogastroenterol Motil, 2018. **30**(9): p. e13400.

35. Sloan, T.J., et al., *A low FODMAP diet is associated with changes in the microbiota and reduction in breath hydrogen but not colonic volume in healthy subjects.* PLoS One, 2018. **13**(7): p. e0201410.
36. Wilkinson-Smith, V.C., et al., *Insights Into the Different Effects of Food on Intestinal Secretion Using Magnetic Resonance Imaging.* JPEN J Parenter Enteral Nutr, 2018. **42**(8): p. 1342-1348.
37. Pentafragka, C., et al., *The impact of food intake on the luminal environment and performance of oral drug products with a view to in vitro and in silico simulations: a PEARRL review.* J Pharm Pharmacol, 2019. **71**(4): p. 557-580.
38. Varum, F.J., H.A. Merchant, and A.W. Basit, *Oral modified-release formulations in motion: the relationship between gastrointestinal transit and drug absorption.* Int J Pharm, 2010. **395**(1-2): p. 26-36.
39. Mudie, D.M., G.L. Amidon, and G.E. Amidon, *Physiological parameters for oral delivery and in vitro testing.* Mol Pharm, 2010. **7**(5): p. 1388-405.
40. Sjogren, E., et al., *In vivo methods for drug absorption - comparative physiologies, model selection, correlations with in vitro methods (IVIVC), and applications for*

formulation/API/excipient characterization including food effects. Eur J Pharm Sci, 2014. **57**: p. 99-151.

41. Hens, B., et al., *Gastrointestinal transfer: in vivo evaluation and implementation in in vitro and in silico predictive tools.* Eur J Pharm Sci, 2014. **63**: p. 233-42.
42. Buhmann, S., et al., *Assessment of colonic transit time using MRI: a feasibility study.* Eur Radiol, 2007. **17**(3): p. 669-74.
43. Hahn, T., et al., *Visualization and quantification of intestinal transit and motor function by real-time tracking of 19F labeled capsules in humans.* Magn Reson Med, 2011. **66**(3): p. 812-20.
44. Chaddock, G., et al., *Novel MRI tests of orocecal transit time and whole gut transit time: studies in normal subjects.* Neurogastroenterol Motil, 2014. **26**(2): p. 205-14.
45. Savarino, E., et al., *Measurement of oro-caecal transit time by magnetic resonance imaging.* Eur Radiol, 2015. **25**(6): p. 1579-87.
46. Lam, C., et al., *Distinct Abnormalities of Small Bowel and Regional Colonic Volumes in Subtypes of Irritable Bowel Syndrome Revealed by MRI.* Am J Gastroenterol, 2017. **112**(2): p. 346-355.
47. Pritchard, S.E., et al., *Assessment of motion of colonic contents in the human colon using MRI tagging.* Neurogastroenterol Motil, 2017. **29**(9).

48. Zhi, M., et al., *Clinical application of a gadolinium-based capsule as an MRI contrast agent in slow transit constipation diagnostics.* Neurogastroenterol Motil, 2017. **29**(6).

49. Khalaf, A., et al., *MRI assessment of the postprandial gastrointestinal motility and peptide response in healthy humans.* Neurogastroenterol Motil., 2018.

50. Reppas, C., et al., *Characterization of Contents of Distal Ileum and Cecum to Which Drugs/Drug Products are Exposed During Bioavailability/Bioequivalence Studies in Healthy Adults.* Pharm Res, 2015. **32**(10): p. 3338-49.

51. Rump, A., et al. *In Vivo Evaluation of a Gastro-Resistant HPMC-Based “Next Generation Enteric” Capsule*. Pharmaceutics, 2022. **14**, DOI: 10.3390/pharmaceutics14101999.

52. Rump, A., et al., *The Effect of Capsule-in-Capsule Combinations on In Vivo Disintegration in Human Volunteers: A Combined Imaging and Salivary Tracer Study.* Pharmaceutics, 2021. **13**(12).

53. Muraoka, M., et al., *Evaluation of intestinal pressure-controlled colon delivery capsule containing caffeine as a model drug in human volunteers.* J Control Release, 1998. **52**(1-2): p. 119-29.

54. Philip, A.K. and B. Philip, *Colon targeted drug delivery systems: a review on primary and novel approaches.* Oman medical journal, 2010. **25**(2): p. 79-87.

55. Ibekwe, V.C., et al., *A new concept in colonic drug targeting: a combined pH-responsive and bacterially-triggered drug delivery technology.* Aliment Pharmacol Ther, 2008. **28**(7): p. 911-6.
56. McCoubrey, L.E., et al., *Colonic drug delivery: Formulating the next generation of colon-targeted therapeutics.* J Control Release, 2023. **353**: p. 1107-1126.
57. Tannergren, C., et al., *Toward an increased understanding of the barriers to colonic drug absorption in humans: implications for early controlled release candidate assessment.* Mol Pharm, 2009. **6**(1): p. 60-73.
58. Yang, L., J.S. Chu, and J.A. Fix, *Colon-specific drug delivery: new approaches and in vitro/in vivo evaluation.* Int J Pharm, 2002. **235**(1-2): p. 1-15.
59. Kostewicz, E.S., et al., *In vitro models for the prediction of in vivo performance of oral dosage forms.* Eur J Pharm Sci, 2014. **57**: p. 342-66.
60. Lennernas, H., et al., *Oral biopharmaceutics tools - time for a new initiative - an introduction to the IMI project OrBiTo.* Eur J Pharm Sci, 2014. **57**: p. 292-9.
61. Khan, A.K.A., J. Piris, and S.C. Truelove, *An experiment to determine the active therapeutic moiety of sulphasalazine.* The Lancet, 1977. **310**(8044): p. 892-895.
62. Riley, S.A., *What dose of 5-aminosalicylic acid (mesalazine) in ulcerative colitis?* Gut, 1998. **42**(6): p. 761.

63. Klotz, U., *Clinical Pharmacokinetics of Sulphasalazine, Its Metabolites and Other Prodrugs of 5-Aminosalicylic Acid.* Clinical Pharmacokinetics, 1985. **10**(4): p. 285-302.

64. Chan, R.P., et al., *Studies of two novel sulfasalazine analogs, ipsalazide and balsalazide.* Digestive Diseases and Sciences, 1983. **28**(7): p. 609-615.

65. Wadworth, A.N. and A. Fitton, *Olsalazine.* Drugs, 1991. **41**(4): p. 647-664.

66. Mark, E.B., et al., *Assessment of colorectal length using the electromagnetic capsule tracking system: a comparative validation study in healthy subjects.* Colorectal Dis, 2017. **19**(9): p. O350-O357.

67. Phillips, S.F., *Absorption and secretion by the colon.* Gastroenterology, 1969. **56**(5): p. 966-971.

68. Weitschies, W. and C.G. Wilson, *In vivo imaging of drug delivery systems in the gastrointestinal tract.* Int J Pharm, 2011. **417**(1-2): p. 216-26.

69. Wilson, C.G., *The transit of dosage forms through the colon.* Int J Pharm, 2010. **395**(1-2): p. 17-25.

70. Alyami, J., R.C. Spiller, and L. Marciani, *Magnetic resonance imaging to evaluate gastrointestinal function.* Neurogastroenterol Motil, 2015. **27**(12): p. 1687-92.

71. Davis, J., et al., *Scintigraphic study to investigate the effect of food on a HPMC modified release formulation of UK-294,315.* J Pharm Sci, 2009. **98**(4): p. 1568-76.

72. Watts, P.J., et al., *The transit rate of different-sized model dosage forms through the human colon and the effects of a lactulose-induced catharsis.* International Journal of Pharmaceutics, 1992. **87**(1): p. 215-221.

73. Adkin, D.A., et al., *Colonic transit of different sized tablets in healthy subjects.* Journal of Controlled Release, 1993. **23**(2): p. 147-156.

74. Abrahamsson, B., et al., *Gastro-intestinal transit of a multiple-unit formulation (metoprolol CR/ZOK) and a non-disintegrating tablet with the emphasis on colon.* International Journal of Pharmaceutics, 1996. **140**(2): p. 229-235.

75. Hardy, J.G., C.G. Wilson, and E. Wood, *Drug delivery to the proximal colon.* J Pharm Pharmacol, 1985. **37**(12): p. 874-7.

76. Proano, M., et al., *Transit of solids through the human colon: regional quantification in the unprepared bowel.* Am J Physiol, 1990. **258**(6 Pt 1): p. G856-62.

77. Hebden, J.M., et al., *Night-time quiescence and morning activation in the human colon: effect on transit of dispersed and large single unit formulations.* Eur J Gastroenterol Hepatol, 1999. **11**(12): p. 1379-85.

78. Coupe, A.J., et al., *Nocturnal scintigraphic imaging to investigate the gastrointestinal transit of dosage forms.* Journal of Controlled Release, 1992. **20**(2): p. 155-162.

79. Hodges, L.A., et al., *Scintigraphic evaluation of colon targeting pectin-HPMC tablets in healthy volunteers.* Int J Pharm, 2009. **370**(1-2): p. 144-50.

80. Barrow, L., et al., *Quantitative, noninvasive assessment of antidiarrheal actions of codeine using an experimental model of diarrhea in man.* Dig Dis Sci, 1993. **38**(6): p. 996-1003.

81. Hebden, J.M., et al., *Stool water content and colonic drug absorption: contrasting effects of lactulose and codeine.* Pharm Res, 1999. **16**(8): p. 1254-9.

82. Hebden, J.M., et al., *Regional Differences in Quinine Absorption from the Undisturbed Human Colon Assessed Using a Timed Release Delivery System.* Pharmaceutical Research, 1999. **16**(7): p. 1087-1092.

83. Marvola, J., et al., *Neutron activation-based gamma scintigraphy in pharmacoscintigraphic evaluation of an Egalet® constant-release drug delivery system.* International Journal of Pharmaceutics, 2004. **281**(1): p. 3-10.

84. Hebden, J.M., et al., *Limited exposure of the healthy distal colon to orally-dosed formulation is further exaggerated in active left-sided ulcerative colitis.* Aliment Pharmacol Ther, 2000. **14**(2): p. 155-61.

85. Cole, E.T., et al., *Enteric coated HPMC capsules designed to achieve intestinal targeting.* Int J Pharm, 2002. **231**(1): p. 83-95.

86. Marvola, T., et al., *Neutron activation based gamma scintigraphic evaluation of enteric-coated capsules for local treatment in colon.* Int J Pharm, 2008. **349**(1-2): p. 24-9.

87. Varum, F.J., et al., *A novel coating concept for ileo-colonic drug targeting: proof of concept in humans using scintigraphy.* Eur J Pharm Biopharm, 2013. **84**(3): p. 573-7.

88. Ibekwe, V.C., et al., *Interplay between intestinal pH, transit time and feed status on the in vivo performance of pH responsive ileo-colonic release systems.* Pharm Res, 2008. **25**(8): p. 1828-35.

89. Moghimipour, E., et al., *In vivo evaluation of pH and time-dependent polymers as coating agent for colonic delivery using central composite design.* Journal of Drug Delivery Science and Technology, 2018. **43**: p. 50-56.

90. Dew, M.J., et al., *An oral preparation to release drugs in the human colon.* Br J Clin Pharmacol, 1982. **14**(3): p. 405-8.

91. Schroeder, K.W., W.J. Tremaine, and D.M. Ilstrup, *Coated oral 5-aminosalicylic acid therapy for mildly to moderately active ulcerative colitis. A randomized study.* N Engl J Med, 1987. **317**(26): p. 1625-9.

92. Ashford, M., et al., *An in vivo investigation into the suitability of pH dependent polymers for colonic targeting.* International Journal of Pharmaceutics, 1993. **95**(1): p. 193-199.

93. Hu, Z., et al., *Application of a biomagnetic measurement system (BMS) to the evaluation of gastrointestinal transit of intestinal*

pressure-controlled colon delivery capsules (PCDCs) in human subjects. Pharm Res, 2000. **17**(2): p. 160-7.

94. Hu, Z., et al., *Colon delivery efficiencies of intestinal pressure-controlled colon delivery capsules prepared by a coating machine in human subjects.* J Pharm Pharmacol, 2000. **52**(10): p. 1187-93.

95. Ishibashi, T., et al., *Design and evaluation of a new capsule-type dosage form for colon-targeted delivery of drugs.* International Journal of Pharmaceutics, 1998. **168**(1): p. 31-40.

96. Tuleu, C., et al., *Colonic delivery of 4-aminosalicylic acid using amylose-ethylcellulose-coated hydroxypropylmethylcellulose capsules.* Aliment Pharmacol Ther, 2002. **16**(10): p. 1771-9.

97. Dvorácková, K., et al., *Coated capsules for drug targeting to proximal and distal part of human intestine.* Acta Pol Pharm, 2010. **67**(2): p. 191-9.

98. Nguyen, D.A. and H.S. Fogler, *Facilitated diffusion in the dissolution of carboxylic polymers.* AIChE Journal, 2005. **51**(2): p. 415-425.

99. Vinner, G.K., et al., *Microencapsulation of Clostridium difficile specific bacteriophages using microfluidic glass capillary devices for colon delivery using pH triggered release.* PLoS One, 2017. **12**(10): p. e0186239.

100. Guo, B.J., Z.L. Yang, and L.J. Zhang, *Gadolinium Deposition in Brain: Current Scientific Evidence and Future Perspectives.* Front Mol Neurosci, 2018. **11**: p. 335.

101. Wang, Y.X., *Superparamagnetic iron oxide based MRI contrast agents: Current status of clinical application.* Quant Imaging Med Surg, 2011. **1**(1): p. 35-40.

102. Sakhno, T., et al., *Polymer Coatings for Protection of Wood and Wood-Based Materials.* Advances in Chemical Engineering and Science, 2016. **6**: p. 93-110.

103. Stippler, E., S. Kopp, and J. Dressman, *Comparison of US Pharmacopeia Simulated Intestinal Fluid TS (without pancreatin) and Phosphate Standard Buffer pH 6.8, TS of the International Pharmacopoeia with Respect to Their Use in In Vitro Dissolution Testing.* Dissolution Technologies, 2004. **11**: p. 6-10.

104. The United States Pharmacopeial Convention, *Disintegration General Chapter.* USP 43-NF 38, 2020. **701**.

105. Yoshikawa, Y., et al., *A dissolution test for a pressure-controlled colon delivery capsule: rotating beads method.* J Pharm Pharmacol, 1999. **51**(9): p. 979-89.

106. Katsuma, M., et al., *Studies on lactulose formulations for colon-specific drug delivery.* Int J Pharm, 2002. **249**(1-2): p. 33-43.

107. Patel, M.M. and A.F. Amin, *Development of a novel tablet-in-capsule formulation of mesalamine for inflammatory bowel disease.* Pharm Dev Technol, 2013. **18**(2): p. 390-400.

108. Staelens, D., et al., *Visualization of delayed release of compounds from pH-sensitive capsules in vitro and in vivo in a hamster model.* Contrast Media Mol Imaging, 2016. **11**(1): p. 24-31.

109. Ishibashi, T., et al., *Evaluation of colonic absorbability of drugs in dogs using a novel colon-targeted delivery capsule (CTDC).* J Control Release, 1999. **59**(3): p. 361-76.

110. Tozaki, H., et al., *Chitosan capsules for colon-specific drug delivery: enhanced localization of 5-aminosalicylic acid in the large intestine accelerates healing of TNBS-induced colitis in rats.* J Control Release, 2002. **82**(1): p. 51-61.

111. Jeong, Y.I., et al., *Evaluation of an intestinal pressure-controlled colon delivery capsules prepared by a dipping method.* J Control Release, 2001. **71**(2): p. 175-82.

112. Macchi, E., et al., *Enteric-coating of pulsatile-release HPC capsules prepared by injection molding.* Eur J Pharm Sci, 2015. **70**: p. 1-11.

113. Kirchhoff, S., et al., *Assessment of colon motility using simultaneous manometric and functional cine-MRI analysis: preliminary results.* Abdom Imaging, 2011. **36**(1): p. 24-30.

114. Hebden, J.M., et al., *Small bowel transit of a bran meal residue in humans: sieving of solids from liquids and response to feeding.* Gut, 1998. **42**(5): p. 685.

115. Wilson, C.G. and N. Washington, *Assessment of Disintegration and Dissolution of Dosage Forms In Vivo Using Gamma Scintigraphy.* Drug Development and Industrial Pharmacy, 1988. **14**(2-3): p. 211-281.

116. Wilding, I.R., A.J. Coupe, and S.S. Davis, *The role of gamma-scintigraphy in oral drug delivery.* Adv Drug Deliv Rev, 2001. **46**(1-3): p. 103-24.

117. Weitschies, W., et al., *Magnetic markers as a noninvasive tool to monitor gastrointestinal transit.* IEEE Trans Biomed Eng, 1994. **41**(2): p. 192-5.

118. Weitschies, W., et al., *Magnetic marker monitoring of disintegrating capsules.* Eur J Pharm Sci, 2001. **13**(4): p. 411-6.

119. Weitschies, W., et al., *Magnetic Marker Monitoring: An application of biomagnetic measurement instrumentation and principles for the determination of the gastrointestinal behavior of magnetically marked solid dosage forms.* Adv Drug Deliv Rev, 2005. **57**(8): p. 1210-22.

120. Weitschies, W., H. Blume, and H. Mönnikes, *Magnetic marker monitoring: high resolution real-time tracking of oral solid dosage forms in the gastrointestinal tract.* Eur J Pharm Biopharm, 2010. **74**(1): p. 93-101.

121. Andrä, W., et al., *A novel method for real-time magnetic marker monitoring in the gastrointestinal tract.* Phys Med Biol, 2000. **45**(10): p. 3081-93.

122. Biller, S., D. Baumgarten, and J. Haueisen, *A Novel Marker Design for Magnetic Marker Monitoring in the Human Gastrointestinal Tract.* IEEE Transactions on Biomedical Engineering, 2011. **58**(12): p. 3368-3375.

123. Hahnemann, M.L., et al., *Motility mapping as evaluation tool for bowel motility: initial results on the development of an automated color-coding algorithm in cine MRI.* J Magn Reson Imaging, 2015. **41**(2): p. 354-60.

124. Major, G., et al., *Colon Hypersensitivity to Distension, Rather Than Excessive Gas Production, Produces Carbohydrate-Related Symptoms in Individuals With Irritable Bowel Syndrome.* Gastroenterology, 2017. **152**(1): p. 124-133 e2.

125. Hoad, C.L., et al., *Colon wall motility: comparison of novel quantitative semi-automatic measurements using cine MRI.* Neurogastroenterology & Motility, 2016. **28**: p. 327–335.

126. Murray, K., et al., *Differential effects of FODMAPs (fermentable oligo-, di-, mono-saccharides and polyols) on small and large intestinal contents in healthy subjects shown by MRI.* Am J Gastroenterol, 2014. **109**(1): p. 110-9.

127. Berger, A., *Magnetic resonance imaging.* Bmj, 2002. **324**(7328): p. 35.

128. Sager, M., et al., *Low dose caffeine as a salivary tracer for the determination of gastric water emptying in fed and fasted state: A MRI validation study.* European Journal of Pharmaceutics and Biopharmaceutics, 2018. **127**: p. 443-452.

129. Grimm, M., et al., *Characterization of the gastrointestinal transit and disintegration behavior of floating and sinking acid-resistant capsules using a novel MRI labeling technique.* Eur J Pharm Sci, 2019. **129**: p. 163-172.

130. Kagan, L., et al., *Gastroretentive Accordion Pill: Enhancement of riboflavin bioavailability in humans.* Journal of Controlled Release, 2006. **113**(3): p. 208-215.
131. Davis, J., et al., *Scintigraphic study to investigate the effect of food on a HPMC modified release formulation of UK-294,315.* Journal of pharmaceutical sciences, 2009. **98**(4): p. 1568-1576.
132. Steingoetter, A., et al., *Analysis of the meal-dependent intragastric performance of a gastric-retentive tablet assessed by magnetic resonance imaging.* Alimentary pharmacology & therapeutics, 2003. **18**(7): p. 713-720.
133. Knörgen, M., et al., *Non-invasive MRI detection of individual pellets in the human stomach.* European journal of pharmaceutics and biopharmaceutics, 2010. **74**(1): p. 120-125.
134. Faas, H., et al., *Monitoring the intragastric distribution of a colloidal drug carrier model by magnetic resonance imaging.* Pharmaceutical research, 2001. **18**(4): p. 460-466.
135. Faas, H., et al., *Effects of meal consistency and ingested fluid volume on the intragastric distribution of a drug model in humans—a magnetic resonance imaging study.* Alimentary pharmacology & therapeutics, 2002. **16**(2): p. 217-224.
136. Grimm, M., et al., *Characterization of the gastrointestinal transit and disintegration behavior of floating and sinking acid-resistant capsules using a novel MRI labeling technique.* European Journal of Pharmaceutical Sciences, 2019. **129**: p. 163-172.

137. Curley, L., et al., *Magnetic Resonance Imaging to Visualize Disintegration of Oral Formulations.* Journal of Pharmaceutical Sciences, 2017. **106**(3): p. 745-750.
138. Sager, M., et al., *Combined application of MRI and the salivary tracer technique to determine the in vivo disintegration time of immediate release formulation administered to healthy, fasted subjects.* Molecular pharmaceutics, 2019. **16**(4): p. 1782-1786.
139. Knörgen, M., et al., *Non-invasive MRI detection of individual pellets in the human stomach.* Eur J Pharm Biopharm, 2010. **74**(1): p. 120-5.
140. Heissam, K., et al., *Measurement of fasted state gastric antral motility before and after a standard bioavailability and bioequivalence 240 mL drink of water: Validation of MRI method against concomitant perfused manometry in healthy participants.* PLOS ONE, 2020. **15**(11): p. e0241441.
141. Eggers, H., et al., *Dual-echo Dixon imaging with flexible choice of echo times.* Magn Reson Med, 2011. **65**(1): p. 96-107.
142. Sager, M., et al., *Combined Application of MRI and the Salivary Tracer Technique to Determine the in Vivo Disintegration Time of Immediate Release Formulation Administered to Healthy, Fasted Subjects.* Mol Pharm, 2019. **16**(4): p. 1782-1786.
143. Das, K.M. and R. Dubin, *Clinical pharmacokinetics of sulphasalazine.* Clin Pharmacokinet, 1976. **1**(6): p. 406-25.
144. Antonin, K.H., et al., *Oxprenolol absorption in man after single bolus dosing into two segments of the colon compared with that*

after oral dosing. British journal of clinical pharmacology, 1985. **19 Suppl 2**(Suppl 2): p. 137S-142S.

145. Godbillon, J., et al., *Investigation of drug absorption from the gastrointestinal tract of man. III. Metoprolol in the colon.* British journal of clinical pharmacology, 1985. **19 Suppl 2**(Suppl 2): p. 113S-118S.
146. Staib, A.H., et al., *Measurement of theophylline absorption from different regions of the gastro-intestinal tract using a remote controlled drug delivery device.* Eur J Clin Pharmacol, 1986. **30**(6): p. 691-7.
147. Marvola, M., et al., *Gastrointestinal Transit and Concomitant Absorption of Verapamil from a Single-Unit Sustained-Release Tablet.* Drug Development and Industrial Pharmacy, 1987. **13**(9-11): p. 1593-1609.
148. Wilding, I.R., et al., *Pharmacoscintigraphic evaluation of a modified release (Geomatrix®) diltiazem formulation.* Journal of Controlled Release, 1995. **33**(1): p. 89-97.
149. Edsbäcker, S. and T. Andersson, *Pharmacokinetics of Budesonide (Entocort™ EC) Capsules for Crohn's Disease.* Clinical Pharmacokinetics, 2004. **43**(12): p. 803-821.
150. Edsbäcker, S., P. Larsson, and P. Wollmer, *Gut delivery of budesonide, a locally active corticosteroid, from plain and controlled-release capsules.* European Journal of Gastroenterology & Hepatology, 2002. **14**(12).

151. Bode, H., et al., *Investigation of nifedipine absorption in different regions of the human gastrointestinal (GI) tract after simultaneous administration of 13C- and 12C-nifedipine.* Eur J Clin Pharmacol, 1996. **50**(3): p. 195-201.

152. Hahn, T.W., et al., *Pharmacokinetics of rectal paracetamol after repeated dosing in children.* Br J Anaesth, 2000. **85**(4): p. 512-9.

153. Kimura, T., et al., *Drug absorption from large intestine: physicochemical factors governing drug absorption.* Biol Pharm Bull, 1994. **17**(2): p. 327-33.

154. Gittings, S., et al., *Characterisation of human saliva as a platform for oral dissolution medium development.* Eur J Pharm Biopharm, 2015. **91**: p. 16-24.

155. Ali, J., et al., *Development and optimisation of simulated salivary fluid for biorelevant oral cavity dissolution.* Eur J Pharm Biopharm, 2021. **160**: p. 125-133.

156. Paton, C.D., T. Lowe, and A. Irvine, *Caffeinated chewing gum increases repeated sprint performance and augments increases in testosterone in competitive cyclists.* Eur J Appl Physiol, 2010. **110**(6): p. 1243-50.

157. Morris, C., et al., *Caffeine release and absorption from caffeinated gums.* Food Funct, 2019. **10**(4): p. 1792-1796.

158. De Mey, C. and I. Meineke, *Prandial and diurnal effects on the absorption of orally administered enteric coated 5-aminosalicylic acid (5-ASA).* Br J Clin Pharmacol, 1992. **33**(2): p. 179-82.

159. Talattof, A., J.C. Price, and G.L. Amidon, *Gastrointestinal Motility Variation and Implications for Plasma Level Variation: Oral Drug Products.* Mol Pharm, 2016. **13**(2): p. 557-67.

160. Augustijns, P., et al., *Unraveling the behavior of oral drug products inside the human gastrointestinal tract using the aspiration technique: History, methodology and applications.* European Journal of Pharmaceutical Sciences, 2020. **155**: p. 105517.

161. Kimura, T. and K. Higaki, *Gastrointestinal transit and drug absorption.* Biol Pharm Bull, 2002. **25**(2): p. 149-64.

162. Goodman, K., et al., *Assessing gastrointestinal motility and disintegration profiles of magnetic tablets by a novel magnetic imaging device and gamma scintigraphy.* Eur J Pharm Biopharm, 2010. **74**(1): p. 84-92.

163. Sugihara, M., et al., *Analysis of Intra- and Intersubject Variability in Oral Drug Absorption in Human Bioequivalence Studies of 113 Generic Products.* Mol Pharm, 2015. **12**(12): p. 4405-13.

164. Khan, E., *Pharmacokinetics and Pharmacodynamics*, in *Understanding Pharmacology in Nursing Practice*, P. Hood and E. Khan, Editors. 2020, Springer International Publishing: Cham. p. 27-56.

165. Liu, C., et al., *Manometry of the Human Ileum and Ileocaecal Junction in Health, Disease and Surgery: A Systematic Review.* Frontiers in Surgery, 2020. **7**.

166. Dent, J., et al., *Manometric demonstration of duodenal/jejunal motor function consistent with the duodenal brake mechanism.* Neurogastroenterology & Motility, 2020. **32**(10): p. e13835.

167. Faas, H., et al., *Pressure-geometry relationship in the antroduodenal region in humans.* American Journal of Physiology-Gastrointestinal and Liver Physiology, 2001. **281**(5): p. G1214-G1220.

168. Wright, et al., *Validation of antroduodenal motility measurements made by echo-planar magnetic resonance imaging.* Neurogastroenterology & Motility, 1999. **11**(1): p. 19-25.

169. FDA, *Guidance for industry: food-effect Bioavailability and fed Bioequivalence studies.* U.S. Department of Health and Human Services, Centre for Drug Evaluation and Research (CDER), 2002.

170. FDA, *Guidance for industry. Bioavailability and bioequivalence studies for orally administered drug products: general considerations.* U.S. Department of Health and Human Services, Centre for Drug Evaluation and Research (CDER), 2003.

171. Gollifer, R.M., et al., *Relationship between MRI quantified small bowel motility and abdominal symptoms in Crohn's disease patients-a validation study.* Br J Radiol, 2018. **91**(1089): p. 20170914.

172. de Jonge, C.S., et al., *Dynamic MRI for bowel motility imaging—how fast and how long?* The British Journal of Radiology, 2018. **91**(1088): p. 20170845.

173. Menys, A., et al., *Dual registration of abdominal motion for motility assessment in free-breathing data sets acquired using dynamic MRI.* Phys Med Biol, 2014. **59**(16): p. 4603-19.
174. Fragkos, K.C., et al. *Serum Scoring and Quantitative Magnetic Resonance Imaging in Intestinal Failure-Associated Liver Disease: A Feasibility Study*. Nutrients, 2020. **12**, DOI: 10.3390/nu12072151.
175. Åkerman, A., et al., *Computational postprocessing quantification of small bowel motility using magnetic resonance images in clinical practice: An initial experience.* Journal of Magnetic Resonance Imaging, 2016. **44**(2): p. 277-287.
176. Brasseur, J.G. and W.J. Dodds, *Interpretation of intraluminal manometric measurements in terms of swallowing mechanics.* Dysphagia, 1991. **6**(2): p. 100-119.
177. Hoad, C., et al., *Will MRI of gastrointestinal function parallel the clinical success of cine cardiac MRI?* Br J Radiol, 2018. **91**.
178. Menys, A., et al., *Global Small Bowel Motility: Assessment with Dynamic MR Imaging.* Radiology, 2013. **269**(2): p. 443-450.
179. Froehlich, J.M., et al., *Small bowel motility assessment with magnetic resonance imaging.* Journal of Magnetic Resonance Imaging, 2005. **21**(4): p. 370-375.
180. Steingoetter, A., et al., *Magnetic resonance imaging for the in vivo evaluation of gastric-retentive tablets.* Pharm Res, 2003. **20**(12): p. 2001-7.

181. Grimm, M., et al. *Comparing Salivary Caffeine Kinetics of 13C and 12C Caffeine for Gastric Emptying of 50 mL Water*. Pharmaceutics, 2023. **15**, DOI: 10.3390/pharmaceutics15020328.

182. Grimm, M., et al., *Comparing the gastric emptying of 240 mL and 20 mL water by MRI and caffeine salivary tracer technique.* Eur J Pharm Biopharm, 2023.

183. Vinarov, Z., et al., *Impact of gastrointestinal tract variability on oral drug absorption and pharmacokinetics: An UNGAP review.* Eur J Pharm Sci, 2021. **162**: p. 105812.

184. O'Farrell, C., et al., *Luminal Fluid Motion Inside an In Vitro Dissolution Model of the Human Ascending Colon Assessed Using Magnetic Resonance Imaging.* Pharmaceutics, 2021. **13**(10).

185. Stamatopoulos, K., et al., *Dynamic Colon Model (DCM): A Cine-MRI Informed Biorelevant In Vitro Model of the Human Proximal Large Intestine Characterized by Positron Imaging Techniques.* Pharmaceutics, 2020. **12**(7): p. 659.

186. Schütt, M., et al. *Simulating the Hydrodynamic Conditions of the Human Ascending Colon: A Digital Twin of the Dynamic Colon Model*. Pharmaceutics, 2022. **14**, DOI: 10.3390/pharmaceutics14010184.

187. Sánchez-Sánchez, E., et al. *Consumption of over-the-Counter Drugs: Prevalence and Type of Drugs*. International Journal of

Environmental Research and Public Health, 2021. **18**, DOI: 10.3390/ijerph18115530.

188. Poole, C., D. Jones, and B. Veitch, *Relationships between prescription and non-prescription drug use in an elderly population.* Archives of Gerontology and Geriatrics, 1999. **28**(3): p. 259-271.

189. Bendezu, R.A., et al., *Colonic content: effect of diet, meals, and defecation.* Neurogastroenterol Motil, 2017. **29**(2).

190. Nilsson, M., et al., *Opioid-induced bowel dysfunction in healthy volunteers assessed with questionnaires and MRI.* Eur J Gastroenterol Hepatol, 2016. **28**(5): p. 514-24.